Isolation and characterization of bioactive metabolites from two ethno pharmacologically important Zingiberaceae plants of Bangladesh and their endophytic fungi

A DISSERTATION SUBMITTED TO THE UNIVERSITY OF DHAKA IN PARTIAL FULFILLMENT OF THE REQUIREMENTS FOR THE DOCTOR OF PHILOSOPHY DEGREE IN BIOCHEMISTRY AND MOLECULAR BIOLOGY

SUBMITTED BY

Examination Roll No: 103

Registration No: 2019-20/103

(Re.) **Session:** 2019-20

November, 2025

DEPARTMENT OF BIOCHEMISTRY AND MOLECULAR BIOLOGY FACULTY OF BIOLOGICAL SCIENCES

UNIVERSITY OF DHAKA

DHAKA-1000,

BANGLADESH

DEDICATED

TO MY

FAMILY

DECLARATION

I, Kazi Jannatul Ferdous, Reg. No. 2019-20/103, Roll No. 103, student of PhD in the department of Biochemistry and Molecular Biology, Session 2019-2020 (Re.) hereby declare that the topic printed in the dissertation titled, "Isolation and characterization of bioactive metabolites from two ethnopharmacologically important Zingiberaceae plants of Bangladesh and their endophytic fungi" is my own work and has been carried out at the Department of Biochemistry and Molecular Biology, University of Dhaka and in Bangladesh Council of Scientific and Industrial Research (BCSIR). This thesis contains no material previously published or written by another person, except where duly referenced. All information in this document has been obtained and presented in accordance with academic rules and ethical conduct.

Kazi Jannatul Ferdous

PhD student

Roll No. 103

Registration No. 103/2019-20 (Re.)

Session: 2019-2020

CERTIFICATE OF APPROVAL

This is to certify that this benefice research work titled “Isolation and characterization of bioactive metabolites from two ethnopharmacologically important Zingiberaceae plants of Bangladesh and their endophytic fungi” was carried out by the author and the dissertation prepared from this work is suitable for submission in partial fulfillment for the degree of Doctor of Philosophy (PhD) in Biochemistry and Molecular Biology in the Faculty of Biological Science at the University of Dhaka, Bangladesh.

(Signature of the Supervisor) **Dr. Md. Rakibul Islam** Professor Department of Biochemistry and Molecular Biology University of Dhaka, Dhaka, Bangladesh	**(Signature of the Co-supervisor)** **Dr. Md. Abdul Mazid** Professor Dept. of Pharmaceutical Chemistry, University of Dhaka, Dhaka, Bangladesh	**(Signature of Co-supervisor)** **Dr. Md. Hossain Sohrab** Chief Scientific Officer (CSO) BCSIR Laboratories, Dhaka, Bangladesh

ACKNOWLEDGEMENT

First and foremost I express my gratitude to the almighty Allah, the most gracious and the most merciful. All the applauses belong to the Almighty to accomplish this thesis work.

I am most sincerely grateful and express my heartfelt thanks to my supervisor Dr. Rakibul Islam, Professor, Department of Biochemistry and molecular Biology, University of Dhaka who gave his kind consent for being the supervisor and gave me the opportunity to work with him and also enriched my work with valuable comments and suggestions. He also very kindly provided the necessary support in all phases of this study. I am also grateful to express my sincere thanks for honorable teachers of the Department of Biochemistry and Molecular Biology for their kind cooperation and encouragement to me.

I wish to express my gratitude to my co-supervisor and advisor Dr. Md. Hossain Sohrab, Chief Scientific Officer (CSO), Pharmaceutical Sciences Research Division (PSRD), BCSIR Dhaka Laboratories, Bangladesh Council of Scientific and Industrial Research, Dhaka, for giving me the opportunity to work in his group and let me use the excellent work facilities of his lab. He guided me with excellent scientific knowledge, constructive comments, valuable advices, continuous cooperation and endless inspiration throughout the period of the research work.

I am extremely grateful to my other co-supervisor Dr. Md. Abdul Mazid, Professor, Department of Pharmaceutical Chemistry, University of Dhaka for sharing his scientific thoughtfulness with me and giving continuous inspiration and support.

My heartfelt thanks goes to well known Prof. Dr. Choudhury Mahmood Hasan, Department of Pharmaceutical Chemistry, University of Dhaka for his constructive advices in NMR data interpretation. His skillful help has inspired me to complete this work.

I appreciate all fellow lab mates and Scientists of Pharmaceutical Sciences Research Division (PSRD), BCSIR Dhaka Laboratories for their help and support and for providing a friendly and cooperative environment in the lab. A special thanks to Dr. Farhana Afroze, Shammi Akhter, Suriya Sharmin, Fatema Moni, Satyajit Roy, Nazifa Tabassum, Dr. Mahmuda Nasrin, Zihan Rahman Khan, Rabita Zinnurine, Farhana Afroze, Sadia Noor, Israt Farha Lini, Mita Munshi,

Mr. Zobair Abedin, Mr. Gazi Monjur Murshid, and Mst. Nadira Begum for their assistance and mental support when required.

Finally, I like to express utmost gratitude to my parents Md. Shahjahan Kazi and Jahan Ara Khandoker for their continuous love and inspiration. Without them I cannot be here. My appreciation goes to my husband Dr. Md. Harunur Rashid Bhuyan who sacrificed a lot during my research journey and encouraged me as well. I wish to express my heartiest love to my daughters Nuzaima Naowar Bhuyan and Nureen Nawal Bhuyan for holding their patience and enduring sacrifices during this long journey. Furthermore, I wish to thank the rest of my family members for their enthusiastic support and encouragement.

Table of Contents

List of Table

List of Figures

List of abbreviations

MeOH	Methanol
EtOH	Ethanol
EtOAc	Ethyl acetate
DCM	Dichloromethane
CHCl3	Chloroform
NaOCl	Sodium hypochlorite
DMSO	Dimethyl sulphoxide
PDA	Potato dextrose agar
NA	Nutrient agar
$CDCl_3$	Deuterated chloroform
CD_3OD	Deuterated methanol
CC	Column chromatography
TLC	Thin layer chromatography
PTLC	Preparative Thin Layer Chromatography
h.	Hour
min.	Minute
UV	Ultra violet spectroscopy
NMR	Nuclear magnetic resonance
COSY	Correlation spectroscopy
HMBC	Heteronuclear multiple bond correlation
HSQC	Heteronuclear multiple bond coherence via direct coupling
MTT	Microculture tetrazolium

ABSTRACT

The work explained in this thesis elaborates the isolation and identification of endophytic fungi from two ethnopharmacologically significant Zingiberaceae plants of Bangladesh, namely *Curcuma longa* L. and *Zingiber officinale* Rosc. The term "ethnophamacologically" means that these kinds of plants are traditionally used by specific groups of people for medicine purpose from very ancient period. A detail description was given for chemical screening of the crude extracts of the plants as well as their endophytic fungi. Isolation of secondary metabolites was done from the extracts of plants and their endophytic fungi by a combination of repeated column chromatography and preparative thin layer chromatography (PTLC). Structure clarification of pure compounds was made by their spectral data (GC-MS, 1D and 2D NMR). Finally bioassays of different extracts and isolated pure compounds were performed to observe antioxidant, antimicrobial and cytotoxic effect. The antioxidant activity was measured by the DPPH free radical scavenging method and antimicrobial activity was performed by the disc diffusion method. The cytotoxic activity of various extracts was completed by brine shrimp lethality bioassay. But the pure isolated compounds' cytotoxic activity was analyzed on a variety of cell line cultures, for example, Lung cancer cell line A-549, kidney fibroblast cell line BHK-21, human cervical carcinoma cell line (HeLa). A network pharmacology-based approach in combination with molecular docking analysis was also used to identify a compound's multiple targets that may have linked to its pharmacological action.

A total of seven endophytic fungi were isolated from *C. longa* and, a total of five endophytic fungi were isolated from *Z. officinale*. All the endophytes were segregated from diverse parts of the plants (petiole, leaf, root, bark). Through morphological and molecular analysis it was revealed that among twelve endophytic fungi, eight are *Fusarium* species, three are *Clonostacys* species, and one is *cladosporium* species. All crude extracts contain flavonoids, coumarins, anthrocyanins, isocoumarins or their derivatives types of compounds which was revealed through chemical screening by thin layer chromatography (TLC). The crude methanolic extract of *C. longa* showed significant antioxidant (IC_{50} value 19.85 µg/ml) and cytotoxic activity (LC_{50} value1.81 µg/ml) compared to their standards. Its vaccuum liquid chromatography (VLC) fractions also showed significant antioxidant and cytotoxic activity. In case of *Z. officinale*, the plant methanolic crude extracts showed very significant antioxidant activity (IC_{50} value 2.08

μg/ml) and mild to moderate antibacterial activity (zone of inhibition 7-10 mm). Its fractions obtained through the modified Kupchan partition method also showed good antioxidant and antibacterial activity. The obtained results prove the phytochemical as well as pharmacological significance of these plants.

A total of 27 metabolites and 21 metabolites were discovered through GC-MS analysis of crude methanolic extracts of *C. longa* and *Z. officinale* respectively. Most of them are bioactive constituents. Two compounds have been isolated from the plant *C. longa*, which were characterized as 4-hydroxy-3-methoxy cinnamic acid (CL-1) and methyl ferulate (CL-4). Among seven endophytic fungi isolated from this plant, CLRE-3 (*Clonostachys rosea*) was selected for large-scale cultivation based on chemical and biological investigation. From its ethyl acetate extract four compounds were isolated and characterized as Bassiatin (CLE-7), Nectriafurone (CLE-14), 8-O-methyl nectiafurone (CLE-11) and 8-O-methyl bostrycoidin (CLE-18)). Bassiatin, 8-O-methyl nectiafurone and 8-O-methyl bostrycoidin were obtained from this endophytic fungus for the first time. Among five endophytic fungi isolated from *Z. officinale* ZOLE-2 (*Cladosporium cladosporoides*) was selected for large-scale cultivation by observing its chemical and biological analysis. From its ethyl acetate extract two compounds were isolated and characterized as ergosterol (ZOE-1) and 3, 5, dihydroxy-ergosta-7, 22-diene-6-one (ZOE-6).

Following biological investigation it was revealed that almost all isolated compounds were bioactive. CLE-18(2) and ZOE-6 indicated mild to moderate antibacterial activity against *E. coli*, *P. aeruginosa* and *S. aureus* bacteria with a zone of inhibition of 10 to 16 mm. CL-4 and CLE-7 showed moderate antibacterial activity against *E. coli* bacteria with a zone of inhibition of 10 mm. CL-1 showed noteworthy antioxidant activity with IC_{50} value 4.77 μg/ml in comparison with standards ASA (IC_{50} value 9.01 μg/ml) and BHA (IC_{50} value 11.42 μg/ml). It also exhibited cytotoxic activity against A-549 cancer cell line which was done by the trypan blue exclusion method. CLE-14 showed cytotoxic activity against BHK-21 cell line with IC_{50} value of 663.4μg/ml compared to standard doxorubicin (IC_{50} value of 327.1 μg/ml). It did not exhibit any activity against the HeLa cell line. CLE-7 also displayed cytotoxic activity against the A-549 cancer cell line. A computational study was done against Bassiatin (CLE-7) and lung cancer. Thus MMP9, PTGS2 and ERBB2 were unveiled as the top three common targets between the disease and compound. CLE-7 targets these proteins with fairly good binding score compared to

standards based on molecular docking analysis. Thus it can be considered as a potential candidate for lung cancer treatment.

The isolation of endophytic fungi and their chemical constituents from these plants have been revealed for the first time in Bangladesh through this investigation. From this study it is clear that these plants and their endophytic fungi would be a good resource of reference in the scientific world because of possessing various types of bioactive compounds. This analysis meets up the overall aims and objectives of the study for isolation and characterization of bioactive metabolites which can be used as a scaffold for innovative medicinal chemistry amendment to build up new drugs.

Chapter 1
INTRODUCTION

INTRODUCTION

1.1. Medicinal plants, its bioactivity and compounds

The various combination of natural substances known as phytochemicals such as phenolic compounds, nitrogen compounds, vitamins and terpenes are usually responsible for the medicinal traits found in plants. The pharmacological activity of various phytochemicals may vary; for example, terpenoids have antiviral, antibacterial, anticancer and antimalarial properties. The majority of alkaloids have anaesthetic qualities. Phenolic molecules are crucial for scavenging free radicals. Phenolic chemical flavonoids have a number of therapeutic uses, including antiviral, anticancer, anti-inflammatory consequences. Natural substances are now used as an alternative medical treatment to address global health issues. Researchers may find it useful to study phytochemicals and their therapeutic values in order to create novel medications to treat various illnesses.

1.2. Endophytic fungi

Endophytic fungi are a variety of polyphyletic groupings of microorganisms that can live in various parts of living plants, among other healthy tissues, both above and below ground without showing any symptom. More than a million endophytic fungus species are thought to exist in nature. Endophytic fungi can be divided into three primary ecological groups: (a) mycorrizal; (b) pasture or balansicaeous and (c) non-pasture [Faeth & Fagan, 2002]. Over the course of their lengthy coexistence and evolutionary processes endophytic fungi and their host plants have developed a variety of relationships, including mutualism, antagonism, and neutralism. The inhabitant structure of the endophytic fungi is thought to be influenced by the genetic background, nutritional status, and conservation habitats of the host plants. These factors confer various benefits, including increased resistance to disease, induced growth and build up bioactive constituents [Fiáková et al., 2007], some of which can be processed by humans as useful medicines. Consequently, the way endophytic fungi and their host plants interact with one another can have an impact on the development of specific bioactive chemicals that humans can use as valuable medical resources.

1.3. Endophytic fungi and secondary metabolites

The primary sources of novel medications and treatments are the secondary metabolites formed by endophytic fungi. The isolation of penicillin from the fungus *Penicillium notatum* was one of the first discoveries in 1928 [Wainwright, 1993]. The anti-cancer medication Taxol was created by *Taxus brevifolia* which is a Pacific yew tree in the 1990s [Bolsinger & Jaramillo, 1090]. The anticancer medication vincristine was formed from the endophytic fungus *Mycelia sterilia*, which grew on the rose periwinkle plant, is another example. The antibiotic Clavatol is made by the coniferous tree-dwelling fungus *Aspergillus clavatonanicus* [https://biologydictionary.net/endophytic-fungi/]. Thus endophytes persist to be a source of potential drug leads with diverse properties. Recent developments in endophyte-based drug discovery focus on influencing advanced technologies like genomics, artificial intelligence, and metabolic engineering to unlock the prospective of these microorganisms for producing novel therapeutic compounds. A specific review paper which published in *Molecules* in June 2023, systematically analyzes 296 newly discovered compounds from endophytic fungi reported in journal articles between 2011 and 2022 [Gupta et al., 2023]. The review article provides an inclusive analysis of these 296 compounds that were selected for their novel or rare structures or skeletal frameworks.

1.4. Family: Zingiberaceae

The family of flowering plants known as Zingiberaceae, or the ginger family is made up of roughly 50 genera and 1600 species. They are found in tropical Africa, Asia, and the Americas [Christenhusz et al., 2016]. With their highest diversity in Southeast Asia, the Zingiberaceae are found across the tropics of Africa, Asia, and the Americas. The moist parts of the tropics and subtropics as well as some seasonally dry places are home to these fragrant herbs. The family's members are perennials with fleshy rhizomes (underground stems) that are often sympodial (forked). Their height may be up to 6 meters (20 ft). The Zingiberaceae flower's labellum (two or more fused stamens) gives it an orchid-like appearance.

1.5. *Curcuma longa* Linn. (*C. longa*)

The perennial, upright, leafy plant *Curcuma longa* Linn. has enormous leaves that can reach a length of 1.2 meters. It is frequently referred to as holud in Bangla and turmeric in English. Harvesting takes place between February and April. According to Chatterjee & Pakrashi [2001] and

Hooker [1990], the leaves are big, oblong, and constricted at the base. With overlapping petioles, they are long and borne at the apex of the non-woody subterranean stem. They are 8 to12 cm wide, 30 to 40 cm long and pale green [Ross, 2001]. Cone-shaped and ranging in length from 10 to 15 cm, the inflorescence is affixed to a stem that is encased in a sheathing petiole. The flower has two 5–6 cm long, pale green bracts. Each blossom is either yellow or yellowish white [Thomas, 2000]. Flowering occurs during rainy season [Chatterjee & Pakrashi, 2001]. The primary rhizome develops several roots and thickens to a tuber. The thick, branching rhizomes have a vivid orange to yellow inside [Ross, 2001].

1.5.1. Taxonomy of *C. longa*

Kingdom: Plantae
Division: Magnoliophyta
Class: Liliopsida
Subclass: Zingiberidae
Order: Zingiberales
Family: Zingiberaceae
Genus: *Curcuma*
Species: *Curcuma longa* Linn.

1.5.2. Traditional uses of *C. longa*

Traditionally this plant is used in various medications for example digestive disorders, arthritis, cardiovascular conditions, cancer, bacterial infections etc.

1.5.3. Previous Chemical studies on the genera *C. longa*

The main species that has been the focus of numerous studies is *C. longa*. The most often utilised portion of *Curcuma* species for chemical extractions is their rhizomes. According to Anjusha & Gangaprasad [2014], it has 69.4% carbohydrate, 6.3% protein, 5.1% fat, and 3.5% minerals. The substance that gives it its yellow hue is curcumin (diferuloylmethane), which is made up of curcumin I (94%), curcumin II (6%), and curcumin III (0.3%) [Xiang et al., 2018].

1.5.4. Previous Biological Investigation on the genera *C. longa*

According to a thorough review of the literature, turmeric is widely recognized as a natural remedy with a broad range of pharmacological properties [Nasri et al., 2014]. Numerous metabolites, including curcuminoid, oil, flavonoids, phenolics, protein, some essential amino acids, and a high alkaloid content, are shown to be associated with its therapeutic applications [Sarangthem &

Haokip, 2010]. Turmeric is a frequently used medicinal plant because of its enormous biological activity. Some important biological activities of compounds obtained from this plant are given in Table 1.1.

Table 1.1: Biological activity of turmeric and its compound

Serial No	Compound/ extract	Biological activity	Reference
1	Turmeric powder	Antitumor, Anti protozoan Anti inflammatory and Wound-healing	Gujral et al., 1953
2	Methylcurcumin	Anti protozoan	Gomes et al., 2002
3	Volatile oil	Anti-inflammatory, Antibacterial, Antifungal	Chandra et al., (1972)
4	Curcumin	Antibacterial, Anti protozoan, Antiviral, Antitumor and Antioxidant, Anti-diabetic, Anti-inflammatory, anticancer, Anti-aging, Anti-fertility, hepactoprotective activity, Anti- HIV, opthamalic, antidepressant, effect on cardiovascular and neurodegenerative disease, Anticoagulant activity, Effect on Alzheimer's disease	Lutomski et al., 1974; Choudhary & Sekhon, 2012; Ammon et.al., 1991; Baum & Ng, 2004
5	p,p'-dihydroxydicinna-moylmethane	Anticoagulant activity	Ammon et.al., 1991
6	p-hydroxycinnamoyl(feruloyl) methane	Anticoagulant activity	Ammon et.al., 1991
7	tetrahydrocurcumin	hepactoprotective activity,	Pari & Murugan, 2004
8	Ethanol extract of *C.longa*	Neuroprotective activity	Issuriya et.al., 2014

1.6. *Zingiber officinale* Rosc. (*Z. officinale*)

It is a herbaceous perennial with narrow leaf blades that grows to a height of around one metre. In Bangla, it is called ada, while in English, it is called ginger. The rhizome gives rise to the upright shoots. Thick lobed, meaty, knobby, and fragrant, rhizomes are covered with scars that resemble rings. The rhizome is pale yellow in hue and grows underground. The green leaves have sheathing bases, are long and 2-3 cm wide, and taper to a point over time. The inflorescences contain flowers of pale yellow petals and purple margins [Sutarno et al., 1999; Kirtikar et al., 1993]. Although it is a tropical plant, it may also thrive in subtropical climates.

1.6.1. Taxonomy of *Z. officinale*

Kingdom: Plantae
Division: Magnoliophyta
Class: Liliopsida
Order: Zingiberales
Family: Zingiberaceae
Genus: *Zingiber*
Species: *Zingiber officinale* Rosc.

1.6.2. Traditional uses of *Z. officinale*

Traditionally this plant is utilized in medication such as abdominal pain, vomiting, cough and cold, respiratory problems etc.

1.6.3. Previous Chemical studies on the genera *Z. officinale*

Gingerol, an alcoholic component of the oleoresin, accounts for 5–8% of ginger's pungency. Bisabolene, zingiberene, and zingiberol are the volatile oils (1–2%) that give ginger its scent.

1.6.4. Previous Biological Investigation on the genera *Z. officinale*

Numerous studies have shown that ginger has a variety of biological properties, such as anti-inflammatory, anti-carcinogenic, respiratory, and antidiabetic properties [Mao et al., 2019]. Some major biological activities of compounds from this plant are mentioned in Table 1.2.

Table 1.2: Biological activity of compounds from *Z. officinale*

Serial No	Compound/ extract	Biological activity	Reference
1	6-gingerol	Anticancer activity	Brown et.al., 2009
2	Leaf extract of *Z. officinale*	Induce apoptosis in cancer cell	Park et.al., 2014
3	6-Paradol	Anticancer	Shukla et.al., 2007
4	6-Shogaol	Anticancer, antioxidant, Anti-inflammatory	Shukla et.al., 2007; Jitoe et.al., 1992; Luettig et.al., 2016
5	Zingerone	Antimutagenic. Anti-inflammatory	Shukla et.al., 2007; Masuda et.al., 2004; Hsiang et.al., 2013
6	6-Gingerol and gingerol-related compounds	Anticancer, antioxidant	Shukla et.al., 2007; Sekiwa et.al., 2000
7	Ginger oleoresin	Antioxidant	Ji et.al., 2017
8	Ginger phenylpropanoids	Antioxidant	Schadich et. al., 2016
9	Gingerenone-A	Antimicrobial	Rampogu et.al., 2018
10	10-gingerol	Cytotoxic activity	Bernard et.al., 2017
11	10-shogaol	Cytotoxic activity	Liu et.al., 2017

1.7. Aim and Objectives of the present study

Zingiber officinale Rosc. and *Curcuma longa* Linn. were chosen for this study because they were both historically utilised by a certain group of people from very ancient times. These plants are significant from an ethnopharmacological perspective in this way. Both of these plants have been researched extensively for chemical and biological investigation but no studies have been conducted in Bangladesh to isolate associated endophytic fungi from various parts of these plants. So, there is a knowledge gap here because endophytic fungi are considered as excellent

makers of secondary metabolites these days. Thus, the aim of this study was to identify the metabolites generated by plants and their endophytic fungi that are found in Bangladesh and to assess the bioactivity of the pure compounds that were recovered.

Chapter 2
MATERIALS AND METHODS

MATERIALS AND METHODS

The present study was intended to explore two ehthnopharmacologically important medicinal plants *Curcuma longa* Linn. and *Zingiber officinale* Rosc. and their endophytic fungi. The protocols are as follows:

- Gathering freshly cut plant pieces from a planting source
- Accurately identifying the appropriate medicinal plants
- Cold extraction of the powdered plants with methanol
- Isolation of endophytic fungi from various parts of plant using Water agar (WA) medium
- The isolated endophytic fungi were purified by Potato Dextrose Agar (PDA) medium.
- Identification of endophytic fungi by following morphological and molecular method
- Small scale cultivation of purified endophytic fungi using potato agar media (PDA) medium
- Extraction of cultured media of endophytic fungi with ethyl acetate
- Bioassay of the crude plant and fungal extracts
- Large scale cultivation of the potential endophytic fungi on potato agar (PDA) medium
- Chromatographic screening of the plant and fungal extracts in TLC plates by visual/UV detection and spray reagents
- Isolation of potential fungal and plant metabolites by various chromatographic (column, sub-column, PTLC) and method.
- Molecular structure may be determined using a variety of methods, the most common are the spectroscopy such as ultraviolet (UV), infrared (IR), nuclear magnetic resonance (NMR), mass, GC-MS etc.
- Bioactivity test of the extracts, fractions and pure compounds

2. 1. Getting the Plant Material and Preparing It

Healthy and mature *Curcuma longa* (*C. longa*) and *Zingiber officinale* (*Z. officinale*) plants were collected from Dhamrai, Dhaka, Bangladesh. Different parts of the plants were observed and confirmed by a taxonomist of Bangladesh National Herbarium (BNH), Dhaka, Bangladesh. The receipts herbarium specimens (DACB: 55762 and 45102) (Figure 2.1) have been dropped in the Herbarium for future use. These two plants were dried by air for several days at room temperature, then dried in an oven at 40 °C and ground into a coarse powder.

Figure 2.1: Photographs of the Herbarium sheets of two plants deposited in the Bangladesh National Herbarium (BNH)

2. 2. Plant Materials Extraction and filtration

The powdered rhizome part (150 g of *C. longa* and 138 g of *Z. officinale*) was immersed in methanol (MeOH) for 7 to 8 days with occasional moving. A rotary evaporator was used for concentrating the filtrate obtaining by filtering the methanolic extracts of the plants. Thus the crude extracts of the plants have been obtained. The whole process was consecutively repeated twice and got the final crude extract (15.69 g for *C. longa* and 14.45 g for *Z. officinale*).

2. 3. Isolation of compounds

Various chromatographic and other methods are used to separate pure compounds from crude and fractionated samples. A brief and basic summary of them are provided below:

2. 3.1. Chromatographic Techniques

Chromatography is an analytical method that is recurrently used to break down a mixture of chemical substances into its component parts so that each part may be examined in detail.

2.3.1.1. Gas chromatography-mass spectrometry (GC-MS)

The chemical components of volatile oil are usually recognized by using GC-MS. The analysis was done with a Clarus®690 gas chromatograph (Perkin Elmer, CA, USA) where 99.999 % pure helium was used as a carrier gas [Rahman et. al., 2017].

2.3.1.2. Column Chromatography

Column chromatography is competent for splitting materials on the basis of disparity adsorption of compounds to the adsorbent. By moving through the column at different rates, compounds can be separated into fractions. The system can be used on scales from μg up to kg.

In general, two methods are popular for column chromatography: the dry method and the wet method. For the dry method, the column is first filled with dry stationary phase powder (kieselgel 60, mesh 70-230), then the mobile phase is poured and flushed through the column until it is completely wet and is hindered from running dry [Shusterman et. al., 1997]. For the wet method, the eluent is mixed with the stationary phase powder to prepare a suspension and then poured into the column with care. A layer of sand was set at the top of the silica to ensure that it would be flat. During the whole chromatographic procedure the eluents are collected in a sequence of fractions which are then investigated.

2.3.1.3. Vacuum Liquid Chromatography (VLC)

It is a kind of chromatographic partition whose flow is activated by vacuum. The column is filled by vacuum-packed silica gel (kieselgel 60H). The extract being investigated determines the size of the column and the height of the adsorbent layer. In order to achieve compact packaging, the column is thoroughly cleansed using petroleum ether. Following

the drying process, a layer of silica gel (specifically kieselgel 60, with a mesh size of 70-230) was applied onto the sample. Subsequently, the sample intended for separation was adsorbed onto the gel. The column is washed with organic solvents that increase in polarity in order to gather fractions.

2.3.1.4. Thin Layer Chromatography (TLC)

It is a one-dimensional ascending procedure which conducts the initial examination of the extracts, column fractions, as well as the assessment of the purity of isolated compounds. TLC examination was performed on aluminium sheets that had been coated with silica gel. UV light with wavelengths of 254 or 365 nm was utilized in order to identify the compounds on TLC plates (Silica gel 60 F254; Merck AG, Darmstadt, Germany). A solution of vanillin-sulfuric acid (containing 1% vanillin in concentrated H_2SO_4) was sprayed onto the plates for a purity check [Stahl, 1969; Touchstone & Dobbins, 1978].

2.3.1.5. Preparative Thin Layer Chromatography (PTLC)

It operates based on the identical principles as TLC. Aluminium sheets of 20cm × 20cm, coated with silica gel (Silica gel 60 F254; Merck AG, Darmstadt, Germany), were used. The sample exhibits solubility in a suitable solvent and is administered in the form of a thin and evenly distributed band. Thin-layer chromatography (TLC) is employed to determine a suitable solvent solution for plate development. Various development methodologies were employed selectively to improve isolation. Once the plates have undergone development, a UV lamp with a wavelength of either 254 nm or 365 nm, or a suitable spray solution, is employed to see the chemical bands. Compounds can be eluted from silica gel plates using different solvents.

2.3.2. Solvent treatment

Selective solvent washing is a method of cleaning a chemical compound consisting predominantly of a heterogeneous mixture of several components. Initially, a solution or a mixture of solutions is selected in which the constituent of interest exhibits a high degree of insolubility. The undesirable components can be eliminated by repeatedly washing with this solvent or a mixture of solvents. Additional solvents or combinations of solvents may be used as needed to obtain a pure chemical substance.

2.3.3. Detection of Compounds

Compounds in TLC/PTLC plates may be detected using the methods listed below.

2.3.3.1. Visual detection

In order to ascertain the existence of pigmented substances, the resulting chromatogram is examined through visual observation.

2.3.3.2. UV light

The plates were examined using UV light at wavelengths of 254 nm and 365 nm to mark any fluorescent or quenching compounds that might be present.

2.3.3.3. Spray reagents (Vanillin/H_2SO_4)

The plates are heated to 100^0C for 10 minutes after being sprayed with 1% vanillin in sulfuric acid.

2.3.4. Retardation factor (R_f) values determination

The R_f value of a material can be utilized to determine the constituent in a specific solvent. It aids in the recognition and categorization of chemicals.

The equation used to determine the R_f value of a chemical is as follows:

$$R_f \text{ value} = \frac{\text{Distance travelled by the compound}}{\text{Distance travelled by the solvent system}}$$

2.4. Instrumentation

2.4.1. UV/VIS Spectroscopy

Spectra of UV light were done on a UV-Visible spectrophotometer (Analytik Jena AG, Germany) using 1.0 cm quartz cells at Bangladesh Council of Scientific and Industrial Research (BCSIR), Dhaka, Bangladesh.

2.4.2. NMR spectra

1D and 2D NMR spectra were acquired by using a deuterated solvent and a BRUKER WH 400 or 600 MHz NMR spectrometer at BCSIR. In order to capture all spectra, they were taken at room temperature (RT). Parts per million (ppm) are used to measure chemical changes.

2.4.3. Mass Spectra

Thermo Scientific's Exactive Orbitrap mass spectrometer was used to assemble the mass spectra, which were processed using ThermoX Calibur 2.2 at King's College London (UK).The base peak was connected to relative intensity.

2.5. Chromatographic separation of plant extracts for compound isolation

2.5.1. GC-MS of plant extract of *Curcuma longa* (*C. longa*) and *Zingiber oficinale* (*Z. officinale*)

The mass spectral analysis was done with methanolic rhizome extracts of *C. longa* and *Zingiber oficinale*. The obtained constituents were recognized by observing various characteristics such as their retention time (RT), molecular weight and formula, percent peak area etc. The spectral similarity was compared with the National Institute of Standards and Technology (NIST) database.

2.5.2. Column chromatography of plant extract of *C. longa*

Vacuum liquid chromatography (VLC) was conducted to swiftly separate the crude extract (15 g) into several fractions. Different solvents with increasing polarity were utilized during the fractionation procedure, and the entire crude extract was done on silica gel powder (kieselgel 60, mesh 60). Initially, a solvent system consisting of pure n-hexane was utilised, which was then replaced by a mixture of n-hexane, Dichloromethane (CH_2Cl_2), and lastly pure CH_2Cl_2. In the final stage, methanol was employed in conjunction with CH_2Cl_2 to enhance the separation of crude extracts. A range of solvent solutions were used as mobile phase in this VLC investigation. The system is presented in Table 2.1.

Table 2.1: Solvent systems used for VLC analysis of crude extract

Fraction no.	Solvent systems	Fraction no.	Solvent systems
1	n-hexane/ 10% CH_2Cl_2	10	n-hexane/100% CH_2Cl_2; CH_2Cl_2 / 2% MeOH
2	n-hexane/ 20% CH_2Cl_2	11	DCM / 3-5% MeOH
3	n-hexane/ 30% CH_2Cl_2	12	DCM / 7-15% MeOH
4	n-hexane/ 40% CH_2Cl_2	13	DCM / 20-65% MeOH
5	n-hexane/ 50% CH_2Cl_2	14	100% MeOH
6	n-hexane/ 60% CH_2Cl_2		
7	n-hexane/ 70% CH_2Cl_2		
8	n-hexane/ 80% CH_2Cl_2		
9	n-hexane/ 90% CH_2Cl_2		

2.5.2.1. Investigation of VLC fractions by TLC

VLC fractions were tested using TLC screening under UV light and spraying with vanillin-sulfuric acid reagent where applicable.

2.5.2.2. Isolation of compounds from column fractions

Various techniques such as sub-column chromatography, PTLC have been used to separate and purify a variety of chemicals from the VLC fractions of *C. longa*.

a) Isolation of compound CL-1

The use of spraying reagent revealed the presence of a compound in VLC fraction 12 (CH_2Cl_2/ 7-15% MeOH). Solvent treatment with n-hexane of this fraction made an orange crystal and characterized compound CL-1.

b) Isolation of compound CL-4

PTLC (Tolune/Ethyl acetate 95-5%v/v) was performed with the sub-column fraction of VLC fraction 4 (n-hexane/ 40% CH_2Cl_2). CL-4 was extracted from TLC plate using various solvents as a pale yellow powder.

2.5.3. Solvent-Solvent separation of crude extract of *Z. officinale*

The crude methanol extract of *Z. officinale* (10 g) was fractionated by modified Kupchan protocol [Kupchan & Tsou, 1973; Van-Wagenen et. al., 1993]. The crude extract was liquefied with 10% aqueous methanol and consequently extracted with n-hexane (Hex), dichloromethane (CH_2Cl_2) and to end with ethyl acetate (EA). The schematic diagram (Scheme 1) of the method is mentioned below. The obtained amounts were n-hexane soluble fraction (HexSF = 5.5 g), dichloromethane soluble fraction (DCMSF = 3.9 g), ethyl acetate soluble fraction (EASF = 80 mg) and aqueous soluble fraction (AQSF = 1.32 g), respectively. All the fractions were rested to desertion to dryness for further investigation.

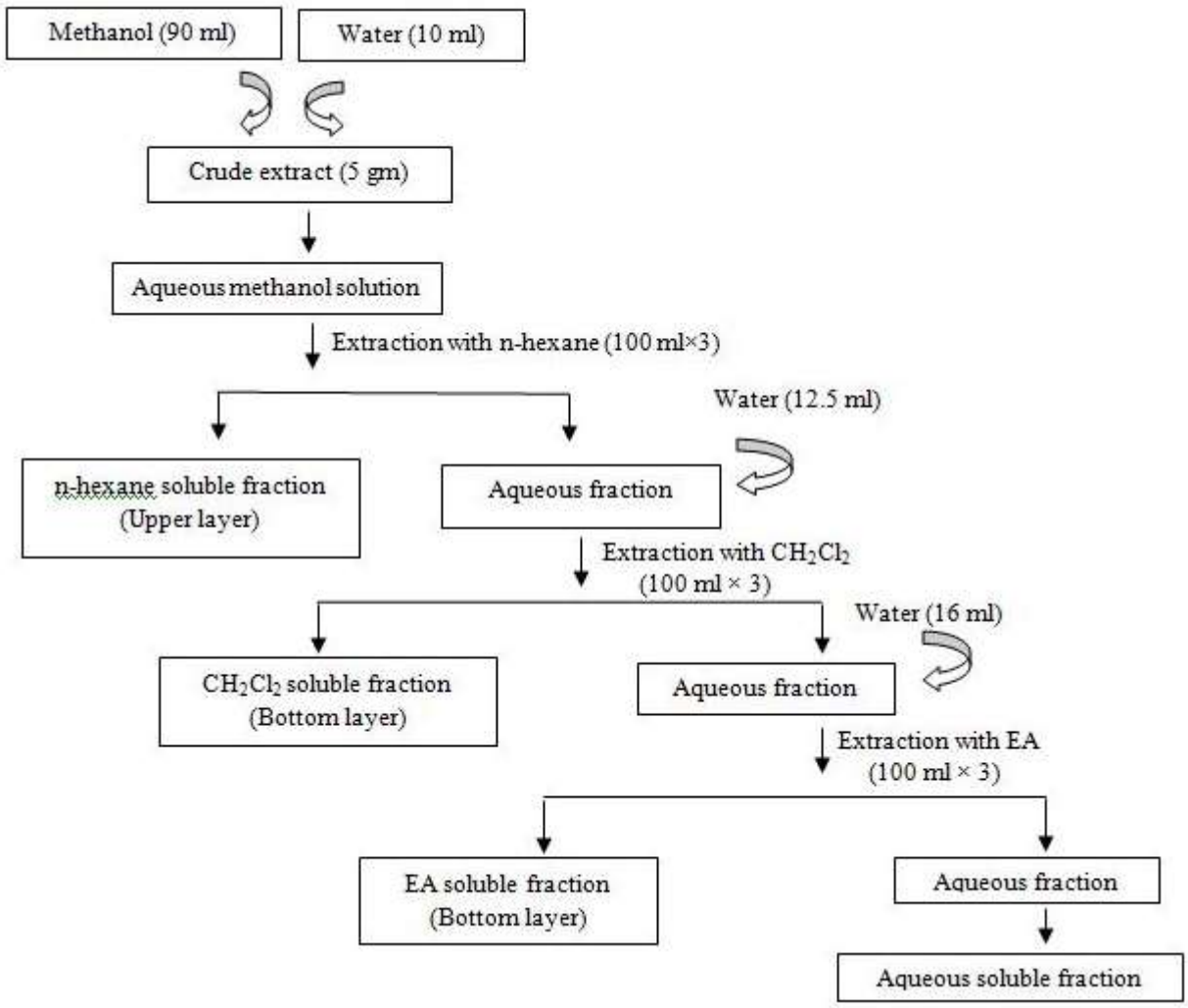

Scheme 1: Modified Kupchan Partitioning of crude extract of rhizome of *Z. officinale*

2.6. Isolation of Endophytic Fungi from Plant

The general scheme for isolation, identification and preparation for fungal extract are mentioned as follow (Scheme 2):

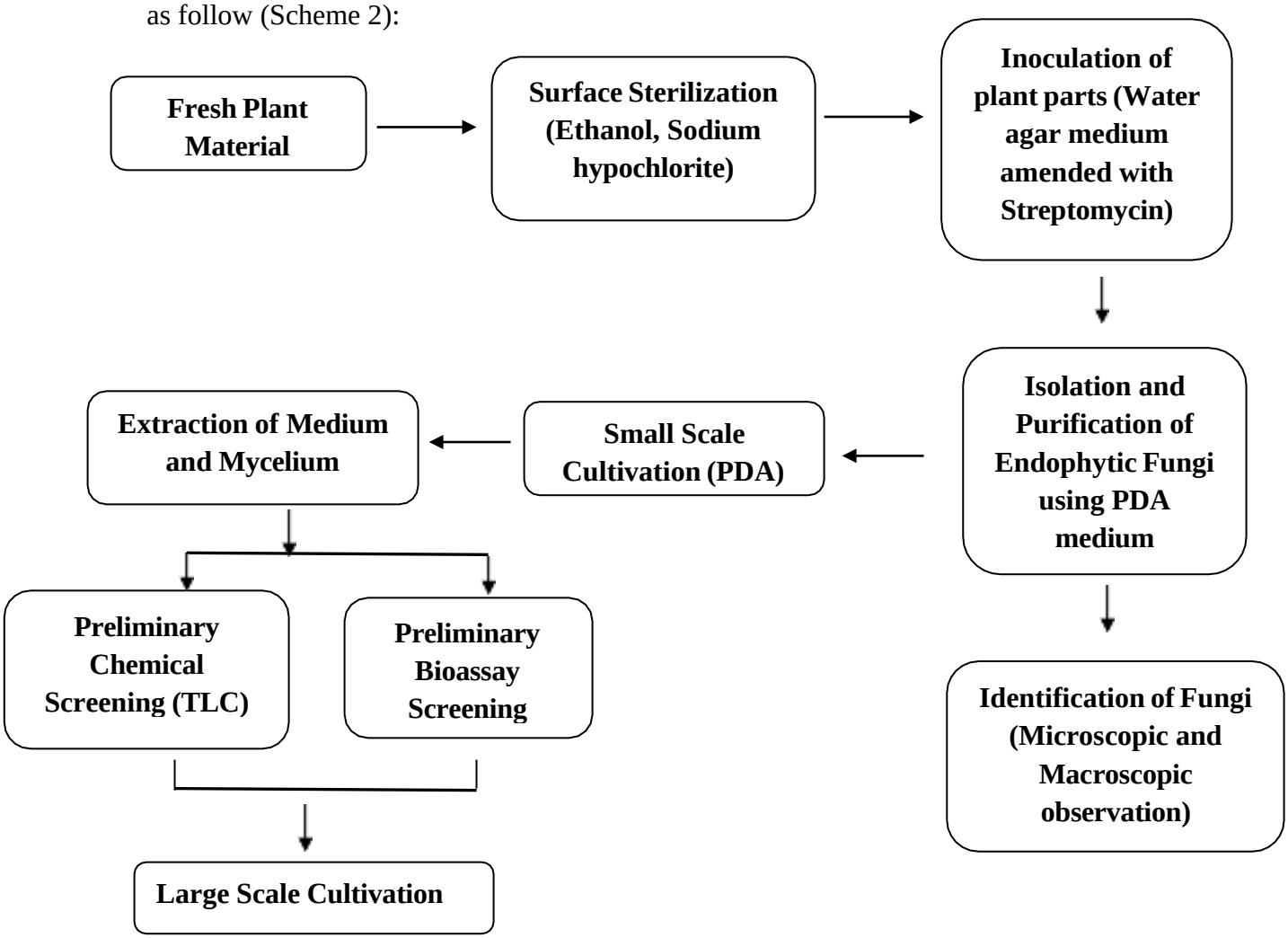

Scheme 2: Isolation of Endophytic Fungi

2.6.1. Sampling

Fresh, healthy (with no visible disease symptoms) and mature plant species were used for isolating endophytic fungi. For research purpose leaves, stems, roots, flowers, and fruits of the plant are usually taken randomly. In this study the following parts of the plants were investigated according to their availability (Table 2.2).

Table 2.2: Investigated plants and their parts

Plant name	Family	Part of the Plant
Curcuma longa	*Zingiberaceae*	Petiole, root and bark /rhizome
Zingiber officinale	*Zingiberaceae*	Leaf, petiole and bark /rhizome

2.6.2. Procedure for isolation, purification and culture of endophytic fungi

Isolation of endophytic fungi from plants was done according to a modified protocol established in the laboratory [Chowdhury et. al., 2016]. The detailed procedures are given below.

- Plants were properly cleaned with running tap water and chopped into little pieces under sterile circumstances (2–3 cm).
- The surface was sterilized by being submerged for three minutes in ethanol with a 70% concentration. The samples were further sterilized in 1.3 M sodium hypochlorite (NaOCl) solution for 3 min followed by surface sterilization in 70 % ethanol for 30s.
- Rinse with sterile water (3 times) for removing any remaining traces of sodium hypochlorite (3 min each).
- Surface sterilized plant parts were positioned on petri dishes which contained Water Agar (WA) media and the media were infused with streptomycin (100 mg/L) (Figure 2.2).
- The petri dishes were kept in a cooled incubator (Froilabo BRE 120, France) at 28 ± 2°C for 21~28 days till any fungal hypha become visible.
- Visualized hyphal tips were transferred to Potato Dextrose Agar (PDA) media to obtain pure fungal colonies.
- To separate the endophytic fungal strains fungal isolates were compared with control fungal isolates (obtained without surface sterilization plant parts).
- These isolated purified endophytic fungal strains were transferred to new PDA containing test tubes for short term storage and for long term storage 10% glycerol is needed.

	
Inoculation of leaf	Inoculation of leaf (3 weeks later)
	
Inoculation of petiole	Inoculation of petiole (3 weeks later)
	
Inoculation of root	Inoculation of root (3 weeks later)
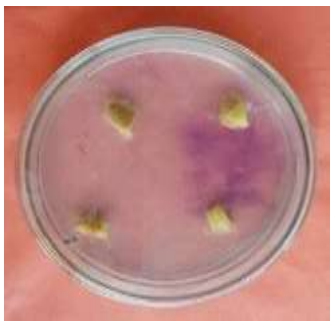	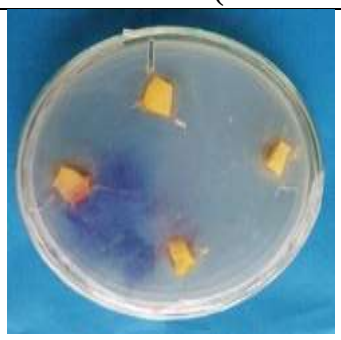
Inoculation of bark (rhizome)	Inoculation of bark (3 weeks later)

Figure 2.2: Inoculation of leaf, petiole, root and bark (rhizome) in water agar medium for the isolation of endophytic fungi

2.6.2.1. Chemicals and instruments used for isolation of endophytes from plants

Chemicals and instruments used for this experiment are given in Table 2.3.

.Table 2.3: Chemicals and instruments used for isolation of endophytes from plants

Reagents & Chemicals	Instruments
1. Sterile water agar medium (20 g water agar in 1000 ml) 2. Streptomycin 3. 1.3 M NaOCl 4. 70% Ethanol (70 mL absolute EtOH and distilled water q.s. to 100 mL) 5. Distilled water 6. Potato dextrose agar medium (39 g PDA in 1000 mL) 7. Solvent for extraction Ethyl Acetate and Chloroform	1. Laminar hood 2. Beaker 3. Petri dish 4. Conical flask 5. Microwave oven 6. Scissors 7. Forceps 8. Scalpel 9. Measuring cylinder 10. Jar 11. Anti-cutter 12. Filter paper 13. Cotton 14. Aluminium foil 15. Razor blade 16. Sterile slant (test tubes) 17. Loop

2.6.2.2. Preparation of solutions

1. Streptomycin (for 100 mg/L):

   By using 5 mL distilled water 1g of streptomycin, contained in vial, was dissolved. For a 200 mL agar medium 20 mg streptomycin was required. Therefore, volume of streptomycin required for 200 mL and 100 mL agar medium was 0.1 mL and 0.05 mL respectively.

2. 1.3 M NaOCl:

   To prepare 1M NaOCl 74.44g is required. Therefore, for 1.3M, 96.772 g amount required in 1 L distilled water. 1000 g of NaOCl is contained in 870 mL of solution. Therefore, 1g was present in 0.87 mL of solution. Thus, for 96.772 g of NaOCl, 84.19 mL volume was required. Therefore for preparing 1 L of 1.3M NaOCl solution, 84.19 mL needs to be

dissolved in distilled water. Thus for 100 mL of 1.3M NaOCl solution, 8.419 mL volume was required.

2.6.2.3. Isolated endophytic fungi from plants

A total of twelve endophytic fungi were isolated from the plants *C. longa* and *Z. officinale* as shown in Table 2.4.

Table 2.4: List of isolated endophytic fungi from plants

Serial no.	Fungi strain name	Source/Plant parts
1	CLPE-1	Isolated from *C. longa* petiole
2	CLPE-2	Isolated from *C. longa* petiole
3	CLPE-3	Isolated from *C. longa* petiole
4	CLPE-4	Isolated from *C. longa* petiole
5	CLRE-1	Isolated from *C. longa* root
6	CLRE-3	Isolated from *C. longa* root
7	CLBE-4	Isolated from *C. longa* bark (rhizome)
8	ZOBE-1	Isolated from *Z. officinale* bark (rhizome)
9	ZOBE-2	Isolated from Z. *officinale* bark (rhizome)
10	ZOPE-3	Isolated from *Z.officinale* petiole
11	ZOLE-1	Isolated from *Z. officinale* leaf
12	ZOLE-2	Isolated from *Z. officinale* leaf

2.7. Endophytic fungi identification

2.7.1. Morphological identification

Matured fungal culture was used to prepare slides. Lactophenol cotton blue solution was used for staining and then observed the slides under phase contrast microscope (Kruss, Germany). The microscope contains objective lens of 40 times magnification [Sadananda et al., 2014]. It was then studied for a characteristics array of spores. Morphological characteristics such as growth pattern, hyphae structure, the color of the colony and medium, margin character, aerial mycelium,

surface texture, the size and coloration of the conidia were examined occasionally upto full growth of fungi and compared with the regular taxonomic key [Devi & Prabakaran, 2014; Barnett & Hunter,1998] (Figure 2.3).

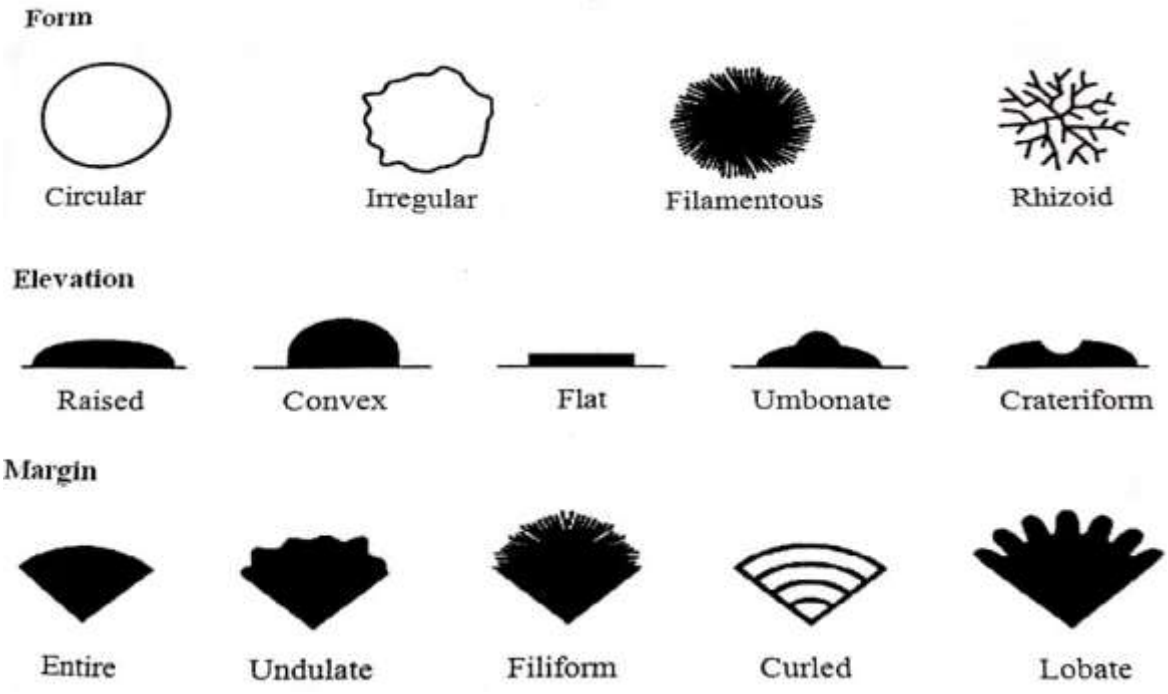

Figure 2.3: Morphological characteristics of fungi in petridish

2.7.2. Molecular identification

Molecular characterization of the endophytes was done by DNA amplification and sequencing of the internal transcribed spacer (ITS) region. Thus the species of the respective fungus can be obtained. Here ITS4 (5′-TCCGTAGGTGAACCTGCGG-3′) (Invitrogen, USA) was used as forward primer and as reverse primer ITS5 (5′- TCCTCCGCTTATTGATATGC-3′) (Invitrogen, USA) was used [White et al., 1990].

2.7.2.1. Fungal DNA extraction

Fungal DNA extraction was going through by using DNeasy Minikit (QIAgen, USA) as per manufacturer's protocol. In brief, glass beads were used to crush and break up the lyophilized fungal mycelia. After that, the cells were lysed using lysis buffer AP-1 and an RNAse-A

solution, which was then incubated at 65^0 C. The buffer AP1 acts as a cleanser to disintegrate the lipids surrounding the cellular membrane. The buffer also keep ups the right atmosphere for the DNA so it is not smashed up during the extraction process. So, buffer API plays a very significant role in the DNA extraction process. Buffer AP-2 was added to the lysate to precipitate the residual detergent, protein, and polysaccharide. The lysate was centrifuged and the cell debris and other precipitates were removed using the QIAshredder TM Mini Spin Column. For each sample different pipette tips were used. Next, a fresh tube was filled with the lysate. The lysate was mixed with a suitable amount of buffer AE and put on the DNeasy Mini Spin Column. Buffer AE elutes DNA from the membrane and allows constant storage of DNA. The filtrate was thrown away after centrifugation. The column was cleaned by adding an ethanolic buffer AW. To remove any remaining ethanol from the membrane in the column, more buffer AW was added and the centrifuge was set to its highest speed.

2.7.2.2. The amplification of DNA

The intended DNA sequence was then augmented by polymerase chain reaction (PCR) using Hot Star Taq Master Mix Kit (QIAgen, USA). For making a 50µL volume of PCR mixture 5-10 ng of genomic DNA, 1 µM each of the primers and 1 U of Hot Star Taq Polymerase were added. The mixture was then put into to the thermal cycler (BioRad, USA) for 35 cycles. Initial pre-heat was at 95°C for 2 minutes, then denaturing for 1 minute at 95°C, annealing for 40 seconds at 56°C, extension for 1 minute at 72°C and finally extension for 10 minutes at 72°C.

2.7.2.3. Purification of PCR products and DNA sequencing

To purify the PCR product agarose gel electrophoresis was used with perfect Prep Gel Cleanup Kit (Eppendorf, USA) as per the manufacturer's protocol. In brief, the electrophoresis was carried out at 75 V for 60 minutes. Ethidium bromide was then used to mark the gel. A 500 bp marked DNA fragment was then cut out from the agarose gel. The binding buffer was blended to the PCR product and sit on at 50° C for 10 minutes at 1000 rpm. A volume of isopropanol was added to the mixture and centrifuged. The filtrate was redundant and the column was washed with wash buffer twice followed by centrifugation. Amplified fungal DNA (PCR product) was eluted by addition of elution buffer. The filtrate (fungal DNA) dissolved in elution buffer was

then collected after centrifugation. The PCR product was sequenced on an ABI370X1 DNA analyzer (Applied Biosystems, USA).

2.7.3. Phylogenetic analysis

Phylogenetic analysis was done to understand the evolutionary relationship. Phylogenetic trees were constructed using MEGA-X software. The statistical method of maximum likelihood including 1000 bootstrap replications was thereafter followed.

2.8. Small scale cultivation of the pure endophytic fungi to produce secondary metabolites

Small scale cultivation was executed primarily to do bioassays for the detection of active metabolites. Fungi were cultured on Potato Dextrose Agar (PDA) medium. After completion of incubation process (28±2°C for ~21 to 28 days) ethyl acetate extractions from the culture medium were done (three times). Evaporation by a rotary evaporator condensed the fungal extracts into a solid residue.

2.9. Bioassay Procedures

The crude extracts of plants, their endophytic fungal crude extract, and isolated pure compounds were subjected to investigate bioactivity such as-

- Antioxidant test by DPPH free radical scavenging assay
- Antimicrobial test by disc diffusion method
- Cytotoxicity test by brine shrimp lethality bioassay
- Toxicity test in cell line

2.9.1. Antioxidant by DPPH free radical scavenging assay

The antioxidant activity of the samples was assayed by measuring the discoloration of a methanol solution of DPPH according to the standard protocol [Williams et. al., 1995]. DPPH methanol solution (20 µg /mL) was combined with samples/control, 2.0 mL of methanol solution at varied concentrations (200 µg /mL to 1.562 µg /mL). After a 30-minute reaction period at room temperature in the dark, the antioxidant potential was measured from the blanching of purple colored methanol solution of DPPH radical by the samples. The scavenging activity of

samples was calculated spectrophotometrically at 517 nm. The calculation was carried out in triplicate and the average value was taken. The scavenging ability was calculated as:

Scavenging ability (I%) = [(A– B/ A] × 100.

Where, A is the absorbance of blank (DPPH solution without sample) and B is the absorbance of sample solution (DPPH solution with sample or positive control).

Concentration of the sample required for 50% inhibition (IC_{50}) was measured by percent inhibition (I%) versus the concentration curve.

2.9.1. 1. Chemicals and instruments used for DPPH free radical scavenging assay

Chemicals and instruments for this experiment are given below.

Table 2.5: Chemicals and instruments used for DPPH free radical scavenging assay

Reagents & Chemicals	Instruments
1. Methanol 2. 0.02 µg/mL methanolic solution of DPPH 3. *tert*-Butylated hydroxy anisole (BHA), and Ascorbic acid (AA) 4. Distilled water.	1. Test tubes 2. Beakers 3. Vials 4. Micropipette 5. UV/VIS spectrophotometer (Analytik Jena AG, Germany) 6. Electronic balance

2.9.1. 2. Preparation of solutions

i) Standard and control preparation

As positive controls in the study BHA and AA were used. A mother solution containing 400 µg /mL of positive control (BHA, AA) was prepared by dissolving the calculated quantity in methanol. The concentration ranged from 200 to 1.562 µg/mL after serial dilution with the mother solution.

ii) Test sample preparation

Methanol was used to make 400 µg /mL mother solution from the calculated amounts of various samples. The concentration ranged from 200 to 1.562 µg/mL after serial dilution with the mother solution.

iii) DPPH solution preparation

A calculated amount of DPPH was weighed and dissolved in methanol to get a DPPH solution to get a concentration of 20 µg/mL. The amber reagent bottle was used to make the solution and placed the solution in a dark place.

2.9.2. Antimicrobial test by disc diffusion method

The antimicrobial activities were screened by the disc diffusion method [Alzoreky & Nakahara, 2003; Rios JL et. al., 1988]. The microorganisms in this antimicrobial study included two gram-positive pathogenic bacterial strains *Bacillus megaterium* (ATCC 28318) and *Staphylococcus aureus* (ATCC 25923), three gram-negative pathogenic bacterial strains *Escherichia coli* (ATCC 28739), *Pseudomonas aeruginosa* (ATCC 27833) and *Salmonella typhi* (ATCC 13311) and three fungal strains *Aspergillus niger, Aspergillus flavus* and *Candida albicans*. Here, ATCC stands for American Type Culture Collection. The bacterial strains were collected as pure cultures from the Institute of Nutrition and Food Science (INFS), University of Dhaka. Samples were measured and dissolved in a determined volume of solvents to produce solutions with known concentrations (mg/mL) of the test samples. Using a micropipette and a dried and disinfected filter paper disc (5 mm in diameter), known concentrations of the tested samples were then permeated. The test microorganisms were evenly planted on medium (NA and PDA) onto discs holding the test substance. To ensure maximal diffusion, the plates were incubated at 37°C (for bacteria) and 25°C (for fungus) for a period of 24 hours. After the incubation period a distinct inhibition zone encircling the medium can be observed if the tested sample has antimicrobial activity. The zone of inhibition's diameter (given in mm) was used to measure the antibacterial activity of the test agent using a visible scale.

2.9.2.1. Chemicals and instruments used for antibacterial test

Chemicals and instruments used for this experiment are given below.

Table 2.6: Chemicals and instruments used for antibacterial test assay

Reagents & Chemicals	Instruments
1. Nutrient Agar Medium (NA) 2. Potato Dextrose Agar Medium (PDA) 3. Methylene chloride (CH_2Cl_2)/ Chloroform 4. Ethanol 5. Methanol	1. Filter paper discs 2. Sterile forceps 3. Petri dishes 4. Micropipette 5. Sterile cotton 6. Inoculating loop 7. Spirit burner 8. Autoclave 9. Laminar air flow hood 10. Refrigerator 11. Incubator 12. Nose mask and Hand gloves

2.9.2.2. Sterilization

The antimicrobial screening was done in a Laminar Hood to prevent any kind of contamination by the test organisms. An hour before working in the Laminar Hood, the UV light was turned on. Glassware, including Petri dishes, was subjected to an autoclaving process for 20 min at 121°C and 15 pounds per square inch of pressure. Sterilized items included blank discs, cotton, forceps, and tips for micropipettes.

2.9.2.3. Medium Preparation

The required volume medium was prepared by taking a calculated amount of each of the constituents and distilled water in a conical flask. The pH (at 25 °C) was adjusted using NaOH or HCl. 10 to 15 ml of the medium was then shifted to screw cap test tubes for preparing plates and 5 ml was taken to test tubes for using in fresh pure culture preparation. The test tubes were then capped and sterilized by autoclaving for 20 minutes at 121°C and 15 pounds per square inch of pressure. The compositions of PDA (Table 2.7) and NA (Table 2.8) media are given below.

Table 2.7: Constituents of potato dextrose agar medium (PDA)

Ingredients	Amount (g/L)
Potato extract	4.0
Dextrose	20.0
Agar	15.0

Table 2.8: Constituents of nutrient agar medium (NA)

Ingredients	Amount (g/L)
Peptone	5.0
Sodium chloride	5.0
Beef extract	1.5
Yeast extract	1.5
Agar	15.0

2.9.2.4. Subculture preparation

The test organisms were transported from the pure cultures to the agar test tubes with the help of a transfer loop for obtaining fresh pure cultures. The whole process was done under laminar air cabinet where aseptic condition is maintained. The inoculated bacterial and fungal strains were then incubated for 24 h at 37 and 25 °C respectively for their optimum growth. These fresh cultures were used for the test.

2.9.2.5. Test plates preparation

Using a sterilized transfer loop in an aseptic environment, the test organisms were moved from the subculture into test tubes holding roughly 10 mL of sterile agar material. To ensure that the organisms were suspended uniformly, the test tubes were shaken by rotation. The sterilized petri dishes were promptly filled with the bacterial suspension. Clockwise and anticlockwise rotations of the petri dishes were performed to ensure that the test organisms were distributed uniformly throughout the medium.

2.9.2.6. Disc preparation

Three types of discs were used for antimicrobial screening:

i) Standard discs

ii) Blank discs

iii) Tested sample discs

i) Standard discs

These were used as positive control to ensure the activity of the standard antibiotic against the test organisms. They were also needed for comparison of the response produced by the known antibacterial agent with that of produced by the test samples. In this experiment, kanamycin (30 µg/disc) and ketoconazole (30 µg/disc) standard discs were used as the antibacterial and antifungal reference.

ii) Blank discs

These were used as negative control which ensures that the left over solvents (left over the discs even after air-drying) and the filter paper were inactive themselves.

iii) Tested sample discs

Depending on the nature of the tested samples (1 mg for pure compound; 2 mg for fungal crude extracts and column fractions; 4 mg for plant crude extracts) they were dissolved with 100 µL

CH_2Cl_2/methanol to obtain the 0.01, 0.02 or 0.04 mg/µL concentration. Then discs were soaked with the 10 µL, 20 µL or 40 µL solutions of the tested samples and dried. Therefore, the concentration for the tested samples can be 100 µg /disc, 200 µg /disc or 400 µg/disc.

2.9.2.7. Diffusion and Incubation

All the discs were placed smoothly on the previously marked zones in the agar plates pre-inoculated with test microorganisms. The plates were then placed in a refrigerator at 4°C for about 24 h to allow sufficient diffusion of the materials from the discs to the surrounding agar medium. The bacterial plates were then inverted and kept in a biological incubator at 37 °C and fungal plates were kept at 25°C in a BOD incubator for 24 h.

2.9.3. Cytotoxicity test by brine shrimp lethality bioassay

The broad toxicity of samples (usually crude extracts) was evaluated by the brine shrimp lethality bioassay test. Brine shrimp eggs were hatched for 24 h in pretend sea water to get nauplii. LC_{50} values were screened against varying concentrations (200-1.562 µg/mL) of fungal extracts in dimethyl sulphoxide (DMSO) obtained by the serial dilution method [Nasrin, et. al., 2019]. The nauplii were calculated by visual observation and were taken in vials containing 5 mL of simulated seawater. Then samples of diverse concentrations were added to the pre-marked vials. The vials were then left for 24 h and the nauplii were counted again using a magnifying glass and the number of surviving nauplii in each vial was counted. The percent (%) of mortality was calculated for each concentration. The median lethal concentration (LC_{50}) of the test agents was determined as the percentage of the shrimp mortality against the logarithm of the sample concentrations.

2.9.3.1. Chemicals and instruments used for brine shrimp lethality bioassay

Chemicals and instruments required for the test are given below.

Table 2.9: Chemicals and instruments used for brine shrimp lethality bioassay

Reagents & Chemicals	Instruments
1. *Artemia salina* leach (brine shrimp eggs) 2. Dimethyl sulfoxide (DMSO) 3. Sea salt (NaCl) 4. Distilled water.	1. A lamp to attract shrimps 2. Pipettes (5 and 25 mL) 3. Micropipette 4. Small tank with a perforated dividing dam to hatch the shrimp 5. Glass vials/test tubes 6. Magnifying glass

2.9.3.2. Seawater Preparation

A transparent solution was obtained by weighing 38 g of sea salt (pure NaCl), dissolving it in one liter of distilled water, and then filtering it off. The purpose of this artificial seawater was to birth brine prawns.

2.9.3.3. Hatching of Brine Shrimps

Eggs of the test organism, *Artemia salinal* leach, were purchased from pet stores. A split tank with holes on one side was filled with simulated saltwater and covered after the shrimp eggs were positioned on that side. The prawns in the tank required 48 h to hatch and develop into nauplii (larvae). An oxygen supply was maintained at all times in the hatching process. The hatchlings were pulled towards the lamp through the perforated dam and 10 living shrimps were added with the help of a Pasture pipette to each of the test tubes containing 5 mL of Brine solution.

2.9.3.4. Test solutions preparation

i) For plants extracts

An amount of 4 mg extracts were measured and dissolved in 60 µL DMSO. A series of solutions of lower concentrations were prepared by serial dilution with DMSO. From each of these test solutions 30 µL were added to pre-marked glass vials/test tubes containing seawater and 10 shrimp nauplii. The volume was then adjusted to 5 mL. So, the final concentrations of samples in the test tubes were 400, 200, 100, 50, 25, 12.5, 6.25, 3.125, 1.5625 and 0.7815 µg /mL.

ii) For fungal extracts

Unlike 4 mg used for plant extracts here 2 mg extracts were measured. The rest of the procedures were the same as described in 2.9.3.4 (i). Lastly the final concentrations of samples in the test tubes were 200, 100, 50, 25, 12.5, 6.25, 3.125, 1.5625, 0.7815 and 0.39062 µg /mL.

2.9.3.5. Positive control preparation

The positive control used in this study was tamoxifen. Tamoxifen 0.2 mg was dissolved in DMSO, and the same solvent was used to create successive dilutions, yielding an initial concentration of 40 µg /mL. The positive control solutions were given to the groups that included 10 live brine shrimp nauplii in 5 mL of simulated seawater.

2.9.3.6. Negative control preparation

30 µL of DMSO was used as a negative control in each of the two pre-marked test tubes that held 10 shrimp nauplii and 5 mL of simulated seawater. If the negative control demonstrated a high death rate, the test was deemed invalid and was rerun.

2.9.4. Toxicity test in cell line

Along with other biological activity described above the toxicity test in cell line culture was carried out with isolated pure compounds from crude extracts of the plants and the endophytic fungi to evaluate whether these molecules are solely responsible for the activity of crude extracts as well as potential lead compound.

2.9.4.1. Toxicity test in lung cancer cell line

The cytotoxicity of isolated pure compounds was assessed against the A-549 lung cancer cell line using the Trypan Blue Exclusion Method [Strober, 2015].

2.9.4.1.1. Chemicals and instruments used for toxicity test in lung cancer cell line

The required chemicals and instruments for the test are given below.

Table 2.10: Chemicals and instruments used for toxicity test in lung cancer cell line

Reagents & Chemicals	Instruments
1. 10% (v/v) fetal bovine serum (FBS) 2. 1% penicillin (100 U/mL) 3. Dulbecco's Modified Eagle's Medium (DMEM) 4. 5% CO_2 (pH 7.4) 5. Phosphate-buffered saline (PBS) 6. Dimethyl sulfoxide (DMSO) 7. HEPES 8. EDTA 9. Trypan blue	1. Biological safety cabinet 2. CO_2 incubator 3. Microscope 4. Hemocytometer 5. Pipettes, Micropipette

2.9.4.1.2. Culture of lung cancer cell line

The cells were grown in sterile 75cm^2 flasks using Dulbecco's Modified Eagles Medium (DMEM), which was supplemented with 10% (v/v) foetal bovine serum (FBS), 1% penicillin(100 U/mL), and 25mM HEPES. Subculture of the cells was done to another 75cm^2 flask once per week under sterile condition. After removing culture medium, cells were washed with phosphate buffered saline (PBS) for 3 times, then 1.0 mL of trypsin (0.25% w/v) plus 0.5 mL EDTA (1 mM) was added and it was left for 2-4 min at 37^{o}C for detaching cells. After detaching cells 9.0 mL of fresh DMEM was added and the cells were re-suspended by pipetting

ups and downs. Lastly, 2 mL of the suspension was transferred to another flask containing 8.0 mL of fresh DMEM. The cells were used for 25-30 passages preserving the morphological /functional characteristics of the cellular line. The composition of PBS is given below (Table 2.11).

Table 2.11: Composition of phosphate buffer saline (PBS)

Ingredients	Conc. (mmol/L)
NaCl	136
KCl	4.7
Na_2HPO_4	3.2
KH_2PO_4	1.3
NaOH (P^H adjusted to)	7.4

2.9.4.1.3. Preparation of tested sample

Stock solutions in DMSO (1.0 mg/mL) were made using the test samples. Filter sterilization was used to sanitize this solution before to administration.

2.9.4.1.4. Incubations for cytotoxic test

Each treatment involved the division of cells into three groups based on the experimental design, with each group having three replicas. The treatment groups were compared to the control group. Prior to the studies, the cells were divided and 2.5×10^6 cells were cultivated in a T-25 flask. The doses that had been manufactured were administered into T-25 cell culture flasks that were 1-day old. The doses were prepared immediately prior to use. The flasks were placed in an incubator for 24 h.

2.9.4.1.5. Measurement of cell viability

After incubation cells were collected using trypsin and a 1.0 mL cell solution was obtained for the purpose of cell counting. The quantification of live cells was conducted by the utilization of trypan blue and a hemocytometer. The surface of the haemocytometer was treated with two drops of cell suspension with 0.4% w/v trypan blue (1:1). The number of viable cells (unstained)

and non-viable cells (stained) were then counted. The calculation of cell death was performed by determining the proportion of dead cells using the following method:

$$\%\,\text{Dead cells} = \frac{\text{no. of stained (dead cells)}}{\text{Total number of cells}} \times 100$$

2.9.4.2. Toxicity test in HeLa and BHK-21 cell line (qualitative and quantitative analysis)

The tests were performed by using a human cervical carcinoma cell line (HeLa) and a baby hamster kidney fibroblast cell line (BHK-21). The quantitative analysis was done by MTT (Microculture tetrazolium) assay.

2.9.4.2.1. Chemicals, consumables and instruments used for toxicity test in HeLa and BHK-21 cell line

The required chemicals and other things for the experiment are given below.

Table 2.12: Chemicals, consumables and instruments used for toxicity test in HeLa and BHK-21 cell line

Reagents & Chemicals	Instruments
1. 10% (v/v) fetal bovine serum (FBS) 2. 1% penicillin-streptomycin (1:1) 3. Dulbecco's Modified Eagle's Medium (DMEM) 4. 5% CO_2 (pH 7.4) 5. Phosphate-buffered saline (PBS) 6. Dimethyl sulfoxide (DMSO) 7. Trypsin 8. Gentamycin 9. Cell culture media	1. Biological bio safety cabinet (Model: NU-400E, Nuaire, USA) 2. CO_2 incubator (Nuaire, USA) 3. Trinocular microscope with camera (Optika, Italy) 4. Hemocytometer 5. 96-well plate 6. 15-ml tubes 7. Culture flasks 8. Tips, Gloves

2.9.4.2.2. Experimental procedure

In brief, cell lines were maintained in Dulbecco's Modified Eagles Medium (DMEM) containing 1% penicillin-streptomycin (1:1) and 0.2% gentamycin and 10% (v/v) fetal bovine serum (FBS). HeLa cells ($2x10^4$/100 µL) and BHK-21 cells ($1.5x10^4$/100 µl) were seeded onto a 48-well plate and incubated at 37^0C+ 5% CO_2. The next day, 25 µL of sample (filtered) was added into each well. Cytotoxicity was examined under an inverted light microscope after 48 h of incubation. Duplicate cells were used for each sample. For quantitative analysis cell viability was checked after 48 h of incubation using the Cell Titer 96 Non-Radioactive Cell Proliferation Assay Kit (Promega, USA). Also, duplicate cells were used for each sample.

2.9.4.3. Computational study

Based on cytotoxicity test results of isolated compounds network pharmacology-based approach in combination with molecular docking analysis was analyzed to identify its multiple targets which may contribute to its pharmacological action [Chandran et. al., 2017]. Network pharmacological method revealed the most prevalent targets identified by Cytoscape analysis. The docking interaction was studied using PyRx software. The interaction between protein-ligand was visualized using Biovia Discovery Studio version 2021.

2.10. Large-scale cultivation of selected endophytic fungi

To generate crude fungal extracts at an up-scale amount, chosen endophytes are often grown on a large scale based on chemical screening and bioactivity (*in vitro*). Here internal strain no. CLRE-3 (*Clonostachys rosea*) and ZOLE-2 (*Cladosporium cladosporoide*) were chosen for large-scale cultivation. The taxonomy of fungi *Clonostachys rosea* and *Cladosporium cladosporoides* are given below:

Taxonomy of *Clonostachys rosea*

Kingdom: Fungi
Division: Ascomycota
Class: Sordariomycetes
Order: Hypocreales
Family: Bionectriaceae
Genus: *Clonostachys*
Species: *Clonostachys rosea*

Taxonomy of *Cladosporium cladosporoides*

Kingdom: Fungi
Division: Ascomycota
Subdivision: Pezizomycotina
Class: Dothideomycetes
Order: Capnodiales
Genus: *Cladosporium*
Species: *Cladosporium cladosporoides*

2.10.1. Chromatographic fractionation of endophytic fungal extract CLRE-3 from the plant *C. longa*

The crude extract (1.89 g) was fractionated on a silica gel (Kieselgel 60, 70–230 mesh) by column chromatography employing gradients of n-hexane/CH_2Cl_2, CH_2Cl_2, CH_2Cl_2/methanol, and methanol. For additional purification, a total of 47 fractions of 100 mL each were collected and combined into 15 fractions based on their TLC patterns. Solvent systems used as mobile phases in column chromatography are listed in Table 2.13.

Table 2.13: Different solvent systems used for column analysis of fungal extract from *C. longa*

Fraction no.	Solvent systems	Fraction no.	Solvent systems
1	n-hexane/35-50% CH_2Cl_2	9	CH_2Cl_2/ 1.5-2% MeOH
2	n-hexane /55% CH_2Cl_2	10	CH_2Cl_2/ 2-4% MeOH
3	n-hexane / 60-85 % CH_2Cl_2	11	CH_2Cl_2/5% MeOH
4	n-hexane / 90-95% CH_2Cl_2	12	CH_2Cl_2/5-10% MeOH
5	n-hexane / 100% CH_2Cl_2	13	CH_2Cl_2/15% MeOH
6	CH_2Cl_2/ 0.1-0.2% MeOH	14	CH_2Cl_2/20% MeOH
7	CH_2Cl_2 / 0.3-0.4% MeOH	15	100% MeOH
8	CH_2Cl_2/ 0.4-1.5% MeOH		

2.10.1.1. Analysis of VLC fractions by TLC

All the column fractions were tested using TLC screening under UV light and spraying with vanillin-sulfuric acid reagent.

2.10.1.2. Isolation of compounds from column fractions

Various techniques such as sub-column chromatography, PTLC have been used to separate and purify a variety of chemicals from the column fractions of CLRE-3.

a) Isolation of compound CLE-7

Sub-column chromatography was done with the column fraction 3 (n-hexane / 60-85 % CH_2Cl_2). Bassiatin (CLE-7) was extracted from the n-hexane/10-15% CH_2Cl_2 fraction of this sub-column and eventually obtained in pure form following solvent treatment with methanol.

b) Isolation of compound CLE-14

Sub-column chromatography was done with the column fraction 3 (n-hexane / 60-85 % CH_2Cl_2). Based on the TLC pattern (Ch_2Cl_2/12.5% ethyl acetate to ethyl acetate/4% MeOH) was mixed. This mixed fraction was then subjected to PTLC (toluene/20% ethyl acetate). Nectriafurone (CLE-14) was extracted from the TLC plate using various solvents.

c) Isolation of compound CLE-11

PTLC (chloroform/0.1% MeOH) was done with the column fraction 11 (CH_2Cl_2/5% MeOH). 8-O-methyl nectriafurone (CLE-11) was extracted from TLC plate using various solvent.

d) Isolation of compound CLE-18(2)

PTLC (chloroform/0.1% MeOH) was done with the column fraction 11 (CH_2Cl_2/5% MeOH). 8-O methyl bostrycoidin (CLE-18(2)) was extracted from TLC plate using various solvent.

2.10.2. Chromatographic fractionation of endophytic fungal extract ZOLE-2 from the plant *Z. officinale*

The crude extract (2 g) was fractionated on a silica gel (Kieselgel 60, 70–230 mesh) by column chromatography employing gradients of n-hexane/CH_2Cl_2, CH_2Cl_2, CH_2Cl_2/methanol, and methanol. For additional purification, a total of 39 fractions of 100 mL each were collected and combined into 16 fractions based on their TLC patterns. Solvent systems used as mobile phases in the column chromatography are listed in Table 2.14.

Table 2.14: Different solvent systems used for column analysis of fungal extract from Z. *officinale*

Fraction no.	Solvent systems	Fraction no.	Solvent systems
1	n-hexane/7.5-17.5% CH_2Cl_2	9	CH_2Cl_2/ 85-95% CH_2Cl_2
2	n-hexane /20% CH_2Cl_2	10	CH_2Cl_2/ 100% MeOH
3	n-hexane / 22.5 % CH_2Cl_2	11	CH_2Cl_2/0.1-0.5% MeOH
4	n-hexane / 22.5% CH_2Cl_2	12	CH_2Cl_2/0.7-0.9% MeOH
5	n-hexane / 25-40% CH_2Cl_2	13	CH_2Cl_2/1.2-2% MeOH
6	CH_2Cl_2/ 45-55% CH_2Cl_2	14	CH_2Cl_2/5-7% MeOH
7	CH_2Cl_2 / 60-65% CH_2Cl_2	15	CH_2Cl_2/10-20% MeOH
8	CH_2Cl_2/ 70-80% CH_2Cl_2	16	100% MeOH

2.10.2.1. Analysis of VLC fractions by TLC

All the column fractions were tested using TLC screening under UV light and spraying with vanillin-sulfuric acid reagent.

2.10.2.2. Isolation of compounds from column fractions

a) Isolation of compound ZOE-1

Ergosterol (ZOE-1) was extracted from column fraction 3 (n-hexane / 22.5 % CH_2Cl_2) by solvent treatment with methanol and n-hexane.

b) Isolation of compound ZOE-6

Sub-column chromatography was done with the column fraction 14 (CH_2Cl_2/5-7% MeOH). Based on the TLC pattern (CH_2Cl_2/1.8% MeOH to CH_2Cl_2/2.4% MeOH) was mixed. This mixed

fraction was then subjected to PTLC (Chloroform/6% MeOH). ZOE-6 was extracted from TLC plate using various solvents.

Chapter 3
RESULTS AND DISCUSSION

RESULTS AND DISCUSSION

This chapter is designed to discuss the following results elaborately:

- Identification of compounds obtained from plant extracts through GC-MS
- Identification of endophytic fungi isolated from *C. longa* and *Z. officinale* plants through morphological and molecular methods
- Chromatographic screening of the plant and fungal extracts in TLC plates by visual/UV detection and spray reagents
- Structure elucidation of metabolites isolated from plants and endophytic fungi were done by different spectrophotometric techniques (UV, 1D and 2D NMR)
- Bioassay of the crude extracts (plants and fungi) and isolated pure compounds

3.1. Identification of compounds obtained from plant extracts through GC-MS

The mass spectra analysis revealed 27 peaks and 21 peaks that correspond to the presence of 27 and 21 major compounds from the two plants *C. longa* and *Z. officinale* respectively.

The results of the GC-MS of of *Curcuma longa* are presented in Figure 3.1 and in Table 3.1.

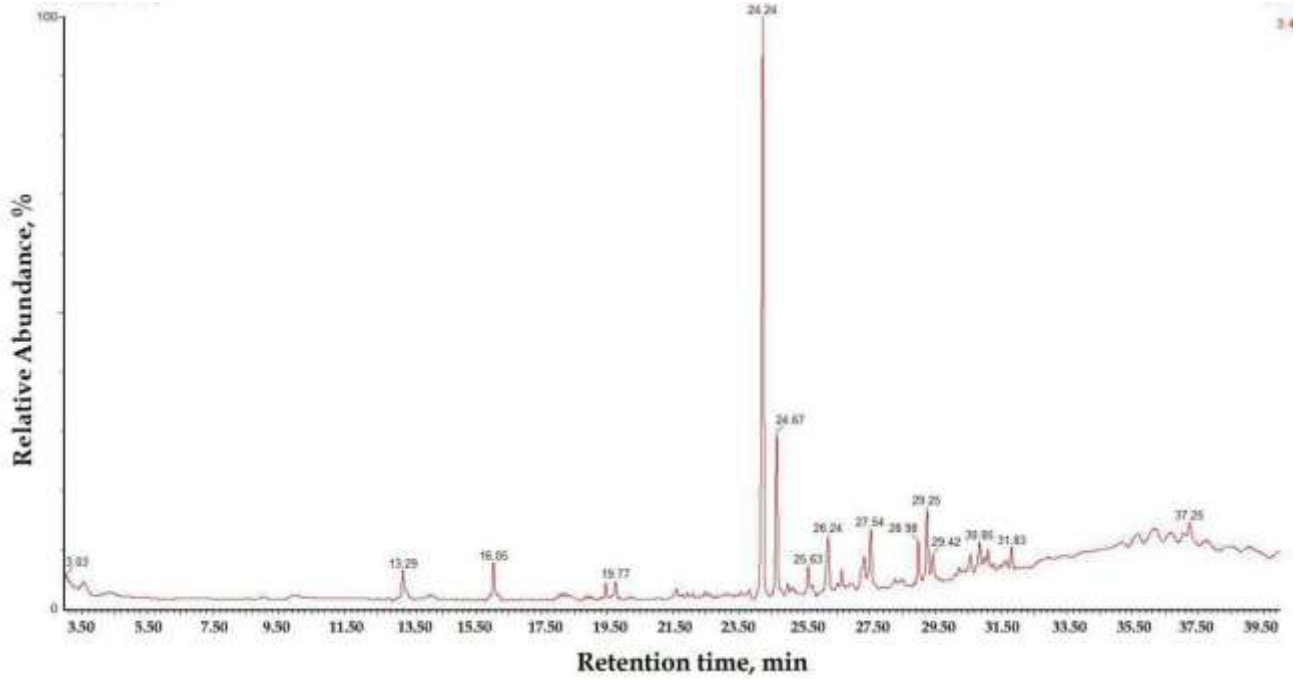

Figure 3.1: GC-MS Chromatogram of methanolic extract of *C. longa* rhizomes

Table 3.1: Phytochemical compounds of methanol extract of *Curcuma longa* via GC-MS

Peak	RT	Peak Area %	Molecular Weight	Molecular Formula	Name of compound	Structure	Compound type
1	8.10	0.22	262	$C_{14}H_{27}O_2Cl$	Chloroacetic acid, Dodecyl ester	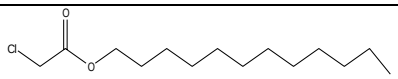	Fatty acid
2	13.29	1.61	120	C_8H_8O	Bezofuran, 2,3-dihydro	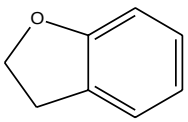	Heterocyclic
3	14.09	0.83	218	$C_{11}H_{22}O_2S$	Trans-2-Methyl-4-N-Pentylthiane,S,S,dioxide	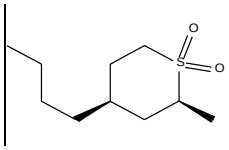	Heterocyclic

4	16.04	1.57	150	$C_9H_{10}O_2$	2-Methoxy-4-Vinyl Phenol	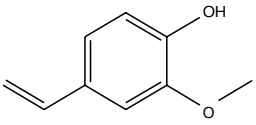	Phenolic
5	18.09	0.33	212	$C_{10}H_9O_3Cl$	4-formylphenyl-3-chloropropanoate	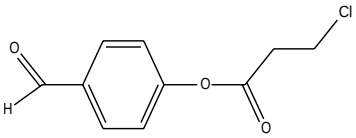	Phenolic
6	18.22	0.59	204	$C_{15}H_{24}$	2-methyl-5-((R)-6-methylhept-5-en-2-yl)bicyclo[3.1.0]hex-2-ene	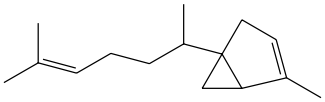	Sesquiterpene
7	19.47	0.37	152	$C_8H_8O_3$	Vanillin	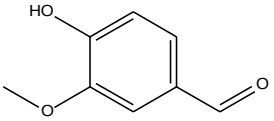	Phenolic
8	19.75	0.54	206	$C_{14}H_{22}O$	2,4-Di-tert-Butyl Phenol	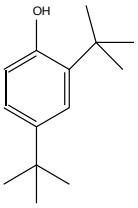	Phenolic
9	20.20	0.18	362	$C_{21}H_{30}O_{3S}$	(2E,6E)3,7,11-trimethyl-9-(phenylsulfinyl)dodeca-2,6,10-trien-1-ol	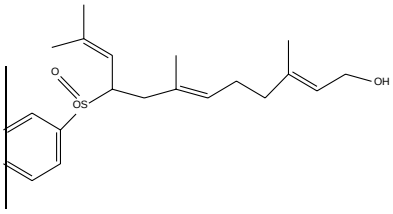	Sesquiterpene
10	21.95	0.08	182	$C_9H_{10}O_4$	Benzoic acid, 4-hydroxy-3-Methoxy- Methyl ester	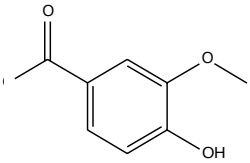	Phenolic
11	22.11	0.08	204	$C_{15}H_{24}$	(1R,4AR,8AR)-2,5,5,8a-tetramethyl-4,5,6,7,8,8a-Hexahydro-1H-	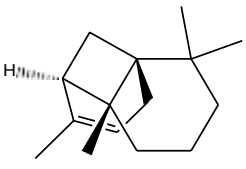	Selinane

					1,4a-methanonaphthalene		
12	22.48	0.19	220	$C_{15}H_{24}O$	2-(4a,8-dimethyl-1,2,3,4,4a,5,6,8a-octahydronaphthalen-2-yl)prop-2-en-1-ol	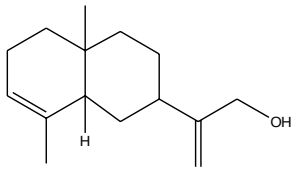	Selinane
13	23.58	0.37	180	$C_{10}H_{12}O_3$	Cyclohexadien-4-one-1-Propiolic acid, Methyl ester	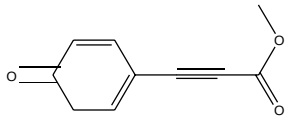	Phenolic
14	23.83	0.36	218	$C_{15}H_{22}O$	Tumerone	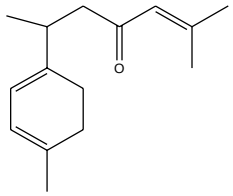	Bisabolane
15	24.25	4.71	216	$C_{15}H_{20}O$	ar- Turmerone	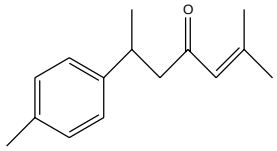	Bisabolane
16	24.67	0.31	218	$C_{15}H_{22}O$	2-Methyl-6-(4-Methylene Cyclohex-2-en-1-yl) Hept-2-en-4-one	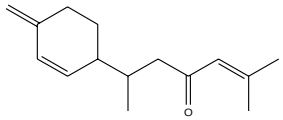	Bisabolane
17	26.23	2.31	218	$C_{15}H_{22}O$	E-Atlantone	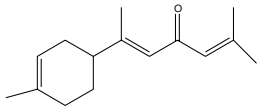	Bisabolane
18	26.65	0.78	372	$C_{16}H_{22}Br_2$	P-Menthane,2,3-Dibromo-8-Phenyl-	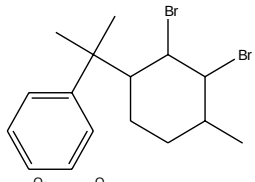	Monoterpenoid
19	27.53	2.04	178	$C_{10}H_{10}O_3$	(E)-methyl 3-(3-hydroxyphenyl)acrylate	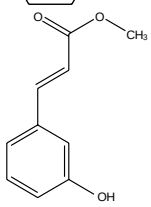	Phenylpropene

20	28.99	1.26	192	$C_{11}H_{12}O_3$	(E)-4-(4-hydroxy-3-methoxyphenyl)but-3-en-2-one	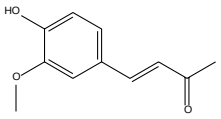	Phenylpropene
21	29.25	2.46	208	$C_{11}H_{12}O_4$	(E)-methyl 3-(4-hydroxy-3methoxyphenyl) acrylate	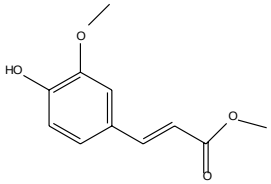	Phenylpropene
22	29.42	1.09	136	$C_9H_{12}O$	(2,5 dimethylphenyl) methanol	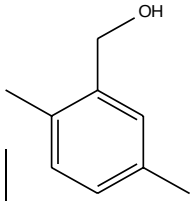	Phenolic
23	30.23	0.43	138	$C_{10}H_{18}$	Napthalene, Decahydro-	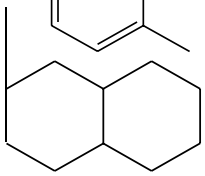	Selinane
24	30.57	1.17	304	$C_{19}H_{28}O_3$	1-(4-hydroxy-3-Methoxy Phenyl) Dodec-4-en-3-one	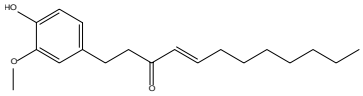	Bisabolane
25	30.85	1.30	232	$C_{15}H_{20}O_2$	6-(3-hydroxy-4-Methyl Phenyl)-2-MethylHept-2-en-4-one	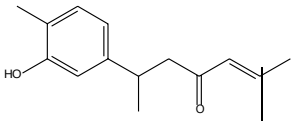	Bisabolane
26	31.83	0.53	218	$C_{15}H_{22}O$	(E)-Gamma-Atlantone	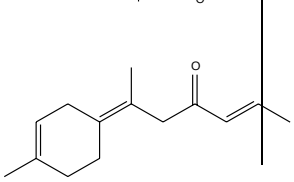	Bisabolane
27	37.25	5.93	281	$C_{18}H_{35}ON$	9-Octadecenamide,(Z)-	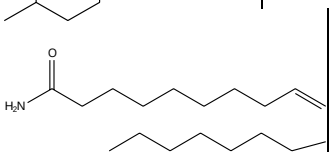	Fatty acid

Among 27 phytochemical compounds identified from the rhizome methanolic extracts of *C. longa* through GC-MS the most abundant component was 9-octadecenamide (Z) (5.93%). The component present in the lowest amount was 4-hydroxy-3-methoxy benzoic acid methyl ester (0.08%).

The results of the GC-MS of *Zinger officinale* are presented in Figure 3.2 and in Table 3.2.

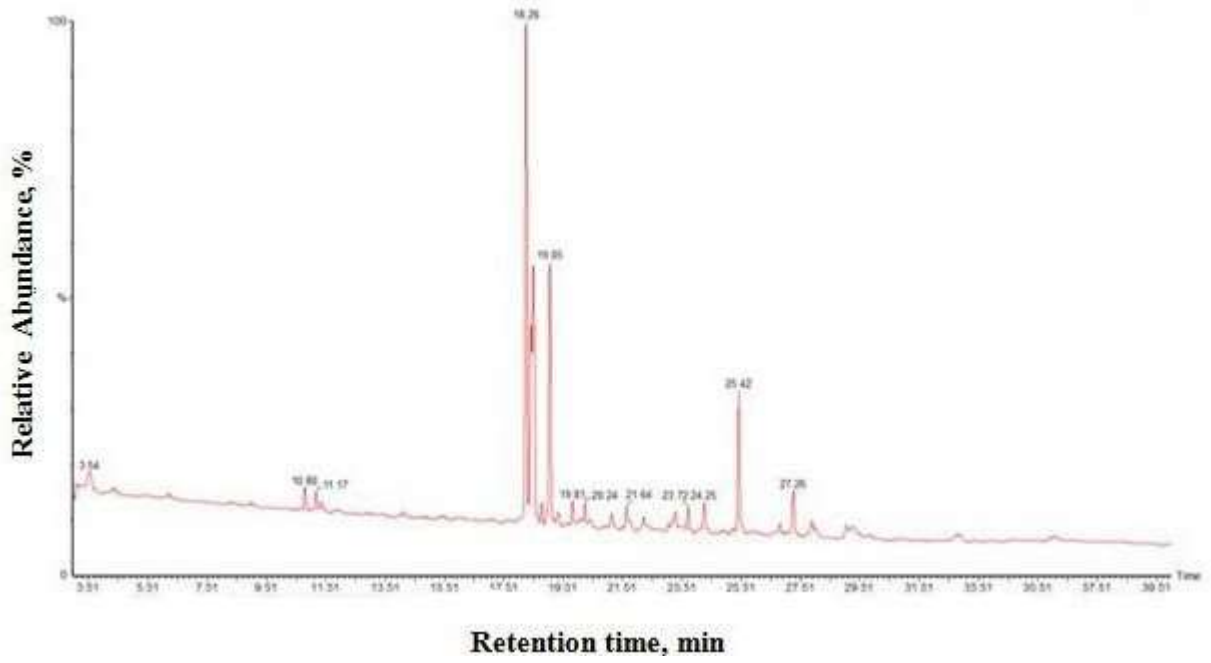

Figure 3.2: GC-MS Chromatogram of methanolic extract of *Z. officinale* rhizomes

Table 3.2: Phytochemical compounds of methanol extract of *Z. officinale* via GC-MS

Peak	RT	Peak Area %	Molecular Weight	Molecular Formula	Name of compound	Structure	Compound type
1	4.36	0.77	386	$C_{18}H_{37}Cl_3Si$	Silane,trichlorooctadecyl	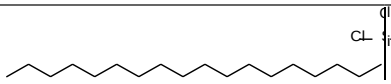	organosilicon
2	6.21	0.60	84	C_4H_8Si	1-Silacyclo-3-pentene	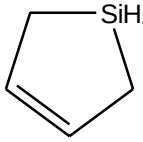	Unsaturated hydrocarbon
3	8.99	0.37	262	$C_{14}H_{27}O_2Cl$	Chloroacetic acid, Dodecyl ester	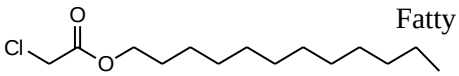	Fatty acid

4	10.80	0.99	154	$C_{10}H_{18}O$	1,7,7-trimethylbicyclo[2.2.1]heptan-2-ol	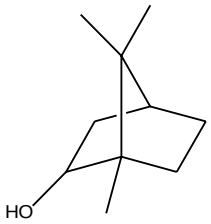	bicyclic monoterpenoids
5	11.17	0.90	156	$C_{10}H_{20}O$	Decanal	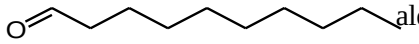	aldehyde
6	11.37	0.61	154	$C_{10}H_{18}O$	4,7,7-trimethylbicyclo[4.1.0]heptan-3-ol	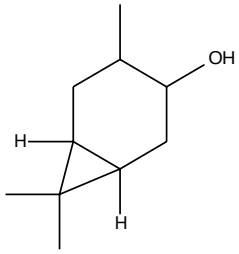	bicyclic monoterpenoids
7	18.26	19.45	204	$C_{15}H_{24}$	2-methyl-5-((R)-6-methylhept-5-en-2-yl)bicycle[3.1.0]hex-2-ene	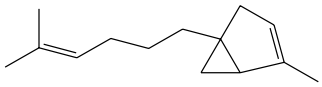	sesquithujene
8	18.49	18.97	204	$C_{15}H_{24}$	Beta-Bourbonene	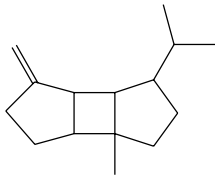	sesquiterpenoids
9	19.05	10.52	204	$C_{15}H_{24}$	3-methylene-6-(6-methylhept-5-en-2-yl)cyclohex-1-ene	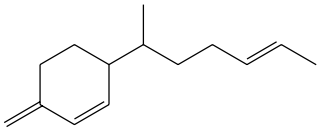	sesquiphellandrene

10	19.81	1.15	206	$C_{14}H_{22}O$	2,4-Di-tert-Butyl Phenol	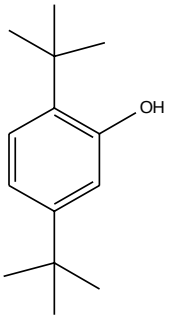	phenylpropanes
11	20.24	1.83	282	$C_{17}H_{30}O_3$	(E)-3,3,7,11-tetramethyldodeca-6,10-dienyl acetate	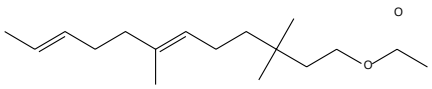	Farnesyl acetate
12	21.15	0.97	204	$C_{15}H_{24}$	Cis-Thujopsene	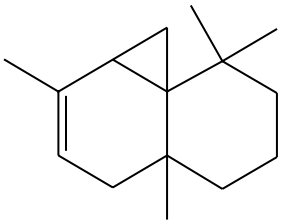	sesquiterpene
13	21.64	1.72	222	$C_{15}H_{26}O$	1,4-dimethyl-4-(6-methylhept-5-en-2-yl) cyclohex-2-enol	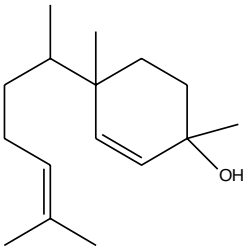	sesquiterpenoid
14	23.29	1.34	222	$C_{15}H_{26}O$	2-(4a-methyl-8-methylene-decahydronaphthalen-2-yl)propan-2-ol	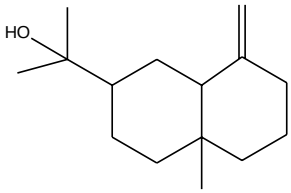	Eudesmane sesquiterpenoid
15	23.72	0.82	204	$C_{15}H_{24}$	(1R,3aS,4aS,8aS)-1,4,4,6-Tetramethyl-1,2,3,3a,4,4a,7,8-octahydro cyclopenta[1,4]cyclobuta[1,2]benzene	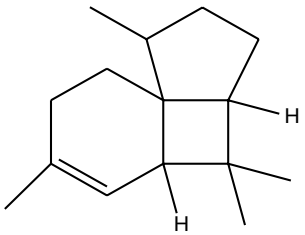	Italicene

16	24.26	2.11	272	$C_{20}H_{32}$	(E)-1-(6,10-dimethylundec-5-en-2-yl)-4-methylbenzene	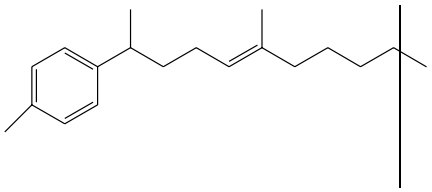	pentylcurcumene
17	25.42	6.43	194	$C_{11}H_{14}O_3$	2-Butanone, 4-(4-hydroxy-3-methoxyphenyl)	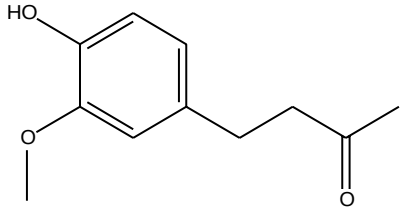	oxygenated hydrocarbon
18	27.26	3.03	222	$C_{15}H_{26}O$	(2,2-dimethyl-4-(3-methylbut-2-enyl)-6-methylenecyclohexyl) methanol	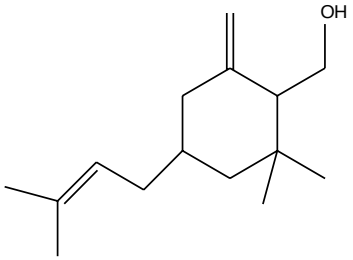	sesquiterpenoids
19	27.89	2.02	270	$C_{17}H_{34}O_2$	Methyl 10,13-dimethyltetradecanoate	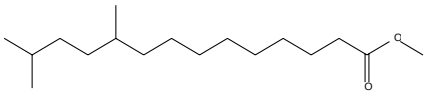	fatty acid methy l ester
20	29.06	0.83	426	$C_{30}H_{50}O$	9,19-cyclolanost-24-en-3-ol,3 beta	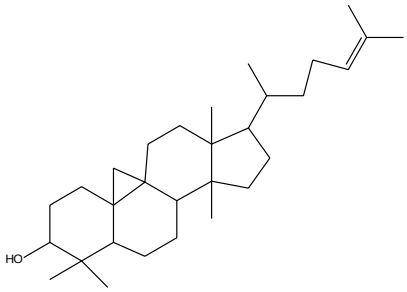	steroids
21	32.81	1.30	222	$C_{15}H_{26}O$	2H-3,9a-Methano-1-benzoxepin, octahydro-2,2,5a,9-tetramethyl-, [3R-(3a,5aa,9a,9aa)]	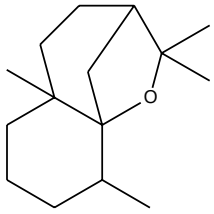	dihydroagarofuran

The most plentiful component was 2-methyl-5-((R)-6-methylhept-5-en-2-yl) bicycle[3.1.0] hex-2-ene (19.45%) and the component present in the lowest amount was Chloroacetic acid, Dodecyl ester (0.37%) among 21 phytochemical compounds identified from rhizome of *Z. officinale* through GC-MS. The comparative phytochemical analysis and their established biological activity of some components identified in these two plants through GC-MS are given in Table 3.3.

Table 3.3: Comparative phytochemical analysis and their biological activity

Serial no.	Name of compound	*Curcuma longa*	*Zingiber officinale*	Biological activity
1	Vanillin	+	-	flavoring agent, anti-mutagenic, anti-carcinogenic [Ohta,1993; Tsuda et. al., 1994]
2	2, 4-Di-tert-Butyl Phenol	+	+	Cytotoxic activity, adulticidal, larvicidal, ovicidal, repellent, and oviposition-deterrent activities,antibacterial activities [Varsha et. al., 2015; Chen et. al., 2015; Aissaoui et. al., 2019]
3	ar-turmerone	+	-	Platelet inhibitor, insulin resistance[Lee, 2006; Kuroda et.al., 2005]
4	9-Octadecenamide	+	-	Anti-inflammatory and antibacterial activity[Hadi et. al., 2016]
5	2-Methoxy-4-Vinyl Phenol	+	-	flavoring agent, antioxidant, antimicrobial, anti-inflammatory[Shareef et. al., 2016]
6	Decanal	-	+	Anti-Salmonella agents and antioxidant activity[Shareef et. al., 2016]
7	1,7,7-trimethylbicyclo[2.2.1]heptan-2-ol	-	+	Antinociceptive and anti-inflammatory activities[Shareef et. al., 2016]
8	Bezofuran	+	-	Antidepressant, anticancer, antiviral, antifungal, antioxidant,

Serial no.	Name of compound	*Curcuma longa*	*Zingiber officinale*	Biological activity
				anti-psychotic activity[Asif, 2016]
9	Napthalene, Decahydro-	+	-	Carcinogenic effect[Jeffrey et. al., 2003]
10	Benzoic acid, 4-hydroxy-3-Methoxy- Methyl ester	+	-	Anti-proliferative, Induce apoptosis[Kumar et. al., 2003]
11	9,19-cyclolanost-24-en-3-ol,3 beta	-	+	Antimicrobial activity[Hasan et. al., 2014]

3.2. Isolation of endophytic fungi from plants

A total seven endophytic fungi were isolated from *C. longa* and a total of five endophytic fungi were isolated from *Z. officinale*. The summary of extracted fractions from the small scale is given below.

Table 3.4: Summary of the extracted fractions of endophytic fungi isolated from *C. longa and Z. officinale*

Endophytic fungi	Isolated from	EtOAc extracts (g)
CLPE-1	Petiole	0.22
CLPE-2	Petiole	0.38
CLPE-3	Petiole	0.12
CLPE-4	Petiole	0.29
CLRE-1	Root	0.42
CLRE-3	Root	0.38
CLBE-4	Bark	0.24
ZOBE-1	Bark	0.09

Endophytic fungi	Isolated from	EtOAc extracts (g)
ZOBE-2	Bark	0.22
ZOPE-3	Petiole	0.29
ZOLE-1	Leaf	0.35
ZOLE-2	Leaf	1.8

Here "E" denotes endophyte

3.2.1. Identification of endophytic fungi through morphological method

All the endophytic fungi displayed characteristic colony and microscopic morphology that could help to distinguish them. Identification of the genus was based on macroscopic and microscopic observation and confirmed as per previous morphological examination of the genus [Ignjatov et. al., 2019; Sutton et. al., 1997; Schroers et. al., 1999; Schroers, 2001; Hanks, 1996; Taylor et. al., 2019]. The characteristics colony and microscopic morphology of endophytic fungi isolated from *C. longa* are given in Figure 3.3 (a, b) and macroscopic as well as microscopic characteristics are elaborately described in Tables 3.5 and 3.6.

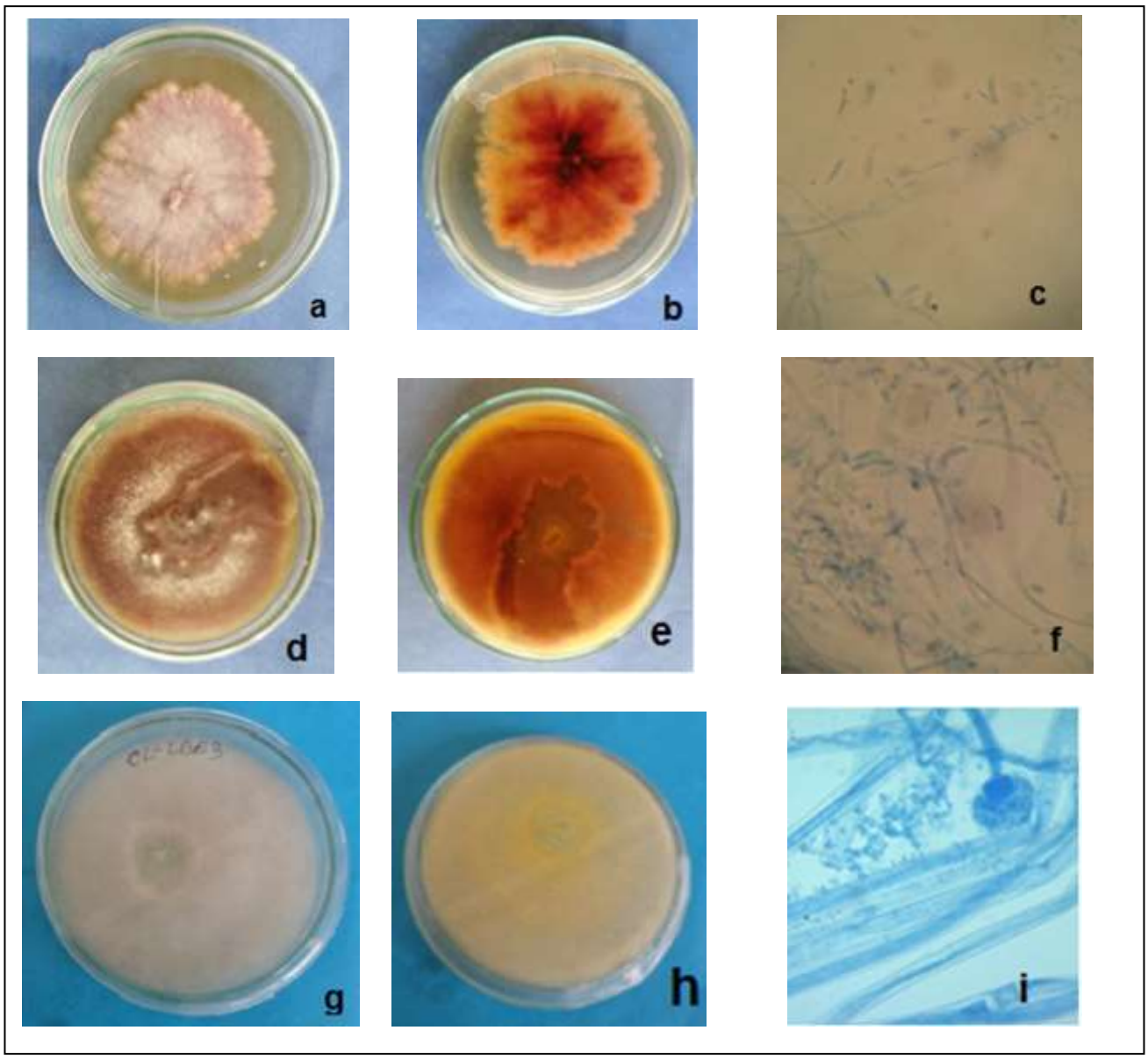

Figure 3.3 (a): Macroscopic and microscopic colony morphologies of the endophytic fungi from *C. longa*. CLPE-1 (a. macroscopic front), (b. macroscopic back) and (c. microscopic view); CLPE-2 (d. macroscopic front), (e. macroscopic back) and (f. microscopic view); CLPE-3 (g. macroscopic front), (h. macroscopic back) and (i. microscopic view).

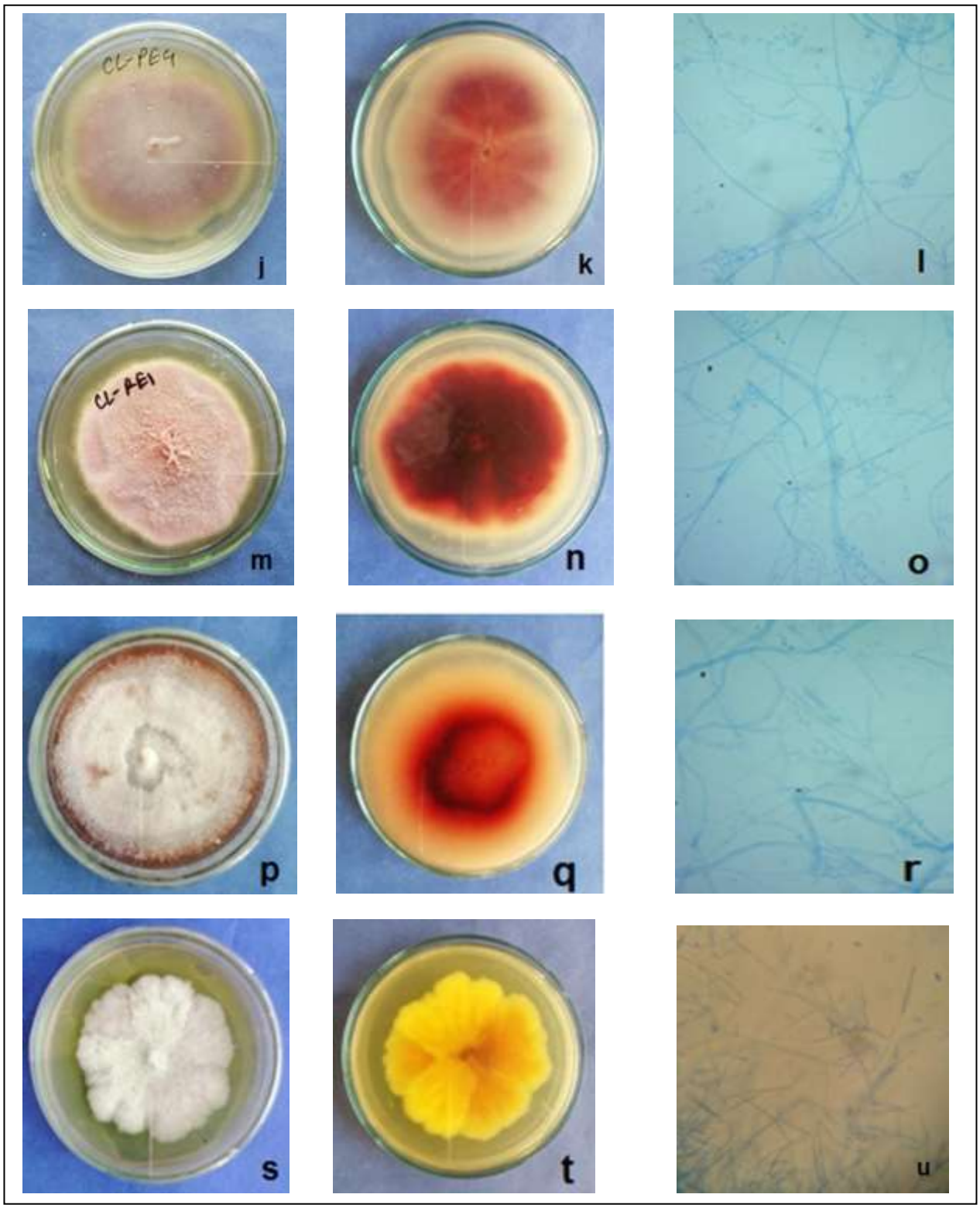

Figure 3.3 (b): Macroscopic and microscopic colony morphologies of the endophytic fungi from *C. longa*. CLPE-4 (j. macroscopic front), (k. macroscopic back) and (l. microscopic view); CLRE-1 (m. macroscopic front), (n. macroscopic back) and (o. microscopic view); CLRE-3 (p. macroscopic front), (q. macroscopic back) and (r. microscopic view); CLBE-4 (s. macroscopic front), (t. macroscopic back) and (u. microscopic view).

Table 3.5: Macroscopic characteristics of isolated endophytes from *C. longa*

Internal strain no.	Identified genus	Colony Morphology						
		Margin	**Texture**	**Growth rate**	**Hyphae**	**Mycelia**	**Color of the front side**	**Color of the back side**
CLPE-1	*Fusarium* sp.	Undulate	Radial	Slow	Surficial	Densely floccose at the center	Pink	Red/ reddish
CLPE-2	*Fusarium* sp.	Entire	Radial	Moderate	Surficial	Soft and dense near center	Brownish white	Reddish brown
CLPE-3	*Clonostachys* sp.	Filiform	Wooly	Rapid	Aerial	Fluffy and elevated	White/light yellow	Yellowish white
CLPE-4	*Fusarium* sp.	Entire	Radial	Slow	Surficial	Soft and grows upward	White purple	White purple
CLRE-1	*Fusarium* sp.	Entire	Radial	Moderate	Surficial	Smooth and slightly raised	White and light pink	Reddish
CLRE-3	*Clonostachys* sp.	Entire	Wooly	Moderate	Aerial	Cottony, filamentous and raised at the center	White/brown	Brown/red
CLBE-4	*Clonostachys* sp.	Undulate	Wooly	Moderate	Aerial	Soft, dense and grows upward	White	Yellow

Table 3.6: Microscopic characteristics of the isolated endophytes from *C. longa*

Internal strain no.	Identified genus	Microscopically visible features		
		Mycelium	**Conidia**	**Conidiophores**
CLPE-1	*Fusarium* sp.	Mass branched	Microconidia slightly sickle-shaped; macroconidia 1 to 3 celled	Septate, hyaline
CLPE-2	*Fusarium* sp.	Branched	Slender sickle-shaped, septate	Septate, hyaline
CLPE-3	*Clonostachys* sp.	Unbranched, narrow	Hyaline and broadly rounded	The primary conidiophores were verticillium-like, secondary conidiophores was penicillate
CLPE-4	*Fusarium* sp.	Branched	Microconidia oval shaped; macroconidia 3 celled with slightly curved apical cell	Chlamydospores was present
CLRE-1	*Fusarium* sp.	Branched	Oval shaped conidia, slightly curved	Short and simple, chlamydospores was present
CLRE-3	*Clonostachys* sp.	Unbranched, narrow	Spindle-like and rough	Verticillium-like
CLBE-4	*Clonostachys* sp.	Unbranched, narrow	Hyaline and broadly rounded	The primary conidiophores were verticillium-like, secondary conidiophores was penicillate

The characteristics colony and microscopic morphology of endophytic fungi isolated from *Z. officinale* are given in Figure 3.4 and macroscopic as well as microscopic characteristics are largely described in Tables 3.7 and 3.8.

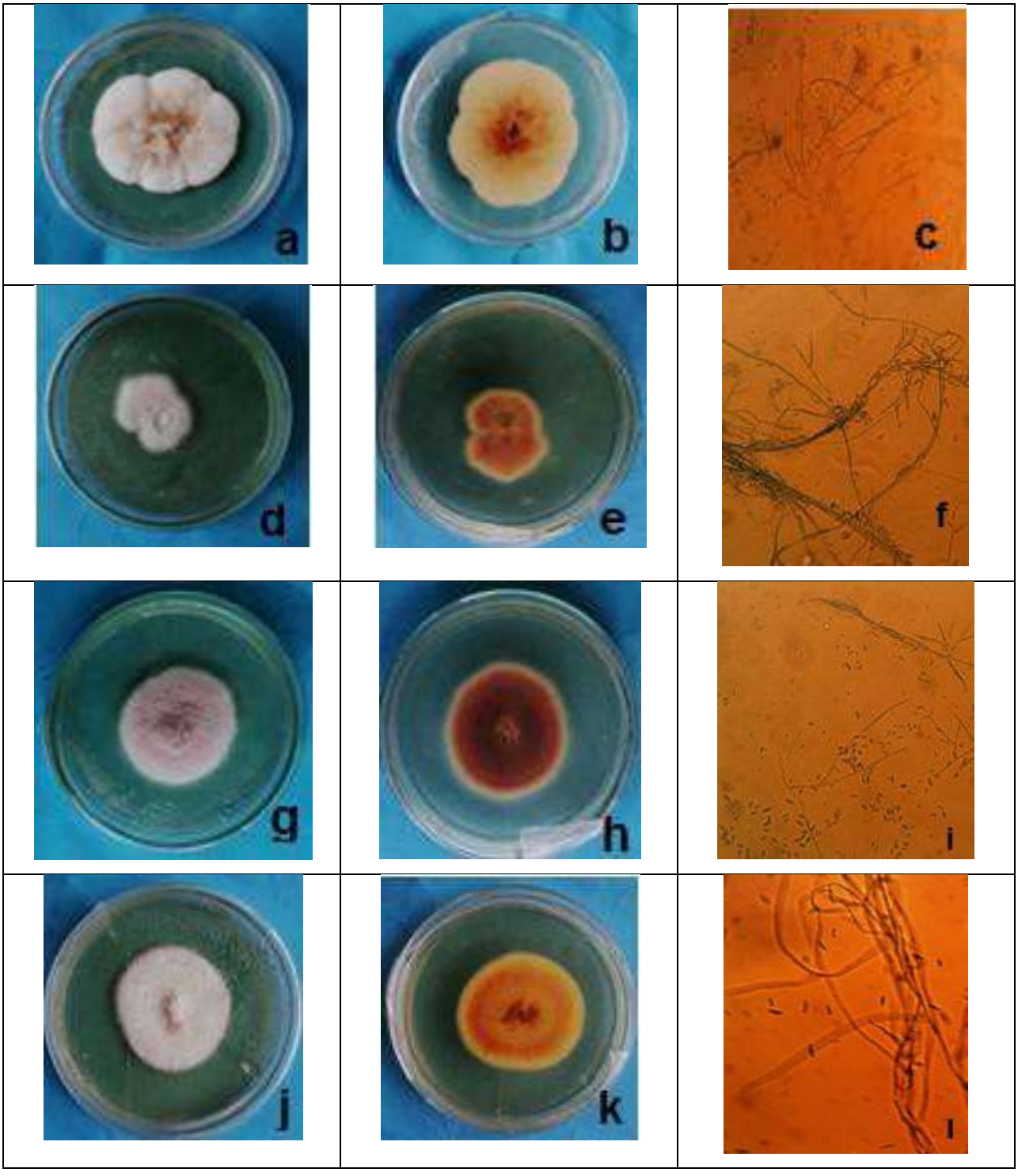
a
b
c
d
e
f
g
h
i
j
k
l

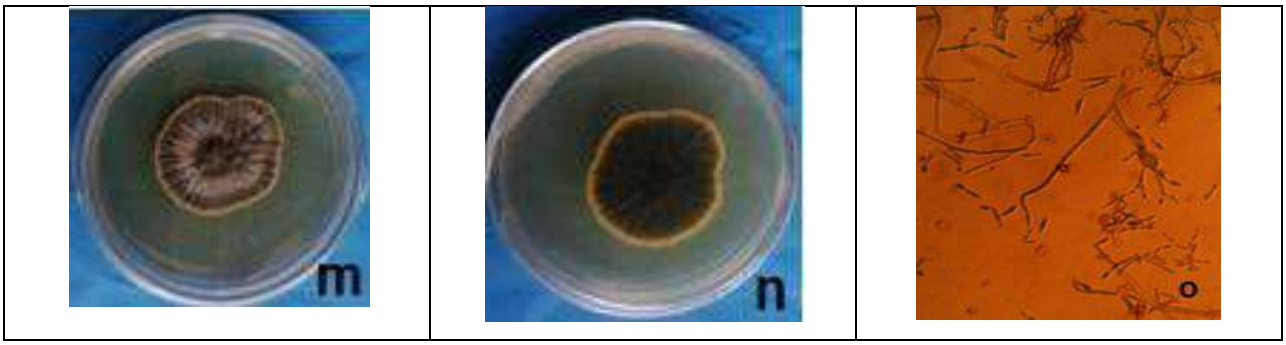

Figure 3.4: Macroscopic and microscopic colony morphologies of the endophytic fungi from Z. *officinale*. ZOBE-1 (a. macroscopic front), (b. macroscopic back) and (c. microscopic view); ZOBE-2 (d. macroscopic front), (e. macroscopic back) and (f. microscopic view); ZOPE-3 (g. macroscopic front), (h. macroscopic back) and (i. microscopic view); ZOLE-1 (j. macroscopic front), (k. macroscopic back) and (l. microscopic view) and ZOLE-2 (m. macroscopic front), (n. macroscopic back) and (o. microscopic view).

Table 3.7: Macroscopic characteristics of isolated endophytes from *Z. officinale*

Internal strain no.	Identified genus	Colony Morphology						
		Margin	**Texture**	**Growth rate**	**Hyphae**	**Mycelia**	**Color of the front side**	**Color of the back side**
ZOBE-1	*Fusarium* sp.	Undulate	Radial	Moderate	Surficial	Soft and dense the near center	Brown color observed in the center with a white side	light yellowish-brown
ZOBE-2	*Fusarium* sp.	Undulate	Wooly	Moderate	Surficial	Fertile, grow vertically	White	Light purple
ZOPE-3	*Fusarium* sp.	Entire	Wooly	Rapid	Aerial	Soft, dense and grows upward	Purple/White	Deep purple in the center with a white side
ZOLE-1	*Fusarium* sp.	Entire	Wooly	Rapid	Aerial	Soft and cottony	White	Light yellow
ZOLE-2	*Cladosporium* sp.	Undulate	Radial	Slow	Aerial	Soft and dense near the center	Grey-olivaceous	Light yellowish olive green

Table 3.8: Microscopic characteristics of the isolated endophytes from *Z. officinale*

Internal strain no.	Identified genus	Microscopically visible features		
		Mycelium	**Conidia**	**Conidiophores**
ZOBE-1	*Fusarium* sp.	Mass branched	Microconidia hyaline, delicate, slightly sickle-shaped or almost straight; macroconidia sickle-shaped, one to three septa	Septate, hyaline
ZOBE-2	*Fusarium* sp.	Branched and thread-shaped	Slender, sickle-shaped, one to three septa	Septate, hyaline
ZOPE-3	*Fusarium* sp.	Branched and unbranched	Microconidia: small, oval, one or two celled; Macroconidia: typically curved like a sickle, three to five septa expanded in the middle of their length	Cylindrical
ZOLE-1	*Fusarium* sp.	Branched	Microconidia: Oval shaped, Macroconidia: curved	Short and simple
ZOLE-2	*Cladosporium* sp.	Sparse, diffuse	Ovoid to limoniform, aseptate	Straight, solitary, unbranched, terminal or lateral and without nodules

3.2.2. Identification of endophytic fungi through molecular method

The fungal isolates (7 from *C. longa* and 5 from *Z. officinale*) had been recognized at the species level by molecular methods which includes the ITS gene sequencing, BLASTN (NCBI) database queries etc. Based on BLAST analysis, the sequence likeness is considered 95% to 100%. Molecular analysis revealed the fungal isolates' accession numbers that are diposited in the U.S National Center for Biotechnology Information (NCBI) Genbank (Figure 3.5 and 3.6) and (Table 3.9).

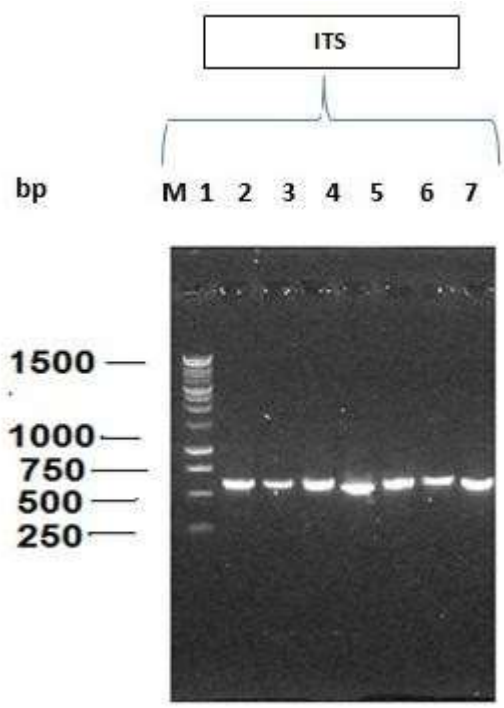

Figure 3.5: ITS profiles of ITS 4 and ITS 5 primers generated based on 5.8s rRNA gene from 7 different fungi of *C. longa*; here, 1= CLPE-1, 2= CLPE-2, 3= CLPE-3, 4= CLPE-4, 5= CLRE-1, 6= CLRE-3, 7= CLBE-4 and M: denotes 1 kb DNA ladder (Marker).

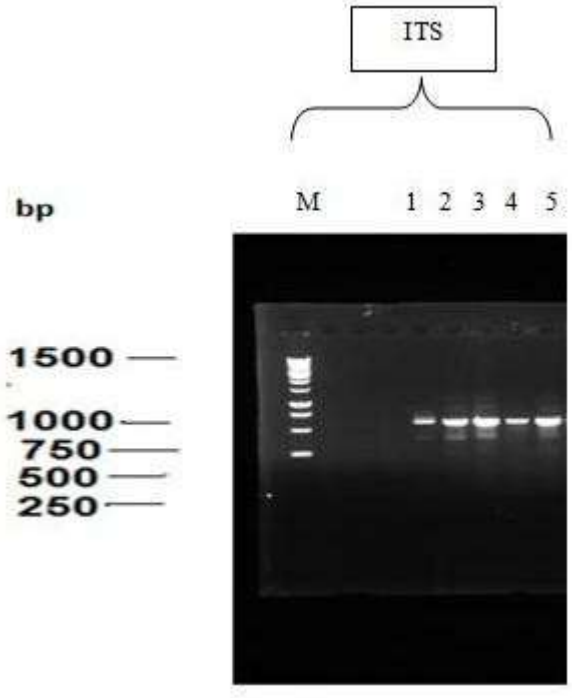

Figure 3.6: ITS profiles of ITS 4 and ITS 5 primers generated based on 5.8s rRNA gene from 5 different fungi of *Z. officinale*; here, 1= ZOBE-1, 2= ZOBE-2, 3= ZOPE-3, 4= ZOLE-1, 5= ZOLE-2 and M: denotes 1 kb DNA ladder (Marker).

Table 3.9: Blast results outputs of the endophytic fungi isolated from *C. longa* and *Z. officinale* plants

Serial no.	Fungal Internal strain no.	Query Cover (%)	Max identity (%)	Identified Fungal Species	Gene bank accession number
1	CLPE-1	99	99	*Fusarium proliferatum*	MZ234162
2	CLPE-2	99	99	*Fusarium proliferatum*	MZ234163
3	CLPE-3	100	99	*Clonostachys rosea*	MZ234164
4	CLPE-4	99	100	*Fusarium oxysporum*	MZ234165
5	CLRE-1	98	100	*Fusarium oxysporum*	MZ234166
6	CLRE-3	99	83	*Clonostachys rosea*	MZ234167
7	CLBE-4	99	98.61	*Clonostachys rosea*	MZ234168
8	ZOBE-1	100	100	*Fusarium proliferatum*	PP346031
9	ZOBE-2	100	100	*Fusarium proliferatum*	PP346434
10	ZOPE-3	98	100	*Fusarium proliferatum*	PP346435
11	ZOLE-1	100	99.64	*Fusarium solani*	PP346437
12	ZOLE-2	100	100	*Cladosporium cladosporoides*	PP346438

3.2.3. Phylogenetic study

A phylogenetic study elucidates the evolutionary history and relationship among a group of organisms. How species or other groups developed from a series of common ancestors are represented by the pattern of branching of a phylogenetic tree. The branch values represent the bootstrap confidence values. Here the evolutionary analysis of the 7 isolated fungi from *C. longa* was conducted using the maximum likelihood method (1000 bootstrap replicates). From morphology and ITS analysis, we found that these 7 active fungal strains belong to 2 genera and 3 species. Through phylogenetic analysis, it can be shown that *Fusarium proliferatum* showed 96% sequence similarity with *Fusarium oxysporum* and *Clonostachys rosea*. Similarly, *Fusarium proliferatum*, *Fusarium oxysporum* and *Clonostachys rosea* showed 100% sequence similarity among them (Figure 3.7).

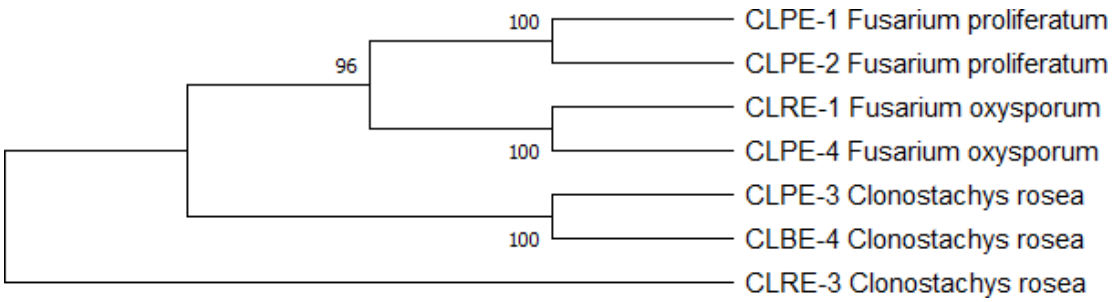

Figure 3.7: Phylogenetic tree based on maximum likelihood method (1000 bootstrap replication) analysis of the rRNA ITS sequence of the endophytic fungi obtained from *C. longa*.

The evolutionary analysis of the 5 isolated fungi from *Z. officinale* was also conducted using the maximum likelihood method (1000 bootstrap replicates). From morphology and ITS analysis, we found that these 5 active fungal strains belong to 2 genera and 3 species. Through phylogenetic analysis, it can be shown that *Fusarium proliferatum* showed 67% sequence similarity with *Fusarium solani* and *Cladosporium cladosporoides*. Similarly, *Fusarium solani* and *Cladosporium cladosporoides* showed 100% sequence similarity within them (Figure 3.8).

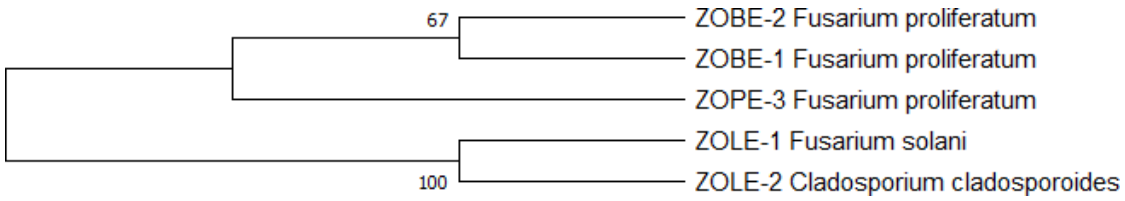

Figure 3.8: Phylogenetic tree based on maximum likelihood method (1000 bootstrap replication) analysis of the rRNA ITS sequence of the endophytic fungi obtained from *Z. officinale*.

3.3. Chromatographic screening of *C. longa, Z. officinale* plant and their associated fungal extracts in TLC plates by visual/UV detection and spray reagents

Preliminary qualitative chemical screening was carried out for all the extracts (methanol extracts of the plants and EtOAc extracts of their associated fungi) by TLC to appraise the presence of various secondary metabolites. The screening was done by visual observation, under UV light (254 and 365 nm) and after spraying with vanillin-H_2SO_4 spray reagent (Figure 3.9 and 3.10) (Table 3.10). Numerous secondary metabolites, including coumarins, isocoumarins, or their derivatives, flavonoids, steroids, terpenoids, anthocyanins, anthraquinones, and naphthoquinones were detected by analyzing TLC spots of the extracts [Harborne, 1998; Mahmud, et. al., 2020].

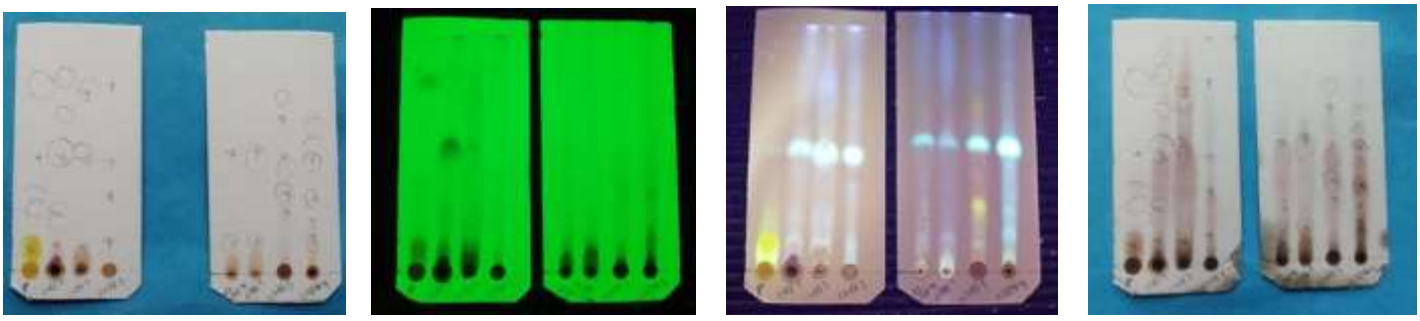

a) visual observation b) 254 nm c) 365 nm d) after spraying

Figure 3.9: Screening of plant and fungal extracts of *C. longa* by Thin Layer Chromatography (TLC) at a) visual observation (b) 254 nm, (c) 365 nm and (d) after spraying with spray reagent.

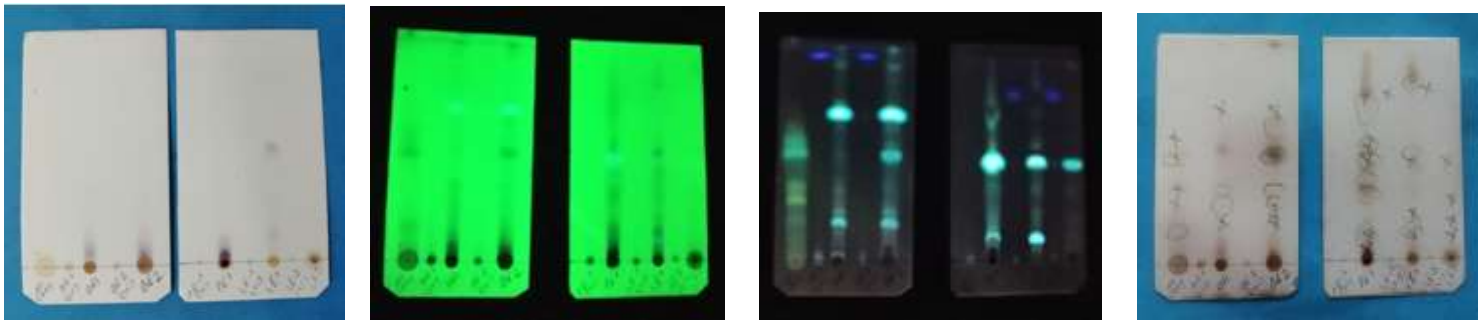

a) visual observation b) 254 nm c) 365 nm d) after spraying

Figure 3.10: Screening of plant and fungal extracts of *Z. officinale* by Thin Layer Chromatography (TLC) at a) visual observation (b) 254 nm, (c) 365 nm and (d) after spraying with spray reagent.

Table 3.10: Chemical screening of crude extract of *C. longa, Z. officinale* and their fungi

Identified genus	Internal strain no.	Visual observation	Visibility under UV light (254 nm)	Visibility under UV light (365 nm)	Visibility with spray reagent	Remarks on probable compounds
Curcuma sp.	CL	Yellow, Brown light quenching, Brown dark quenching	Violet, Grey, Brown	Blue, Yellow, Brown dark quenching	Red	Flavonoid, Steroid, Coumarin or their derivatives
Fusarium sp.	CLPE-1	Brown, Purple light quenching, Purple dark quenching	Grey, Violet, Brown, Black	Sky blue, Light yellow, Black	Purple	Flavonoids, Anthrocyanin, Terpenoid, Coumarin or their derivatives
Fusarium sp.	CLPE-2	Red, Purple light quenching	Grey, Light violet Black	Blue, Sky blue, Yellow, Light blue	Blue, Purple	Flavonoids, Anthrocyanin
Clonostachys sp.	CLPE-3	No color	Brown	Blue, Yellowish, Sky blue, Light blue	Yellow, Light purple, Bluish	Flavonids
Fusarium sp.	CLPE-4	Red, Purple light quenching	Grey, Violet light quenching, Violet dark quenching	Blue, Sky blue, Light blue, Light red	Purple	Anthrocyanin
Fusarium sp.	CLRE-1	Red, Purple light quenching	No color	Blue, Light blue, Yellow, Sky blue, Red	Yellow, Purple	Flavonoids, Terpenoids
Clonostachys sp.	CLRE-3	Yellow, Pink, Purple, Brown light quenching, Brown dark quenching	Grey, Violet, Brown, Black	Blue, Light red, Yellow, Light blue quenching, Red, Orange	Purple, Bluish	Flavonoid, Terpenoid, Coumarin or their derivatives
Clonostachys sp.	CLBE-4	Light brown	Violet, Grey, Violet, dark quenching	Violet, Sky blue, Light blue, Light red, Light yellow	Yellow, Purple, Blue	Flavonoid, Terpenoid, Coumarin or their derivatives
Zingiber sp.	ZO	Yellow	Yellow quenching Brown quenching	Yellow light quenching, Blue light quenching, Brown light quenching	Brown	Steroid, Terpenoids, Coumarin, Isocoumarin or their derivatives
Fusarium sp.	ZOBE-1	Yellow, Purple, Brown	Blue light quenching, Brown quenching, Blue dark quenching	Blue light quenching, Brown light	Brown, Purple	Flavonoids, Anthrocyanin, Terpenoid,

Identified genus	Internal strain no.	Visual observation	Visibility under UV light (254 nm)	Visibility under UV light (365 nm)	Visibility with spray reagent	Remarks on probable compounds
				quenching		Coumarin or their derivatives
Fusarium sp.	ZOBE-2	Yellow, Purple	Blue light quenching, Yellow light quenching, Blue dark quenching	Blue light quenching	Blue, Purple	Terpenoid, Steroids, Coumarin, Isocoumarin or their derivatives
Fusarium sp.	ZOPE-3	Yellow, Pink, Purple, Brown	Blue light quenching, Blue dark quenching	Blue light, quenching, Blue dark quenching	Purple, Brown Blue	Flavonoids, Anthrocyanin, Terpenoid, Coumarin or their derivatives
Fusarium sp.	ZOLE-1	Purple, Pink, Brown	Blue light quenching, Blue dark quenching	Purple dark Quenching, Blue dark quenching	Purple, Blue	Flavonoids, Steroids, Coumarin, Isocoumarin or their derivatives
Cladosporium sp.	ZOLE-2	Yellow, Brown	Blue light quenching	Blue light quenching	Purple	Terpenoid, Steroids, Coumarin, Isocoumarin or their derivatives

3.4. Bioassay of the crude extracts (plants and fungi)

3.4.1. Bioassay of the crude extract of plant *C. longa* and its VLC fractions

A total of 14 fractions were obtained through VLC (described in section 2.5.3). These fractions were mixed based on TLC pattern and obtained 6 fractions named F1 (n-hexane/ 10% CH_2Cl_2), F2 (n-hexane/ 20% CH_2Cl_2- n-hexane/ 50% CH_2Cl_2), F3 (n-hexane/ 60% CH_2Cl_2- DCM / 3-5% MeOH), F4 (DCM / 7-15% MeOH), F5 (DCM / 20-65% MeOH) and F6 (100% MeOH).

3.4.1.1. Antioxidant activity of the crude extract of plant *C. longa* and its VLC fractions

The crude extract and column fractions (F4-F6) showed significant antioxidant activity compared to the positive control BHA and AA. The other column fractions (F1-F3) were reluctant to antioxidant activity and not mentioned in Figure 3.11. Phenolic compounds in spices and herbs are widely responsible for their antioxidant properties as mentioned by a number of studies [Shan et. al., 2005; Wu et. al., 2006; Wong et. al., 2006].

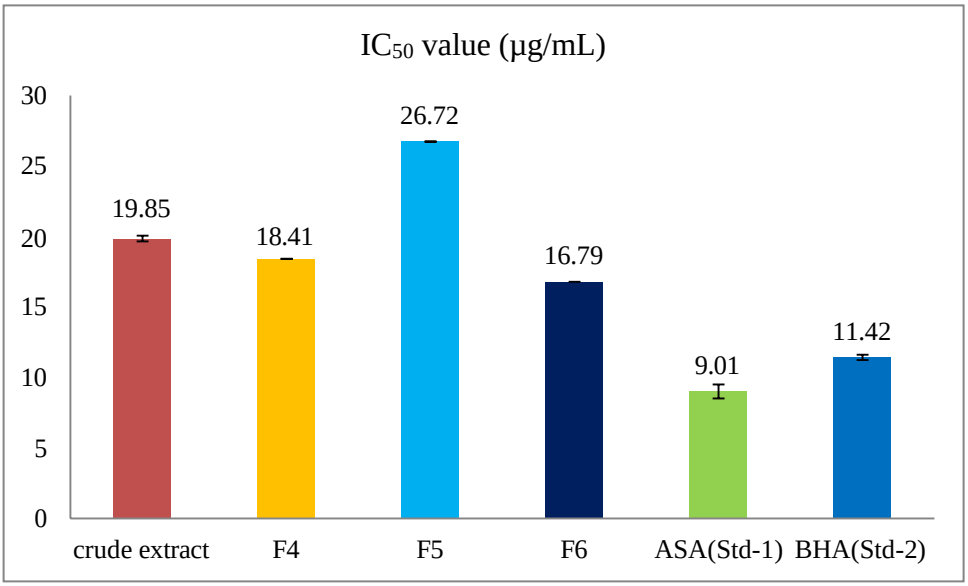

Figure 3.11: Antioxidant activity of the test samples. Values are expressed as mean±SD; n=3.

3.4.1.2. Antimicrobial activity of the crude extract of plant *C. longa* and its VLC fractions

The crude extract as well as VLC fractions, revealed mild antibacterial activity. F1, F2 and F3 fractions showed moderate sensitivities against *B. megaterium*, *S. aureus* and *P. aeruginosa*. F3 and F4 fractions exhibited mild activity against *E. coli*. F5 and F6 showed no activity against the tested bacteria. The fungal strains were also resistant to the test samples (Table 3.11). Alkaloid and flavonoid type compounds may be responsible for the antibacterial actions in higher plants that are suggested by some studies [Cordell et. al., 2001]. Previous studies on the antibacterial activity of this plant extract have often found variable antibacterial activity. Chakraborty et al., reported that *C. longa* ethanol extract had antibacterial activity against *K. pneumoniae, S.aureus, P.aeuroginosa* and *E. coli* in the disc diffusion method [Chakraborty et al., 2014]. In a crude

mixture there are various types of compounds that may interfere with the action of the other [Adwan et. al., 2008]. Sometimes the effectiveness of an antibacterial activity of a plant material depends on the antimicrobial activity test used, the dose applied, the geographical uniqueness of the plant, and the extraction process [Keskın et. al., 2012; Lee & Lee, 2010; Marasini et. al., 2015].

Table 3.11: Antimicrobial screening of crude extract and VLC fractions

Name of the organism	**Zone of inhibition (mm)**							**Standard**
	Sample (200-400 µg/disc)							
Bacteria	**Crude extract**	**F1**	**F2**	**F3**	**F4**	**F5**	**F6**	**Kanamycin (30 µg/disc)**
Escherichia coli (gram –ve)	7	----	-----	8	8	----	-----	17
Pseudomonas aeruginosa (gram –ve)	7	7	8	7	-----	-----	-----	16
Staphylococcus aureus (gram +ve)	7	10	------	8	------	-----	-----	16
Bacillus megaterium (gram +ve)	7	9	9	9	-----	-----	-----	50
Fungi								**Ketoconazole (30 µg/disc)**
Aspergillus niger	-------	------	-----	------	-----	-----	-----	30
Aspergillus flavus	-------	------	------	------	------	-----	-----	48

"-" indicates no sensitivity;

3.4.1.3. Cytotoxicity of the crude extract of plant *C. longa* and its VLC fractions

The crude extract showed significant cytotoxicity with an LC_{50} value of 1.81 µg/mL caompared to the positive control Tamoxifen (0.13 µg/mL). LC_{50} values for other fractions, F4 (2.4 µg/mL), F5 (2.5 µg/mL), F6 (2.3 µg/mL) were also significant. The remaining fractions (F1-F3) exhibited no cytotoxic effect (Figure 3.12). The results of this bioassay also confirmed the previous findings [Chuang et. al., 2000; Khattak et. al., 2005]. The cytotoxic compounds present in the extract may act individually or synergystically and were responsible for the mortality of experimental shrimp.

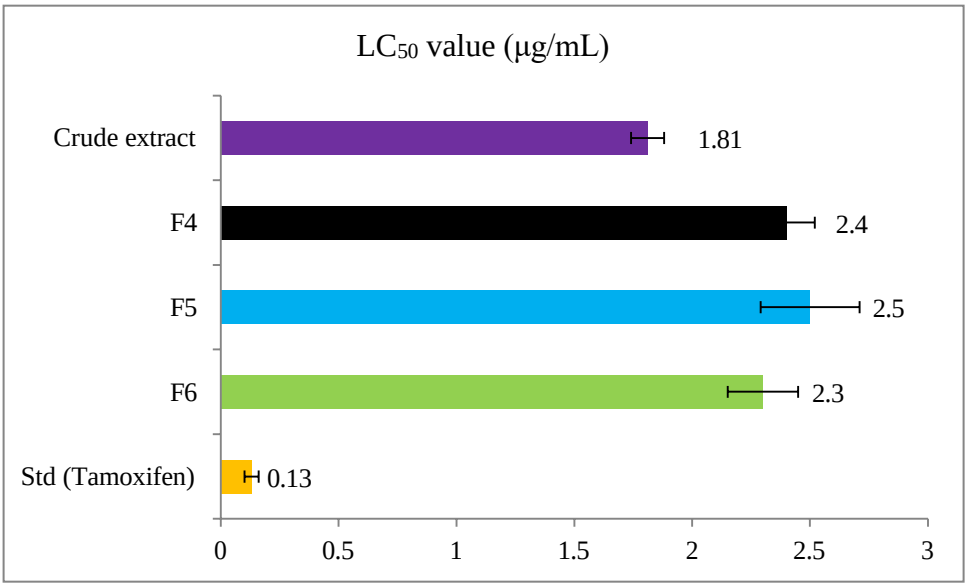

Figure 3.12: Cytotoxicity activity of the test samples. Values are expressed as mean±SD; n=3.

3.4.2. Bioassay of the crude extract of plant *Z. officinale* and its fractions obtained through the Kupchan partition method

3.4.2.1. Antioxidant activity of the crude extract of plant *Z. officinale* and its fractions

The crude extract, DCM and aqueous fractions showed significant antioxidant activity with IC_{50} values of 2.08, 13.14 and 19.19 µg/mL, respectively compared with standard ASA (8.59 µg/mL) (Figure 3.13). The free radical neutralizing capability of the methanol extract might be due to the phenolic acids and flavonoid-type phytoconstituents that are reported to show evidence of high antioxidant potential [Emon et al., 2020; Rudra et al., 2020; Shahidi et al., 1992].

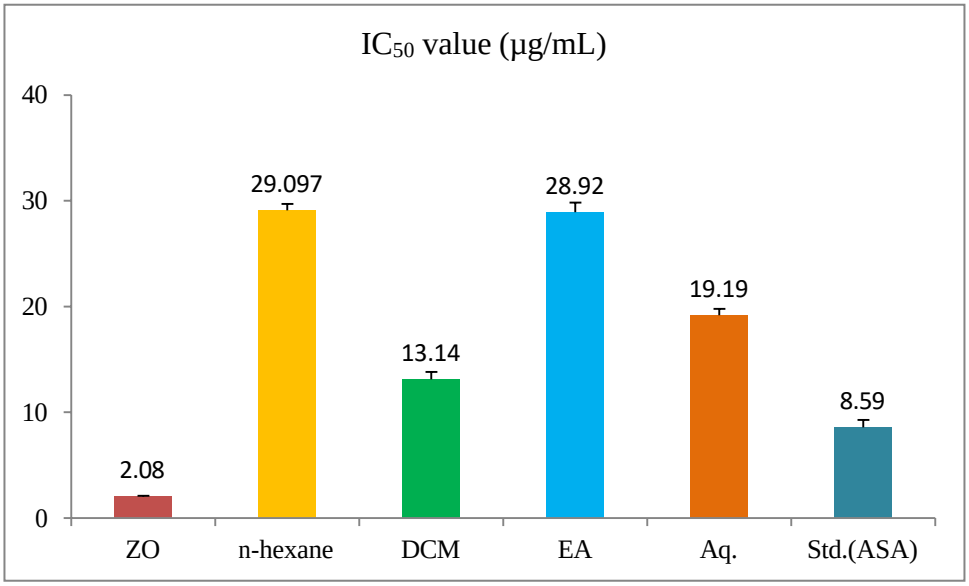

Figure 3.13: Antioxidant activity of fractions obtained through Kupchan method. Values are expressed as mean±SD; n=3.

3.4.2.2. Antibacterial activity of the crude extract of plant *Z. officinale* and its fractions

The crude extract of *Z. officinale* showed mild to moderate activity against all tested bacteria. Among fractions the EA soluble fraction and Aqeuous soluble fraction showed significant antibacterial activity against all tested bacteria except Aqeous soluble fraction against *E. coli*. DCM soluble fraction showed mild to moderate activity. Again DCM and Aq. soluble fraction showed mild activity against the fungal strain *Candida albicans.* No fractions showed antifungal activity against *A. niger* and *A. flavus*. The pictures of some fractions are mentioned in Figure 3.14 and overall antimicrobial activities are given in Table 3.12.

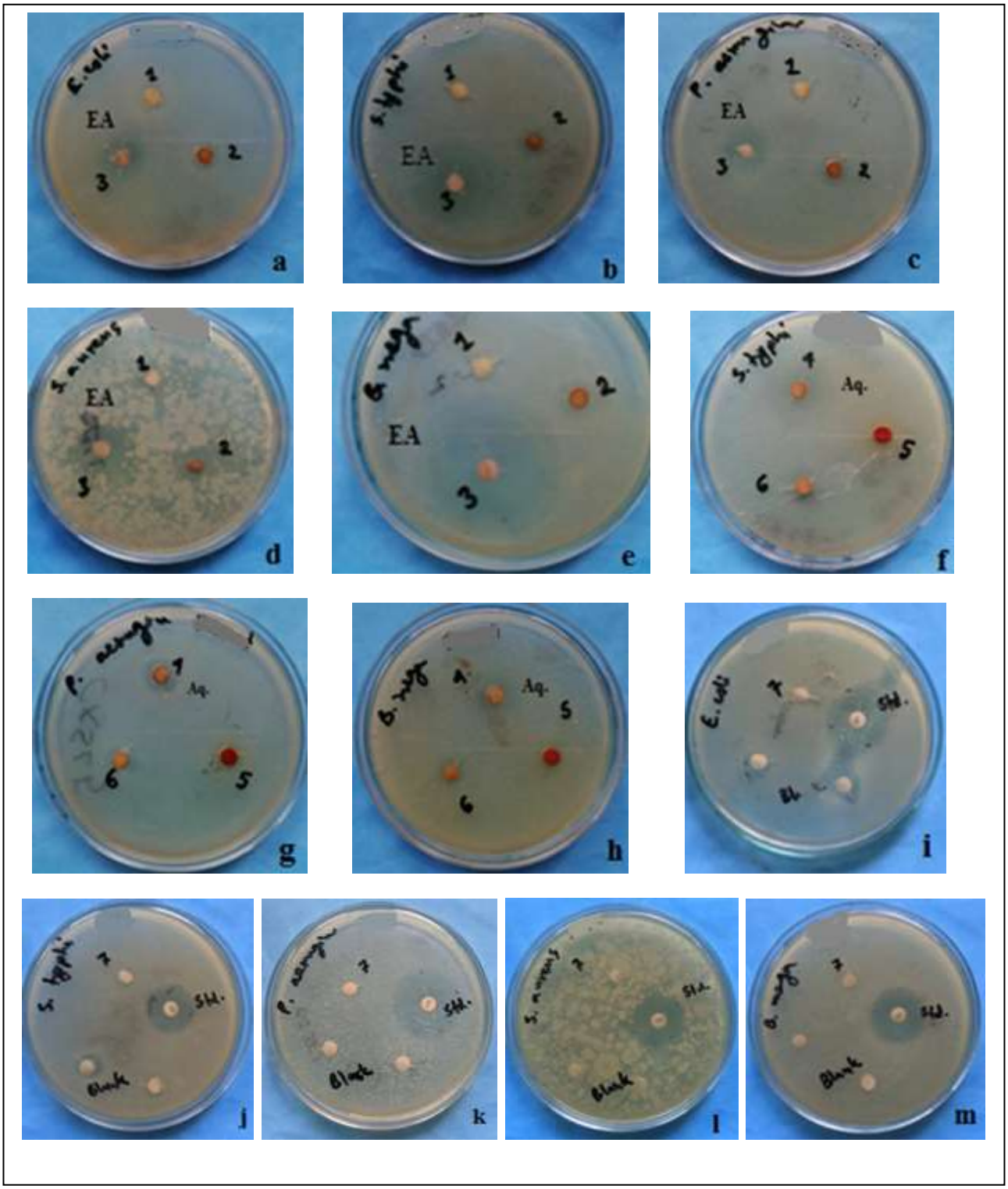

Figure 3.14: Plate pictures of antibacterial activity of EA soluble fractions (a, b, c, d, e); Aq. soluble fractions (f, g, h); Standard (i, j, k, l, m).

Table 3.12: Antimicrobial screening of crude extract and fractions of *Z. officinale*

Name of the organism		**Zone of inhibition (mm)**				**Standard**
		Sample (400 µg/disc)				
Bacteria	***Z. officinale***	**n-hexane soluble fraction**	**Dichloro methane (CH_2Cl_2) soluble fraction**	**Ethyle acetate (EA) soluble fraction**	**Aqueous soluble fraction**	**Kanamycin (30 µg/disc)**
Escherichia coli (gram –ve)	7	-----	7	18	------	21.5
Salmonella typhi (gram –ve)	8	------	10	28	14	18
Pseudomonas aeruginosa (gram –ve)	10	------	10	16	14	27
Staphylococcus aureus (gram +ve)	7	-------	7	17	8	21
Bacillus megaterium (gram +ve)	8	8	10	40	14	21
Fungi						**Ketoconazole (30 µg/disc)**
Aspergillus niger		-------	------	-----	------	38.5
Aspergillus flavus		-------	------	------	------	35
Candida albicans		--------	9	------	8	23

3.4.3. Bioassay of the crude extract of endophytic fungi isolated from *C. longa*

3.4.3.1. Antioxidant activity of the ethyl acetate extracts of endophytic fungi isolated from *C. longa*

Fungal strains CLBE-4 (29.81 µg/mL) and CLPE-1 (49.78 µg/mL) showed potent antioxidant activity compared with the positive controls ASA (9.01 µg/mL) and BHA (11.42 µg/mL). Among other strains, CLPE-2 (168.09 µg/mL), CLPE-3 (149.01 µg/mL) and CLRE-3 (208.38 µg/mL) showed moderate antioxidant activity as shown in Figure 3.15. In a study, a

total of 44 endophytic fungi from several parts of turmeric plant for their antioxidant bioactive potential had been investigated [Bustanussalam et. al., 2015] and it was concluded that filtrate ethylacetate extracts of endophytic fungi have antioxidant activity, which is corroborated with our study.

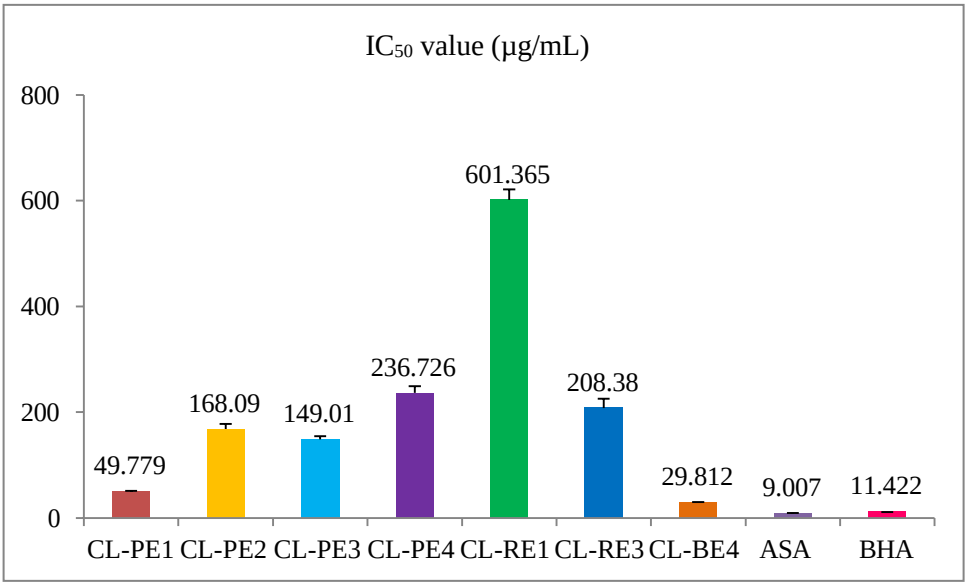

Figure 3.15: Antioxidant activity of the ethyl acetate extracts of endophytic fungi isolated from *C. longa*. Values are expressed as mean±SD; n=3.

3.4.3.2. Antibacterial activity of the ethyl acetate extracts of endophytic fungi isolated from *C. longa*

Isolate CLPE-1 showed moderate activity against all pathogenic bacteria. CLPE-2 showed mild to moderate activity against *E. coli* and *S. typhi*. CLRE-3 showed mild and CLBE-4 showed moderate activity against *S. typhi*. CLPE-3, CLPE-4 and CLRE-1 showed poor activity against all pathogenic bacteria (not mentioned in table). None of the endophytes showed any activity against the tested pathogenic fungi. The results are listed in Table 3.13.

Table 3.13: Antimicrobial screening of ethyl acetate extract of endophytic fungi isolated from *C. longa*

Name of the organism	Zone of inhibition (mm)				Standard
	Sample (200 µg/disc)				
Bacteria	**CLPE-1**	**CLPE-2**	**CLRE-3**	**CLBE-4**	**Kanamycin (30 µg/disc)**
Escherichia coli (gram –ve)	15	11	-----	------	38
Salmonella typhi (gram –ve)	15	13	12	15	30
Staphylococcus aureus (gram +ve)	15	-----	-----	----	28
Bacillus megaterium (gram +ve)	12	7	----	-----	35

3.4.3.3. Cytotoxic activity of the ethyl acetate extracts of endophytic fungi isolated from *C. longa*

From all tested samples, CLPE-1, CLPE-4, CLRE-1 and CLRE-3 showed noteworthy cytotoxicity to brine shrimp nauplii with LC_{50} values of 0.42, 0.46, 2.44 and 0.16 µg/mL respectively. Other fungal strains CLPE-2 and CLBE-4 showed moderate cytotoxicity (Figure 3.16).

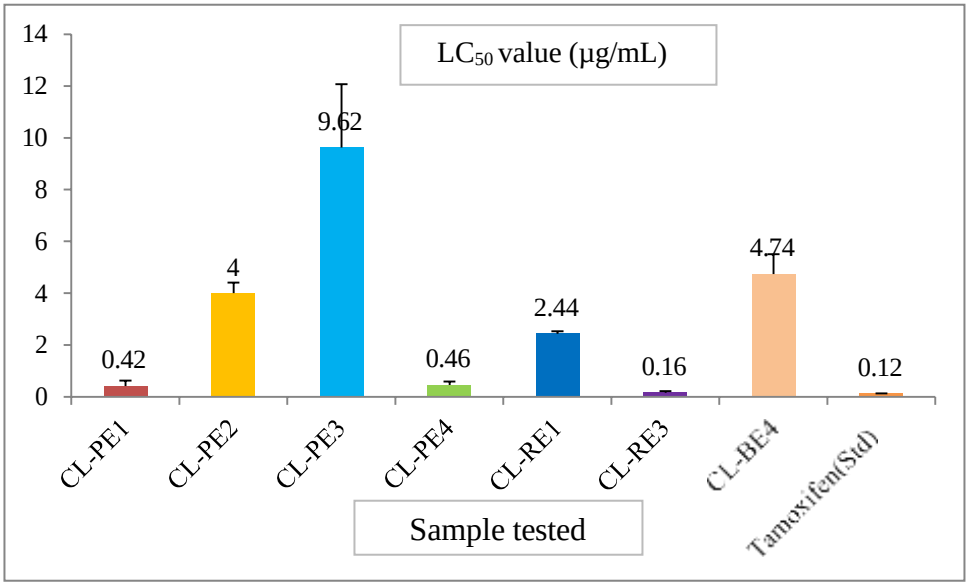

Figure 3.16: Cytotoxic activity of the ethyl acetate extracts of endophytic fungi isolated from *C. longa*. Values are expressed as mean±SD; n=3.

3.4.4. Bioassay of the crude extract of endophytic fungi isolated from *Z. officinale*

3.4.4.1. Antioxidant activity of the ethyl acetate extracts of endophytic fungi isolated from *Z. officinale*

Among the tested samples ZOBE-1, ZOBE-2 and ZOPE-3 showed significant antioxidant activity compared to standard BHA and ASA. Other fungal strains did not show prominent antioxidant activity (Figure 3.17).

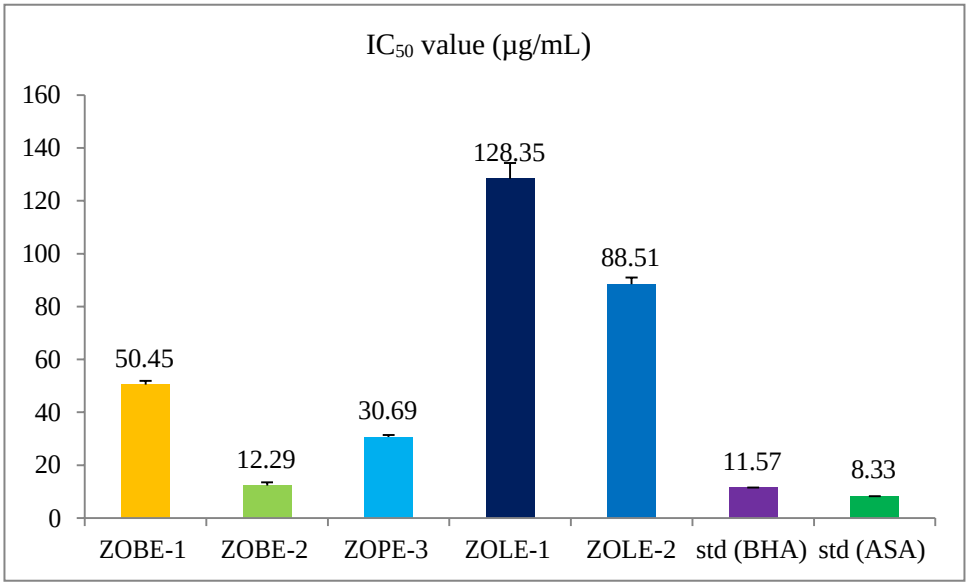

Figure 3.17: Antioxidant activity of the ethyl acetate extracts of endophytic fungi isolated from Z. *officinale*. Values are expressed as mean±SD; n=3.

3.4.4.2. Antimicrobial activity of the ethyl acetate extracts of endophytic fungi isolated from *Z. officinale*

All fungal isolates showed mild to moderate antibacterial activity against all pathogenic bacteria (Table 3.14). ZOLE-2 showed moderate activity against *B. megaterium* and mild activity against *S. typhi*. None of the endophytes showed any activity against the tested pathogenic fungi.

Table 3.14: Antimicrobial screening of ethyl acetate extract of endophytic fungi isolated from *Z. officinale*

Name of the organism	Zone of inhibition (mm)					Standard
	Sample (200 µg/disc)					
Bacteria	**ZOBE-1**	**ZOBE-2**	**ZOPE-3**	**ZOLE-1**	**ZOLE-2**	**Kanamycin (30 µg/disc)**
Escherichia coli (gram –ve)	8	9	10	7	----	33
Salmonella typhi (gram –ve)	12	15	12	----	7	32
Staphylococcus aureus (gram +ve)	10	13	12	----	-----	29
Bacillus megaterium (gram +ve)	10	12	10	7	13	30

3.5. Chemical Investigation

3.5.1. Structure elucidation of the compound isolated from the plant *C. longa*

Two compounds have been isolated from *C. longa*. The obtained NMR data were compared to relevant literature that helped solve the structure of the isolated compound. The compounds are described below.

1. Characterization of compound CL-1 as 4-hydroxy-3-methoxy cinnamic acid

CL-1 was obtained as an orange crystal (30 mg) (R_f = 0.17, toluene/10% EtOAc). ^{1}H NMR ($CDCl_3$, 400 MHz) spectrum showed the presence of the olefinic (cinnamyl) protons by the appearance of a pair of doublets at δ 6.42 and δ 7.52 with J = 16 Hz; while a pair of doublets at δ 7.05 and δ 6.58 (J = 8.0 Hz) for two aromatic protons; broad singlet at 5.76 assisted in the elucidation by indicating one phenolic hydroxyl group. A sharp singlet integrating for three protons at δ 3.88 indicated the methoxy group.

The ^{13} C NMR (100 MHz, $CDCl_3$) spectra further supported the elucidation by indicating nine carbons including the characteristic carbonyl carbon at 183.0. Based on this spectral evidence and comparison with literature data, the compound was characterized as 4-hydroxy-3-methoxy cinnamic acid [Khan et. al., 2008; Han et. al., 2006] which is a phenolic compound. The obtained NMR data are presented in Table 3.15. The structure and NMR spectra are presented in Figure 3.18 to 3.22.

Table 3.15: ^{1}H NMR ($CDCl_3$, 400 MHz) and ^{13} C NMR ($CDCl_3$, 100 MHz) NMR data for CL-1

Position	CL-1	
	δ_H (mult., *J* in Hz)	δ_c
1	----	130.0
2	7.04(1H,br.s)	121.5
3		148.2
4		147.2
5	6.85(1H,d, *J* = 8.0)	115.1
6	7.05(1H,d, *J* = 8.0)	122.9
7	7.52(1H,d, *J* = 16.0)	140.7
8	6.42(1H,d, *J* = 16.0)	110.0
9		183.0
10		55.9
4-OH	5.76br.s,1H	
3-OCH_3	3.89 s, 3H	

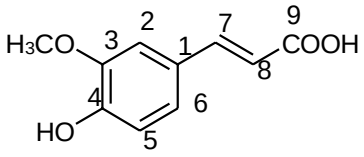

Figure 3.18: Structure of CL-1

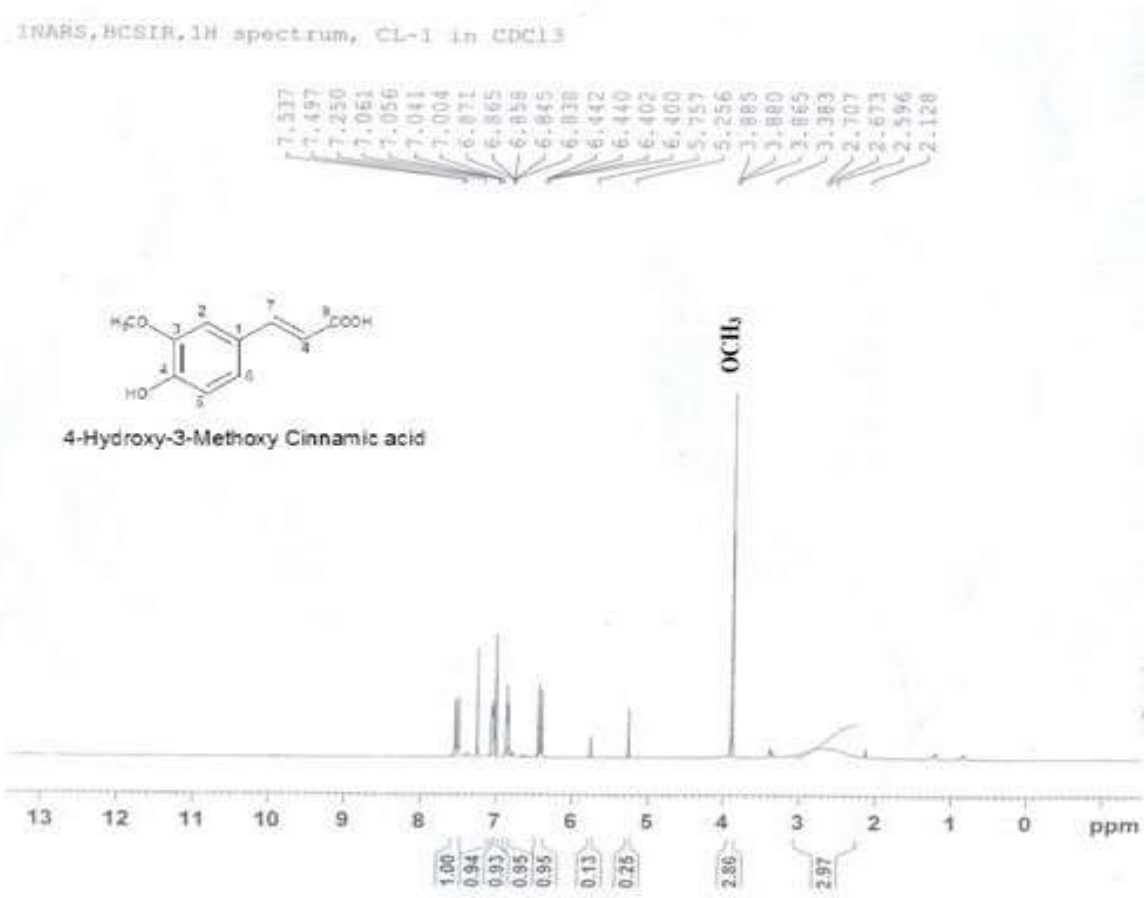

Figure 3.19: ^{1}H NMR (nuclear magnetic resonance) spectrum of CL-1 (Full)

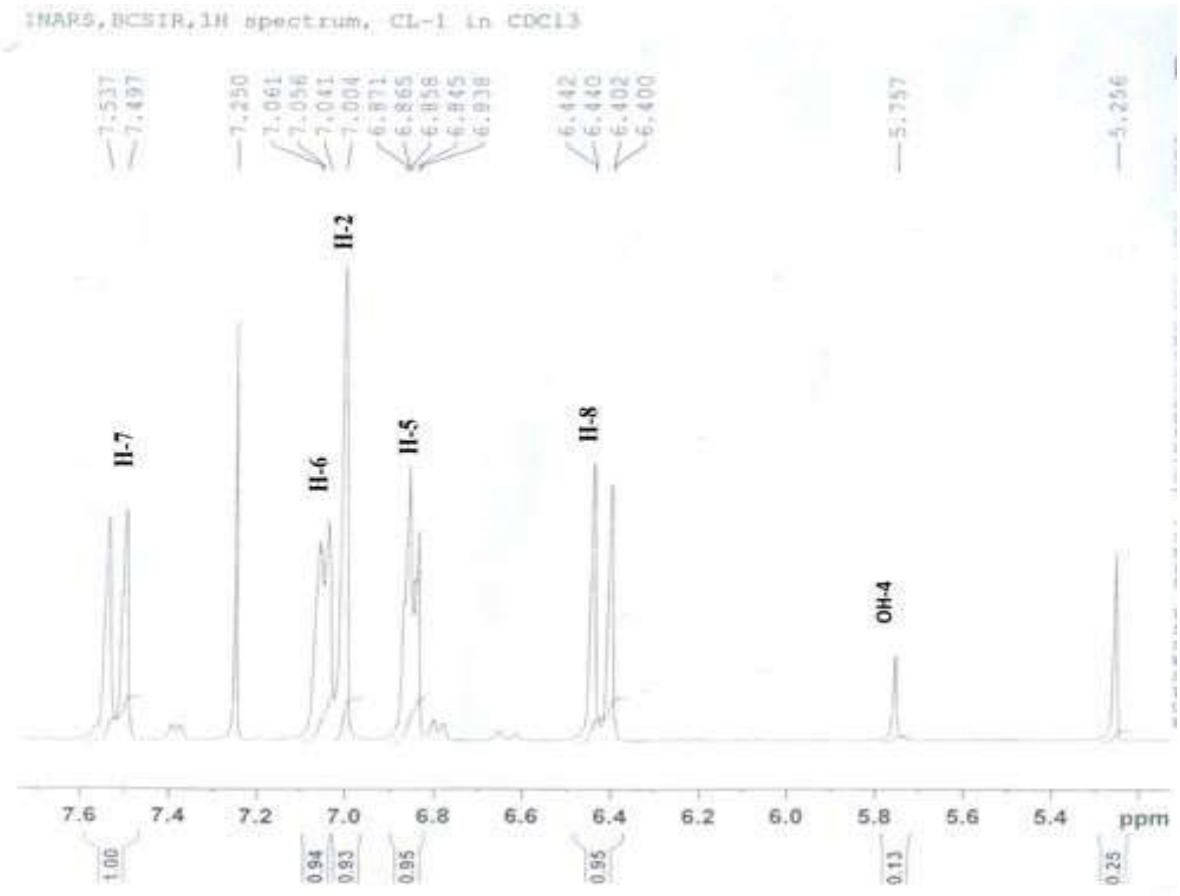

Figure 3.20: ^{1}H NMR spectrum of CL-1 (Expanded)

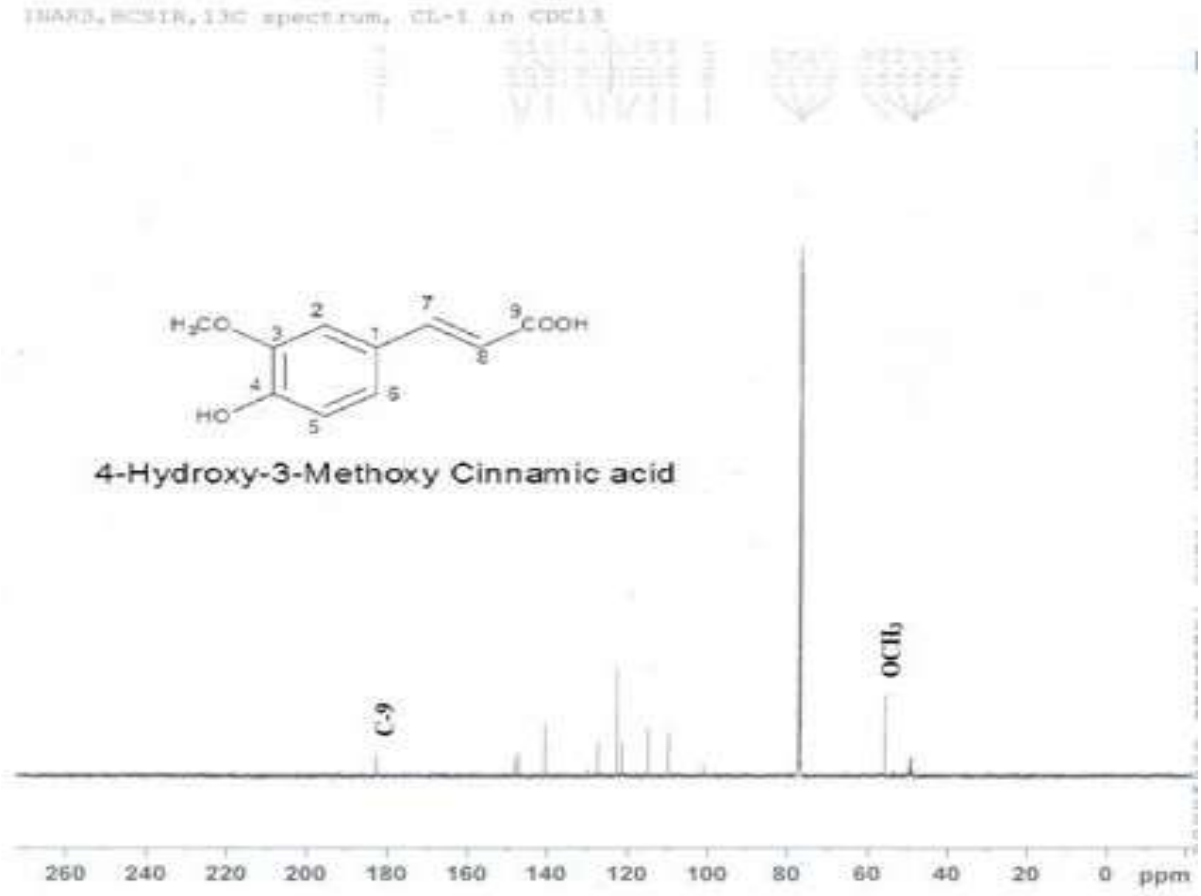

Figure 3.21: ^{13} C NMR of CL-1 (Full)

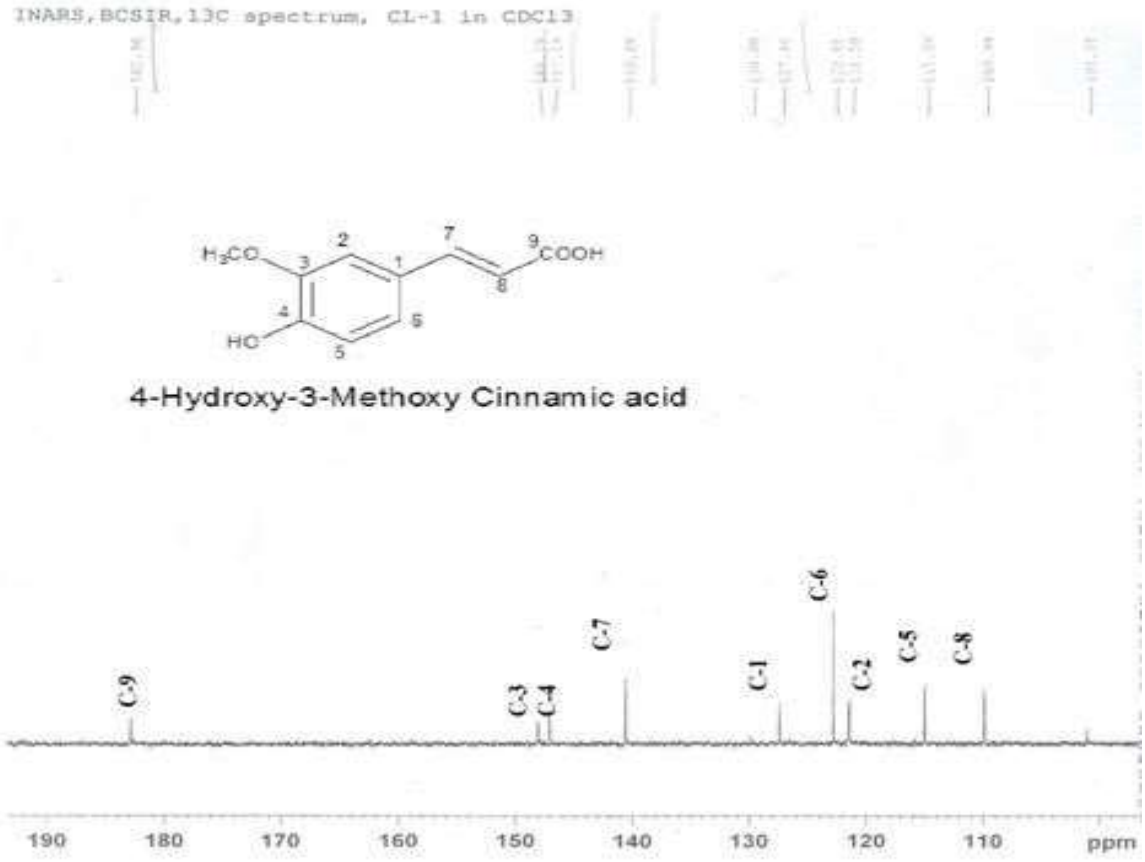

Figure 3.22: ^{13} C NMR of CL-1 (Expanded)

2. Characterization of compound CL-4 as Methyl ferulate

CL-4 was obtained as white crystals (8 mg) (R_f = 0.38, toluene/20% EtOAc). ^{1}H NMR ($CDCl_3$, 400 MHz) spectrum showed that there are suspected aromatic groups, at the chemical shifts (δ_H) of 7.01 (1H, s), 7.05 (1H, d, *J* = 8.0 Hz) and 6.90 (1H, *J* = 8.0 Hz) which symbolizes ABX system in aromatic group. Also at δ_H 6-9 ppm, in addition to aromatic signals, there were also two other signals at δ_H 7.60 and 6.28 ppm with integration 1 proton on each signal. Both of these signals have a coupling constant of 16.0 Hz, which corresponds to signals from trans-alkenes [Supratman, 2010].

In the ^{13}C spectrum there are 4 quaternary carbons (these carbon is not correlated with the proton on the HSQC spectrum), at the chemical shifts (δ_c) 126.98, 148.01, 146.80 and 167.75 ppm. The quaternary carbon at δ_C 167.75 ppm is a typical signal for a carbonyl group. Again in

^{1}H NMR there are two singlet signals with integration equal to 3H at δ_H 3.78 and 3.90, indicating the presence of methoxy. One of the methoxy (δ_H 3.78 ppm) correlates with the carbonyl, indicating presence of an ester. From its HMBC correlations, this ester is attached to a trans-alkene. The other methoxy group (δ_H 3.90 ppm) correlates with carbon at δ_C 146.80 ppm, where that carbon also correlates with C-2 benzene, indicating the methoxy is bound to C-4 benzene.

On the basis of this spectral evidence and comparison with literature data, the compound was characterized as Methyl ferulate, a cinnamate derivative [Ilmiawati1 et. al., 2020] which is a phenolic compound. The obtained NMR data are presented in Table 3.16. The structure and NMR spectra are presented in Figures 3.23 to 3.36.

Table 3.16: ^{1}H NMR ($CDCl_3$, 400 MHz) and ^{13} C NMR ($CDCl_3$, 100 MHz) NMR and 2D spectrum data for CL-4

position	δ_H (mult., *J* in Hz)	δc	COSY	HMBC
1	--------	126.98	---------	--------
2	7.05 (1H, d, *J* = 8.0 Hz)	123.05	6.90	146.80, 148.01, 115.20
3	6.90 (1H, d, *J* = 8.0 Hz)	115.20	7.05	123.05, 146.80, 148.01
4	-------	146.80	------	-------
5	-------	148.01	-------	--------
6	7.01(1H,s)	109.42	------	146.80, 148.01
7	7.60 (1H, d, *J* = 16.0 Hz)	144.98	6.28	109.42, 114.77, 167.75
8	6.28 (1 H, d, *J* = 16.0 Hz)	114.77	7.60	144.98, 167.75, 126.98
9	-------	167.75	------	--------
10	3.90 (3H, s)	56.02	------	146.80
11	3.78 (3H, s)	51.62	-------	144.98

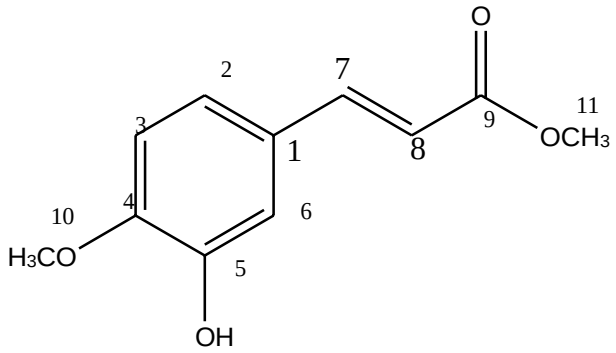

Figure 3.23: Structure of CL-4

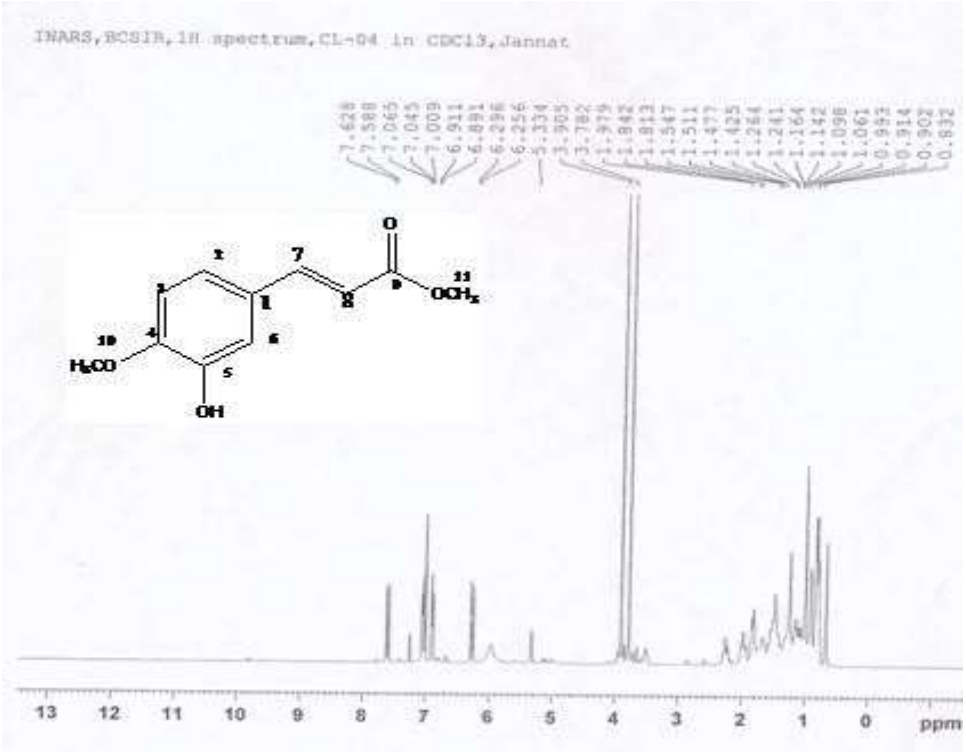

Figure 3.24: ^{1}H NMR spectrum of CL-4 (Full)

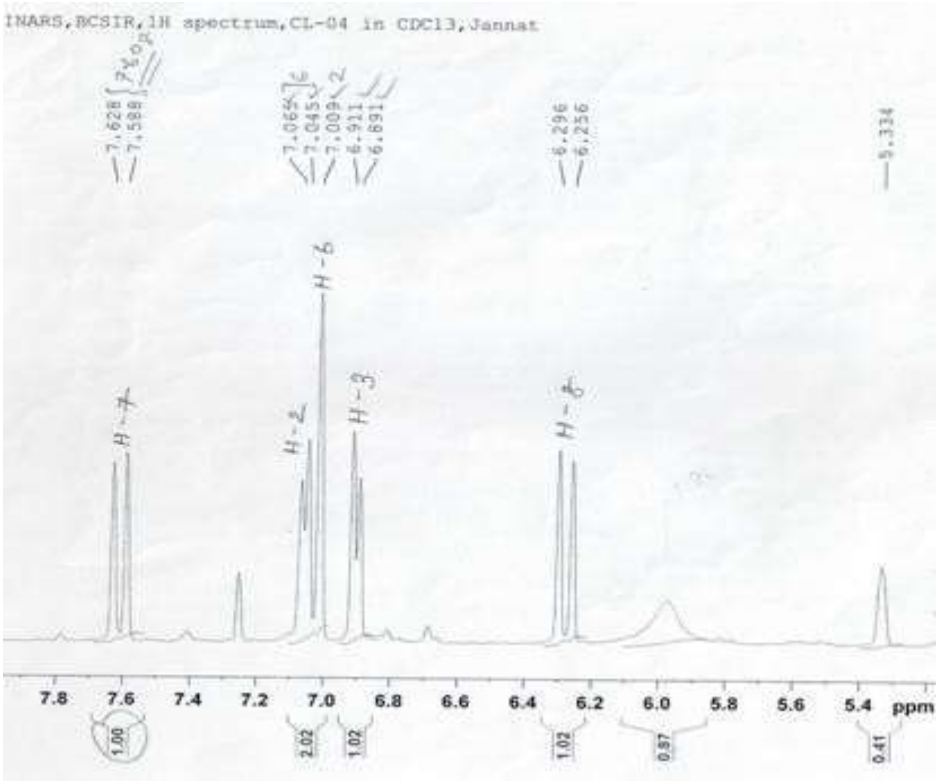

Figure 3.25: ^{1}H NMR spectrum of CL-4 (Expanded)

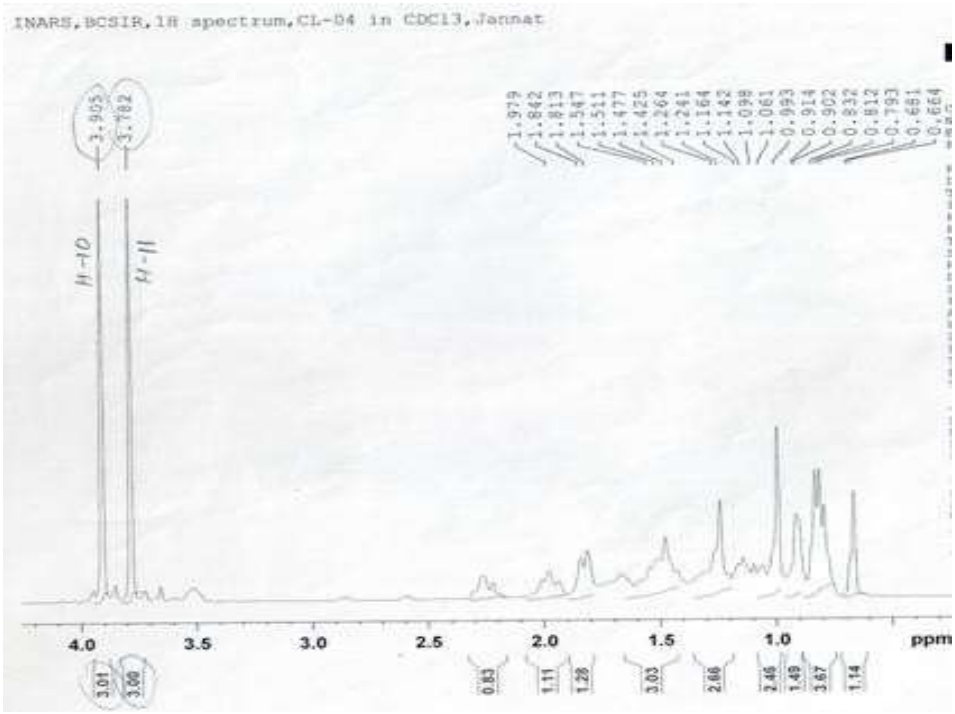

Figure 3.26: ^{1}H NMR spectrum of CL-4 (Expanded)

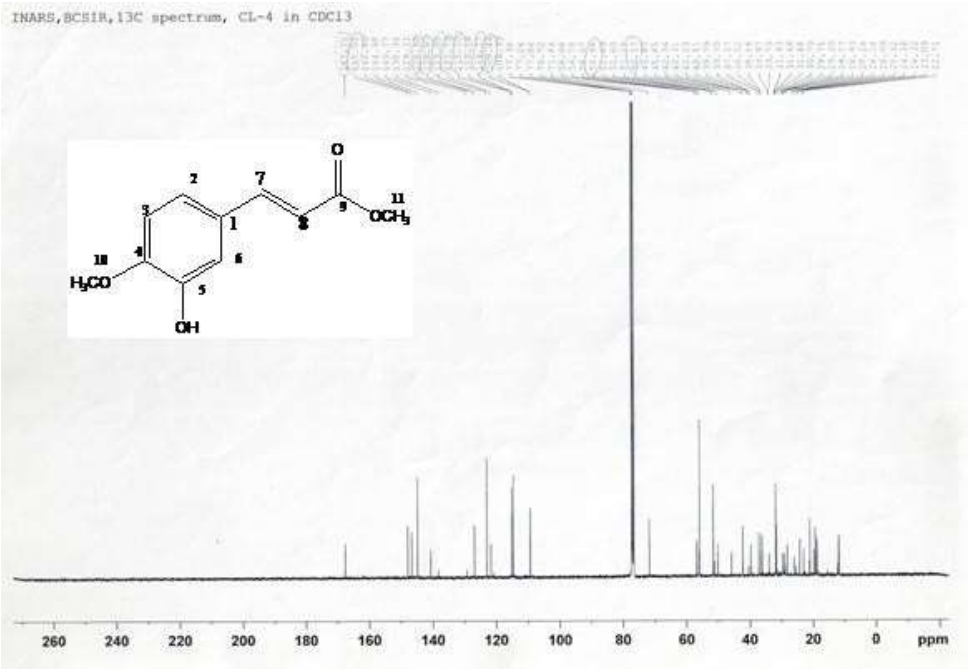

Figure 3.27: ^{13} C NMR of CL-4 (Full)

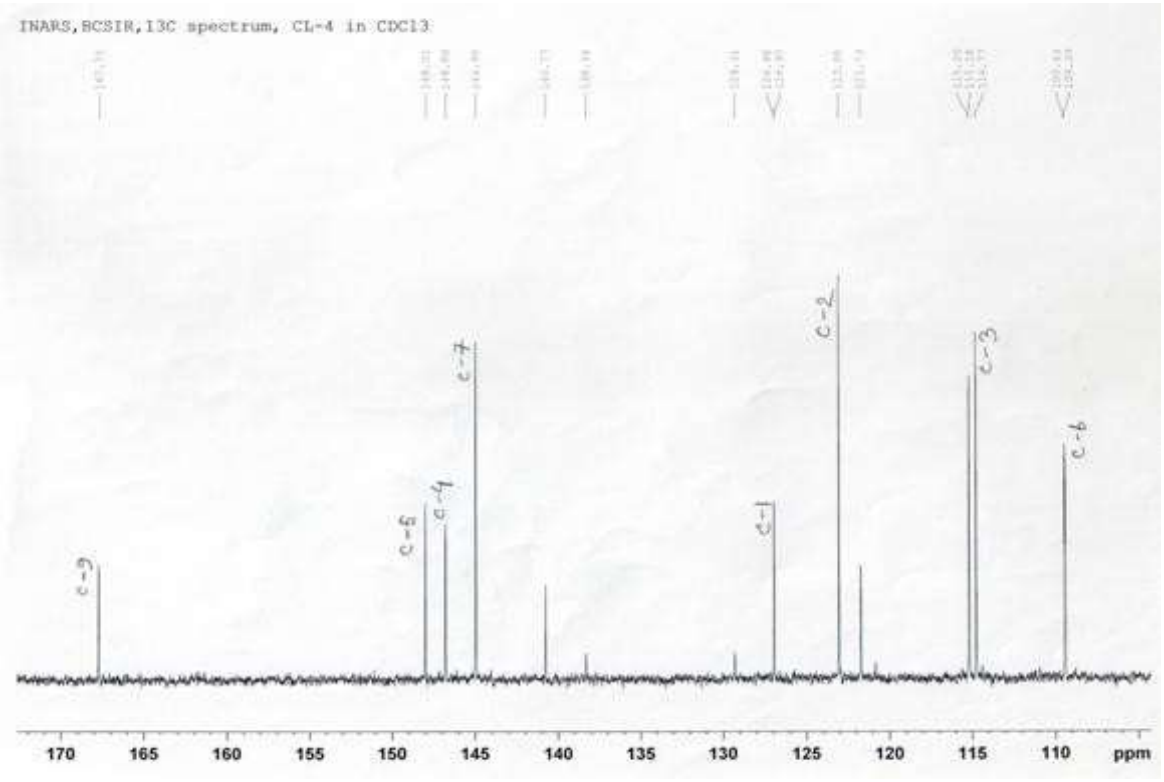

Figure 3.28: ^{13} C NMR of CL-4 (Expanded)

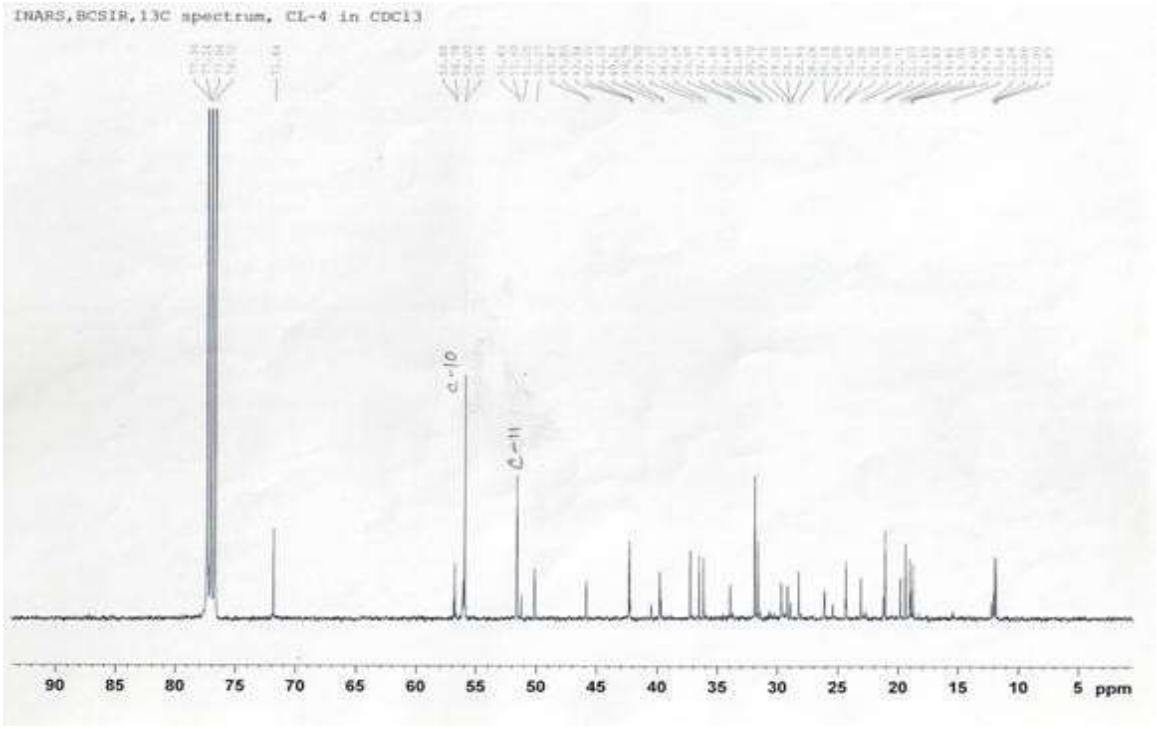

Figure 3.29: ^{13} C NMR of CL-4 (Expanded)

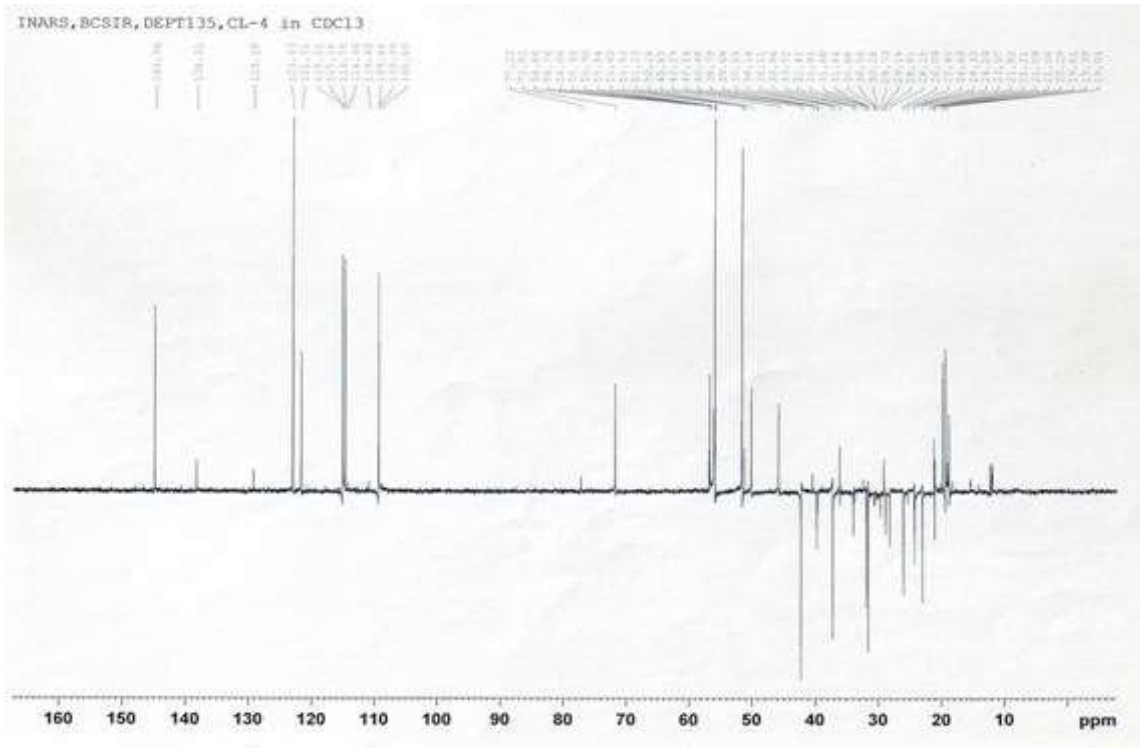

Figure 3.30: DEPT-135 (Distortionless enhancement by polarization transfer) spectrum of CL-4

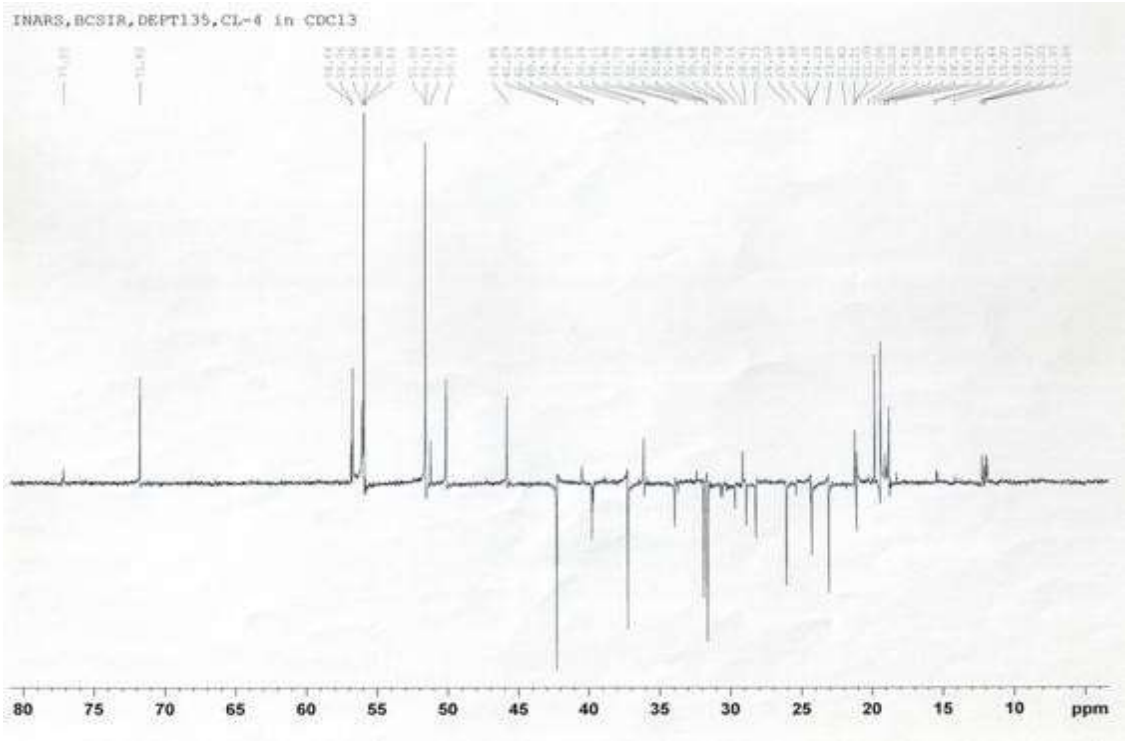

Figure 3.31: DEPT-135 of CL-4

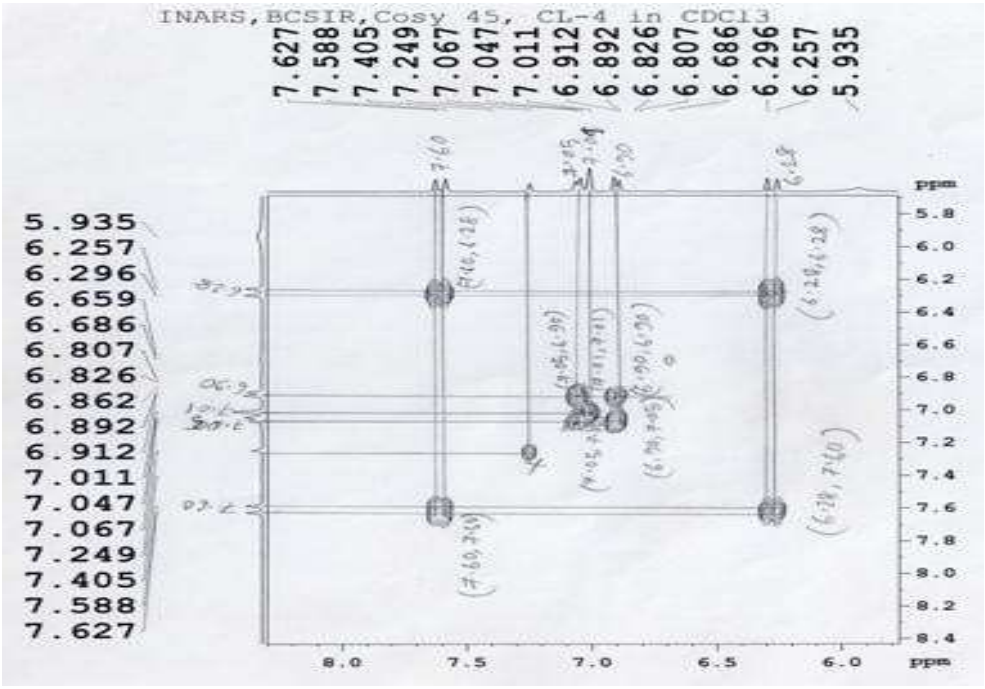

Figure 3.32: COSY (^{1}H-^{1}H Correlation spectroscopy) spectrum of CL-4

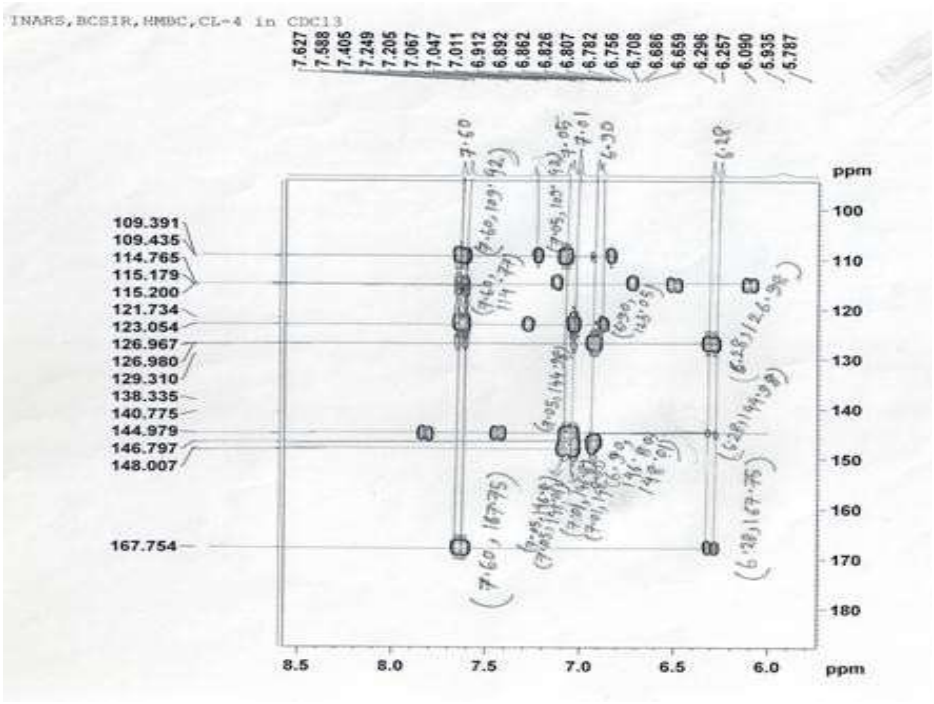

Figure 3.33: HMBC (Heteronuclear multiple bond correlation) spectrum of CL-4

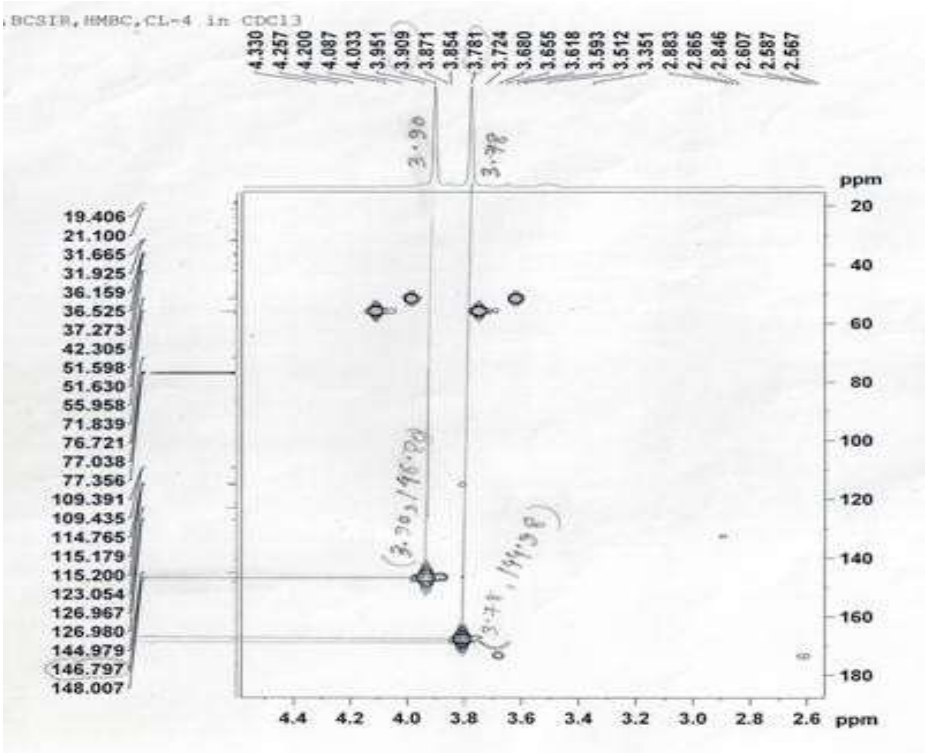

Figure 3.34: HMBC spectrum of CL-4

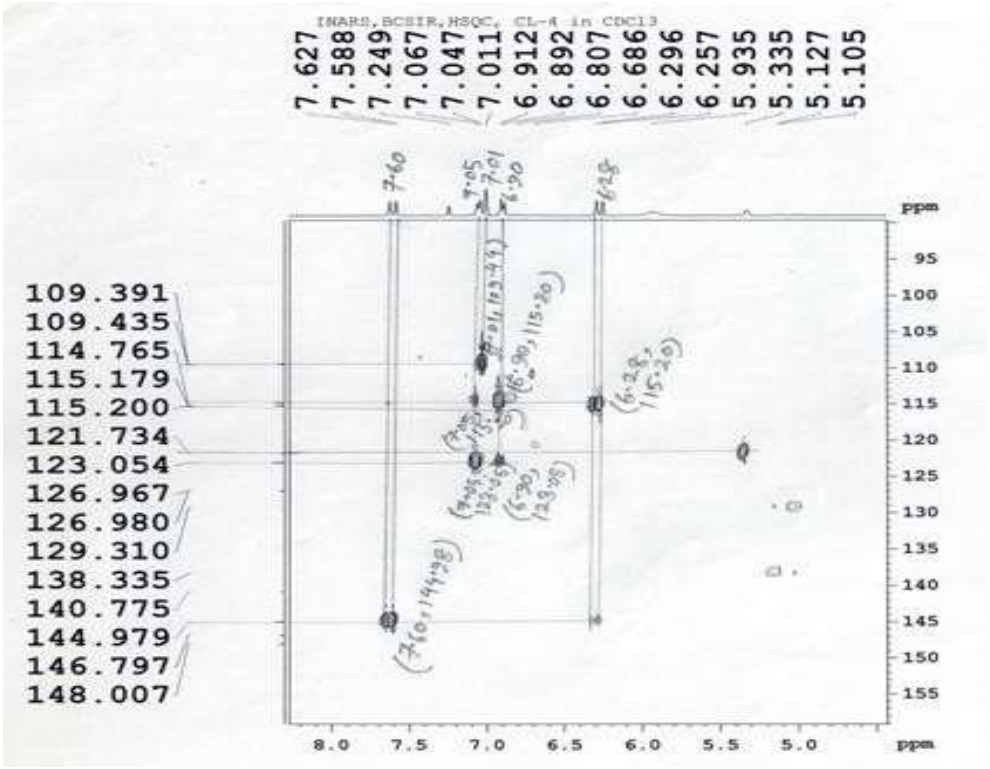

Figure 3.35: HSQC (Heteronuclear single quantum coherence or heteronuclear single quantum correlation) spectrum of CL-4

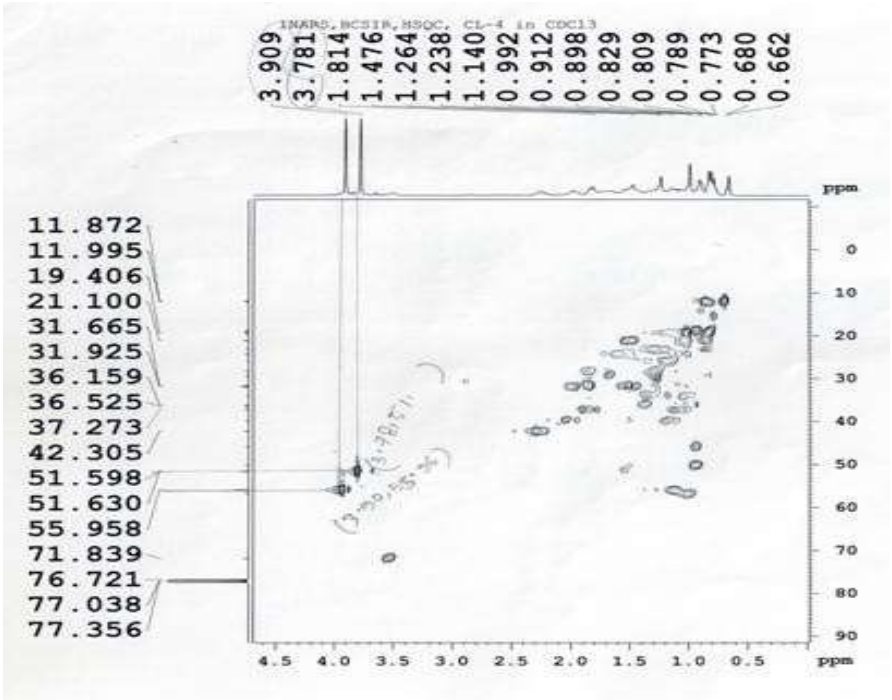

Figure 3.36: HSQC spectrum of CL-4

3.5.2. Structure elucidation of compounds isolated from endophytic fungus *Clonostachys rosea* (CLRE-3) from the plant *C. longa*

The endophytic fungus *Clonostachys rosea* produces a wide range of secondary metabolites, including bioactive substances like terpenoids, polyketides, and nitrogen-containing molecules. Because of their antimicrobial, cytotoxic, antileishmanial, and antimalarial properties, these compounds have a lot of potential for use in pharmaceutical and agrochemical applications. According to a review report published on published on 2020 by Han et.al., several metabolites from *Clonostachys rosea* such as Glioperazine, Verticillin D, Clonostalactam, Alternariol, Alternariol-5-O-methyl ether, Sorbicillin, Dihydrotrichodimer ether A, Dihydrotrichodimer ether B, Tetrahydrotrichodimer ether, Dihydrotrichodimerol, Tetrahydrotrichodimerol, Trichodimerol, 3,5-Dihydroxyfuran-2(5H)-one, Sapinofuranone B, (-)-Vertinolide, (-)-Dihydrovertinolide, TMC-151(A-F), Eburicol, Clonostach acid (A-C) have been reported [Han et.al., 2020]. Again in another review published in 2024, Shi et. al., reported some secondary metabolites isolated from *Clonostachys rosea* such as phenalenones, glycosylated compounds [Shi et. al., 2024]. The structural analysis involved GC-MS analysis.

In the present study, four compounds have been isolated from the *C. rosea* endophytic fungus. Among these, Bassiatin, 8-O-methyl nectriafurone and 8-O-methyl bostrycoidin compounds were isolated from this fungus for the first time. The obtained NMR data were compared to relevant literature that helped solve the structure of the isolated compound. The compounds are described below.

1. Characterization of compound CLE-7 as Bassiatin

CLE-7 was obtained as white crystals (12 mg) (R_f = 0.55, toluene/20% ethyl acetate). In the ^{1}H NMR spectrum, signals of two methyl protons (δ_H 0.87 (3H, d, *J*=6.8 Hz), 0.79 (3H, d, *J*=6.8 Hz)), one N-methyl proton (δ_H 3.05 (3H, s)), three methine protons (δ_H 4.44 (1 H, t, *J*=4.4 Hz), 3.03 (1 H, d, *J*=2.0 Hz), 2.33 (1H,m)), one methylene group (δ_H 3.22 (1H,dd,J=14.0, 4.4 Hz) and 3.31 (1H, dd, J= 14.0, 4.0 Hz)) and five aromatic protons (δ_H 7.35 (3H, m), 7.15 (2H,m)) were observed.

One and two-dimensional NMR spectra analysis, including COSY and HMBC, led to the assignment of the structure ‘a’ as shown in Figure 3.37. In this structure, the (C3-C10), (C12-

C13-C14-C15-C16) and (C9-C7-C8) portions were assigned by tracing of cross peaks in the COSY spectrum. The ring moiety of the structure was also disclosed by HMBC correlation of (4-CH_3/C-5), (4-CH_3/C-3) and (6-H/C-5, 6-H/C-9, 6-H/C-8).

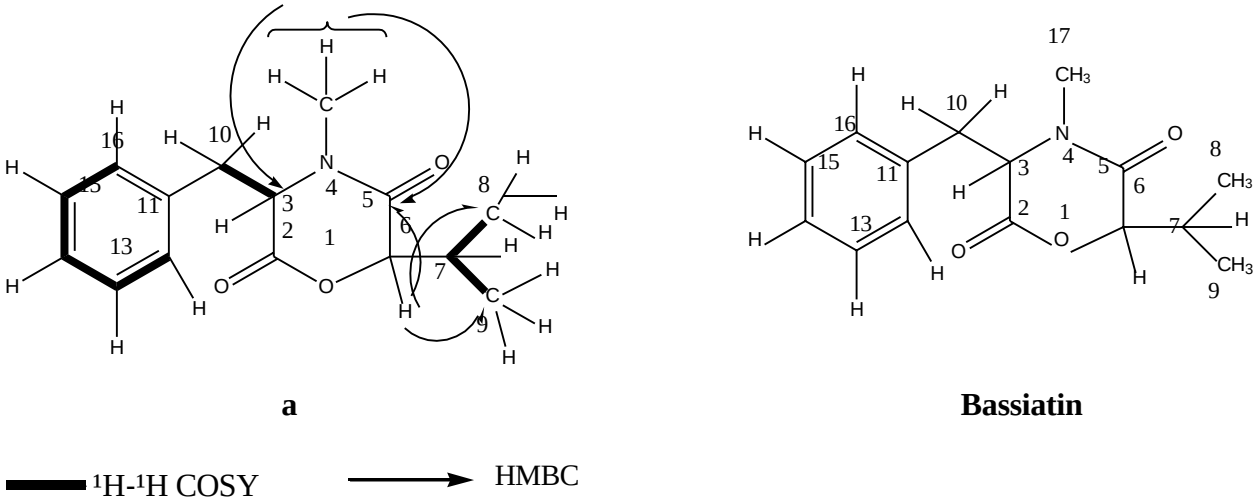

Figure 3.37: Connectivities of CLE-7 (a) and structure of CLE-7

Based on this spectral evidence (^{1}H, ^{13}C-NMR, DEPT-135 and 2D-NMR) and comparison with literature data, the compound was characterized as Bassiatin [Kagamizono et. al., 1995; Ola et. al., 2014], which is a depsipeptide compound composed of N-methyl phenyl alanine and 2-hydroxy-3-methyl butyric acid. The obtained NMR data are presented in Table 3.17. NMR spectra are presented in Figures 3.38 to 3.52.

Table 3.17: ^{1}H NMR ($CDCl_3$, 400 MHz) and ^{13} C NMR ($CDCl_3$, 100 MHz) NMR and 2D spectrum data for CLE-7

position	δ_H (mult., *J* in Hz)	δc	COSY	HMBC
2	---------	167.6	-------	-------
3	4.44 (1H, t, J=4.4 Hz))	62.8	3.22, 3.31	-------
4	3.05 (3H,s)	32.4		165.5, 62.8
5	--------	165.5	--------	
6	3.03 (d, J=2.0 Hz)	81.3	--------	165.5, 15.1, 18.6
7	2.33 (m)	29.7	0.79, 0.87	15.1, 18.6
8	0.87 (3H, d, J= 6.8 Hz)	18.6	2.33	81.3
9	0.79 (3H, d, J= 6.8 Hz)	15.1	2.33	18.6, 29.7, 81.3
10	3.22 (dd, J= 4.4, 14.0 Hz)	37.1	4.44	134.2, 167.2, 129.8, 62.8
	3.31 (dd, J= 4.0, 14 Hz)			129.2, 134.2, 129.8,
11	---------	134.2	-------	--------
12	7.15 m	129.8	7.35	128.2, 129.2, 37.1
13	7.35 m	129.2	7.15	129.8, 134.2
14	7.35 m	128.2	7.15	129.8, 134.2
15	7.35 m	129.2	7.15	129.8, 134.2
16	7.15 m	129.8	7.35	128.2, 129.2, 129.8, 37.1

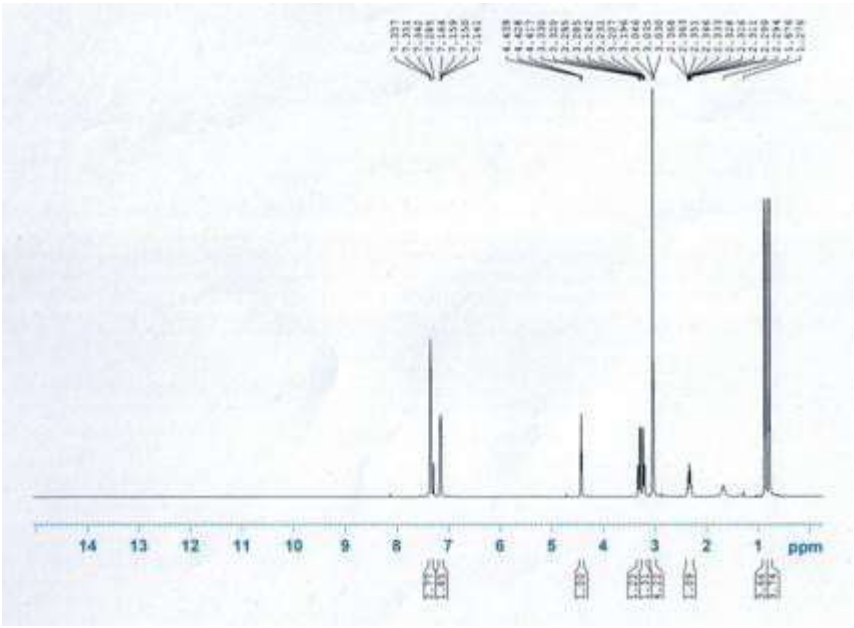

Figure 3.38: ^{1}H NMR spectrum of CLE-7 (Full)

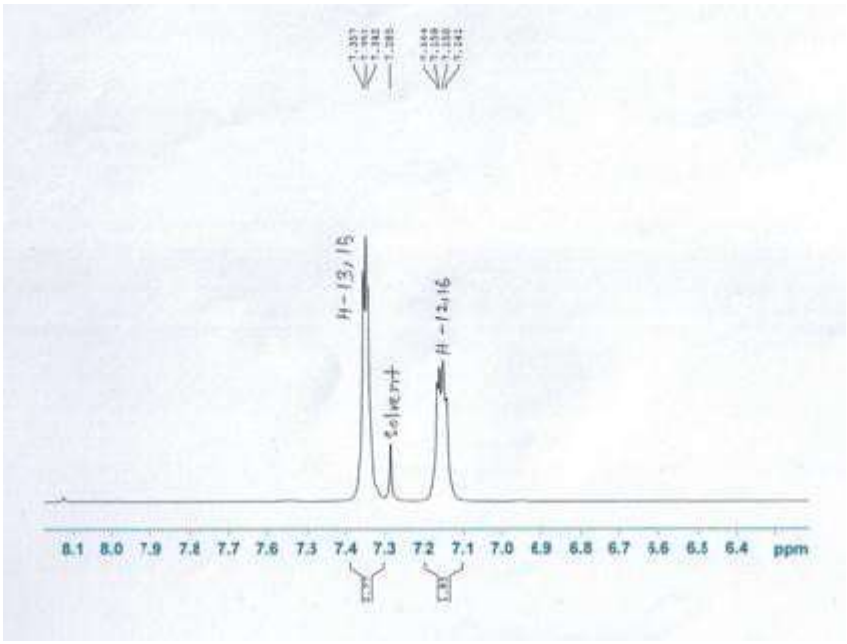

Figure 3.39: ^{1}H NMR spectrum of CLE-7 (Expanded)

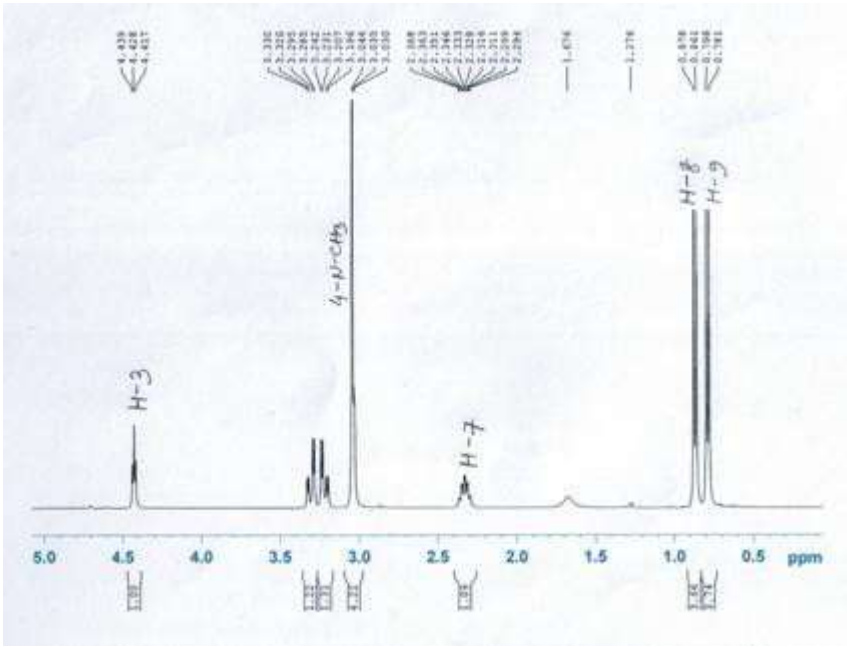

Figure 3.40: ^{1}H NMR spectrum of CLE-7 (Expanded)

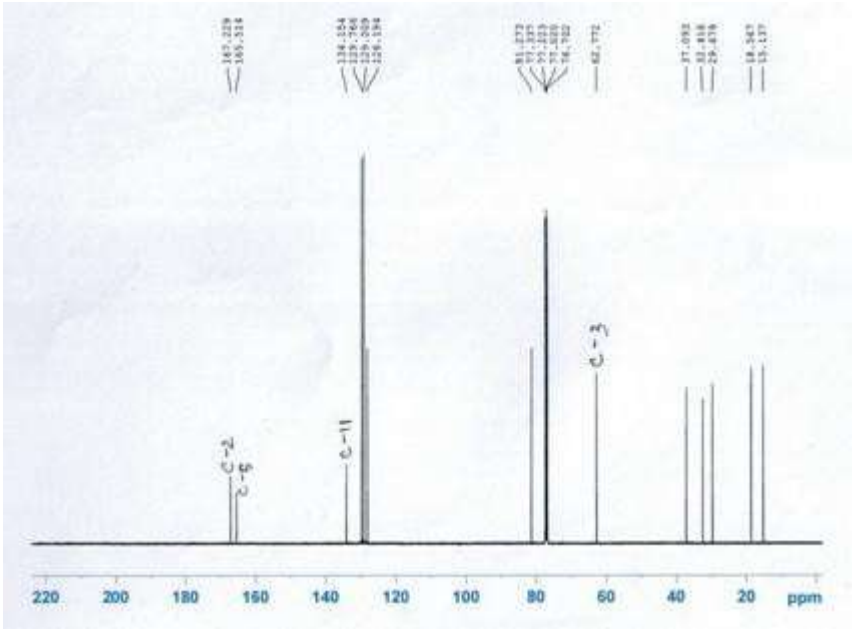

Figure 3.41: ^{13}C NMR spectrum of CLE-7 (Full)

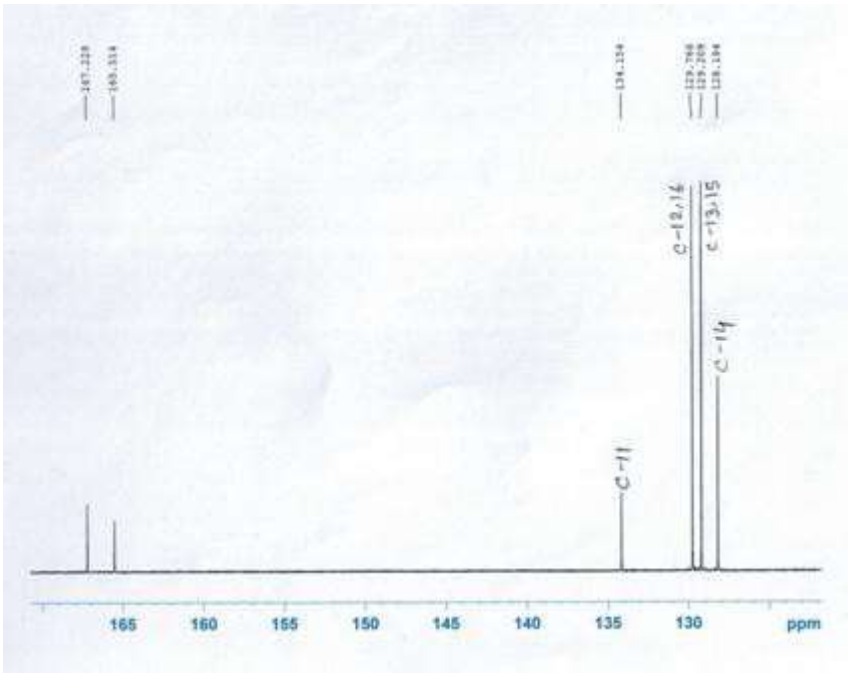

Figure 3.42: ^{13}C NMR spectrum of CLE-7 (Expanded)

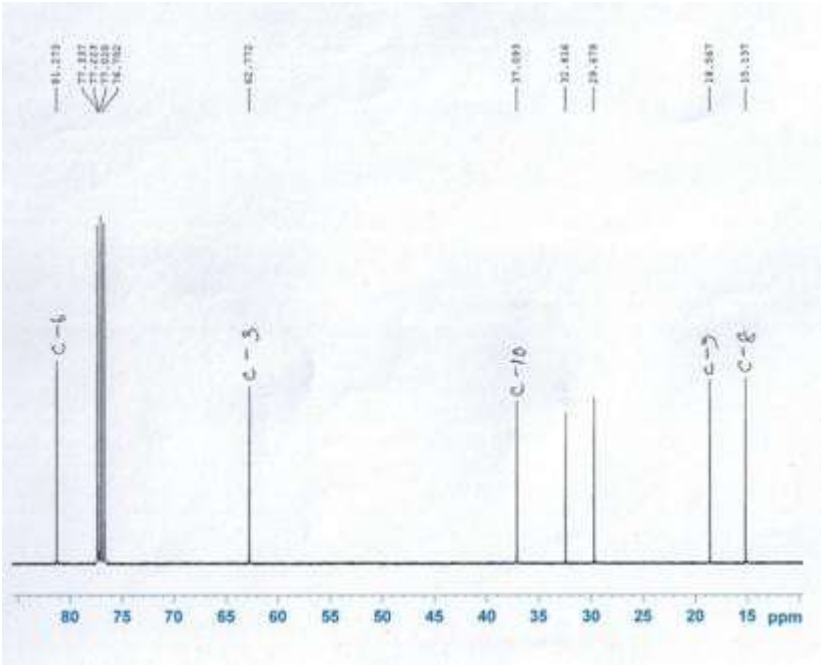

Figure 3.43: ^{13}C NMR spectrum of CLE-7 (Expanded)

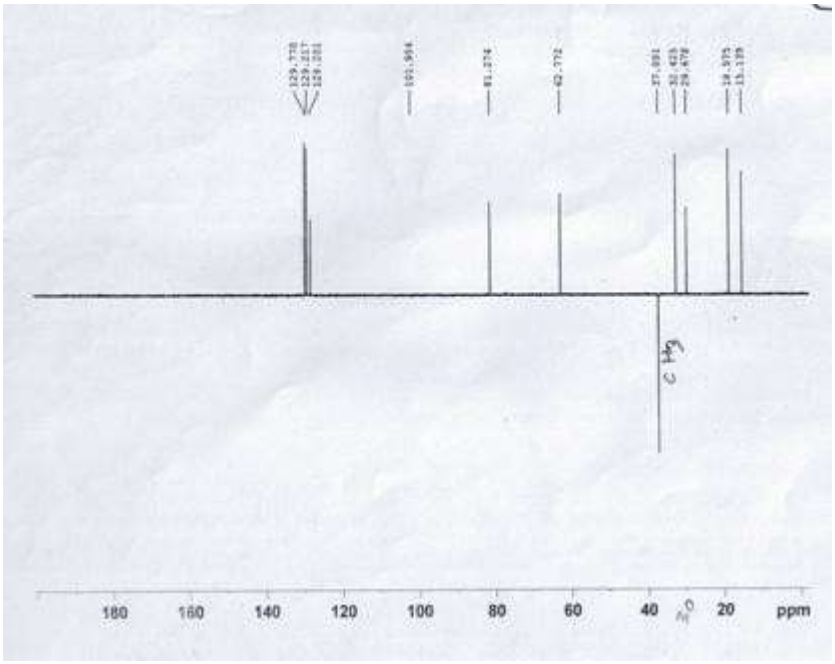

Figure 3.44: DEPT-135 spectrum of CLE-7

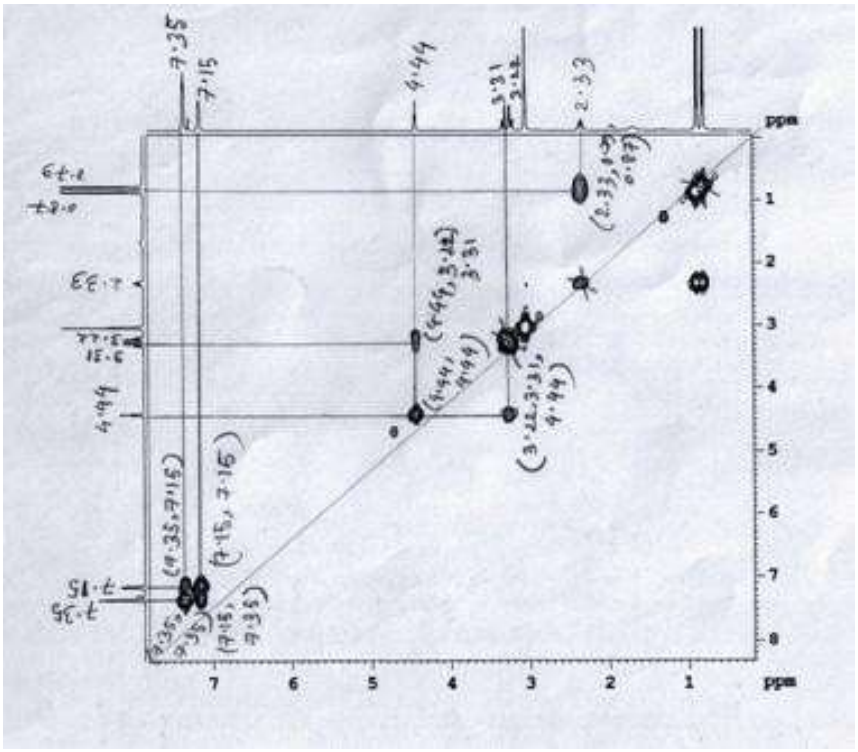

Figure 3.45: ^{1}H-^{1}H COSY spectrum of CLE-7

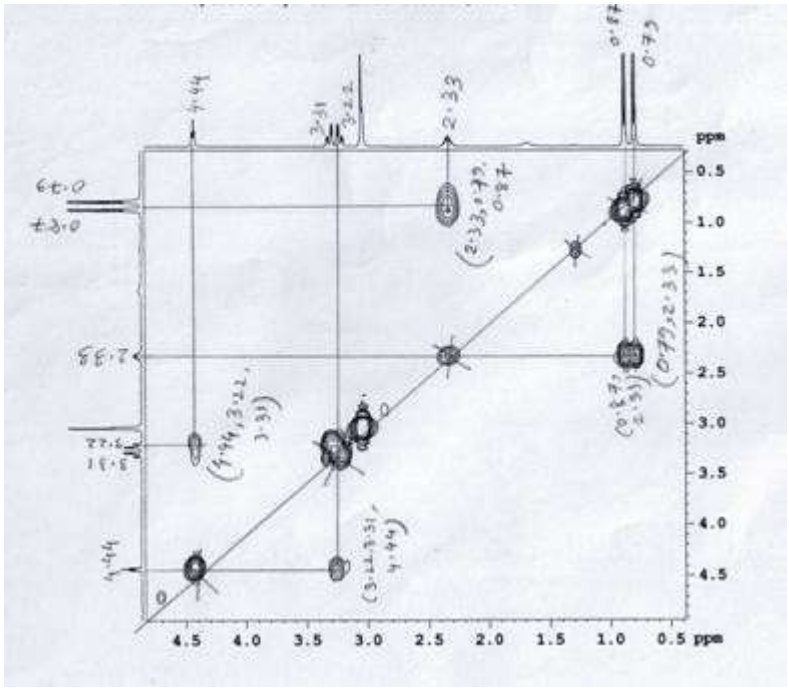

Figure 3.46: ^{1}H-^{1}H COSY spectrum of CLE-7

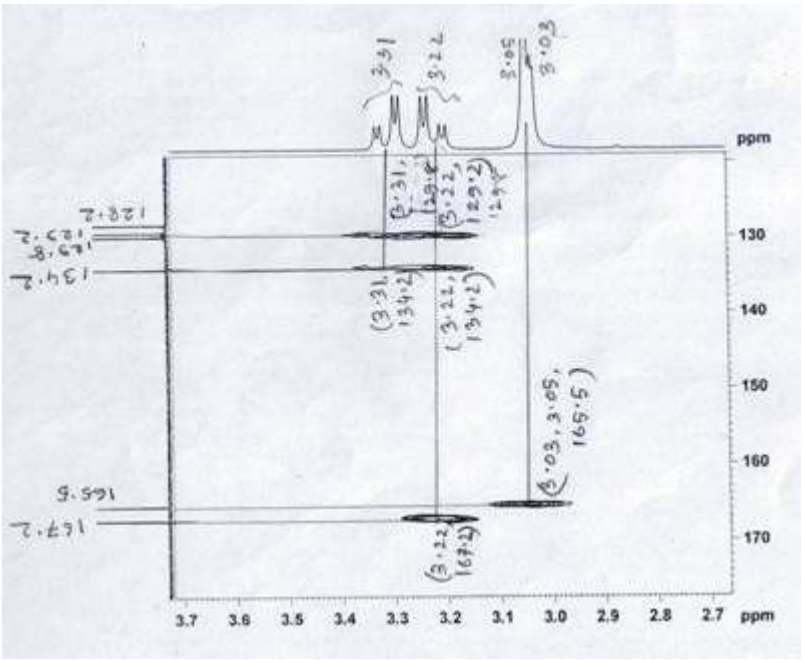

Figure 3.47: HMBC spectrum of CLE-7

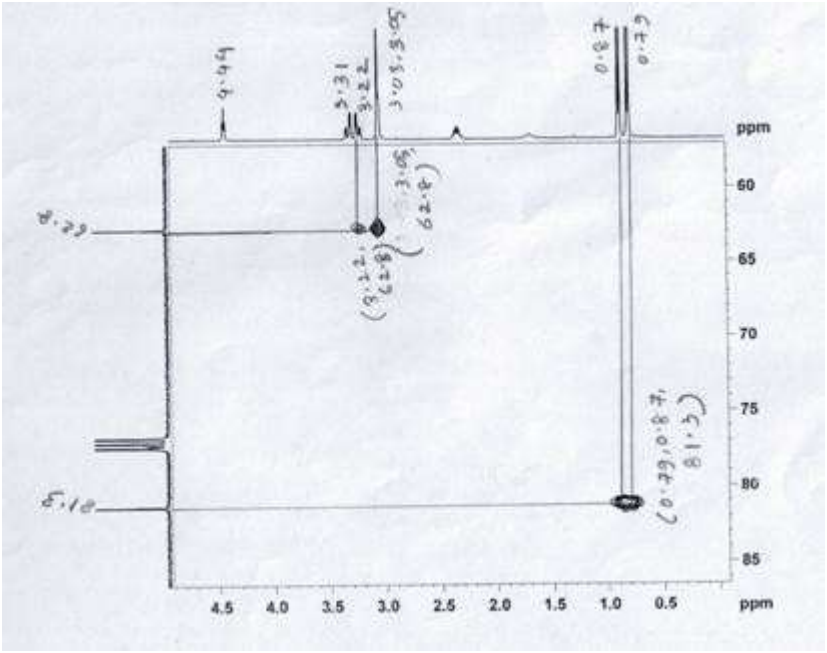

Figure 3.48: HMBC spectrum of CLE-7

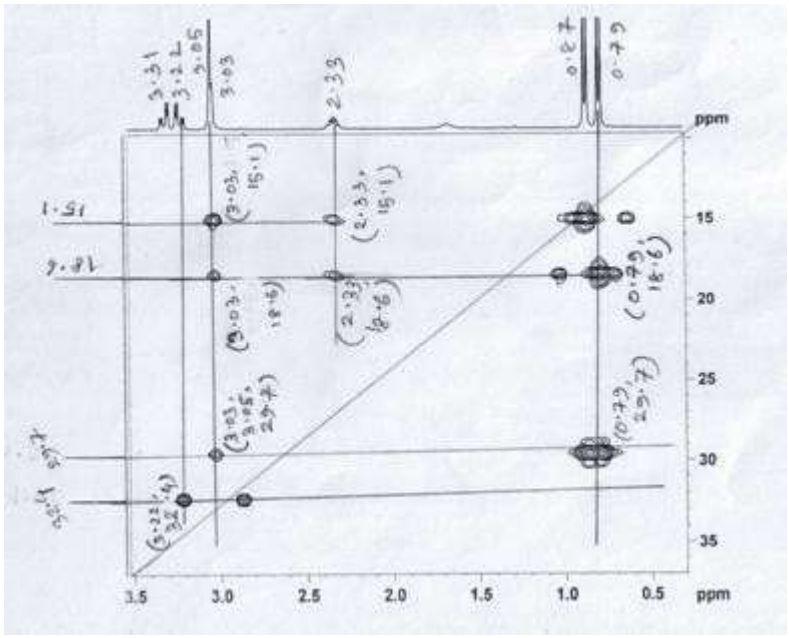

Figure 3.49: HMBC spectrum of CLE-7

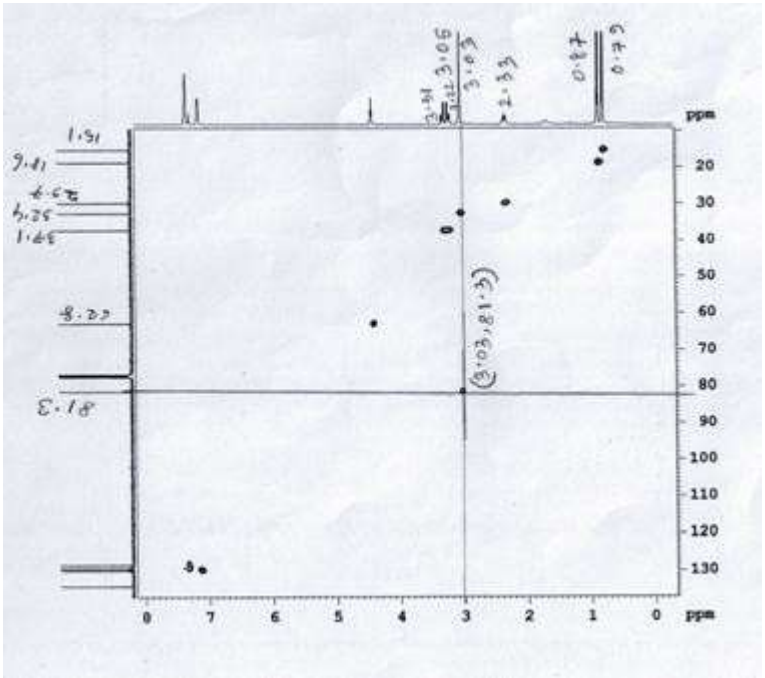

Figure 3.50: HSQC spectrum of CLE-7

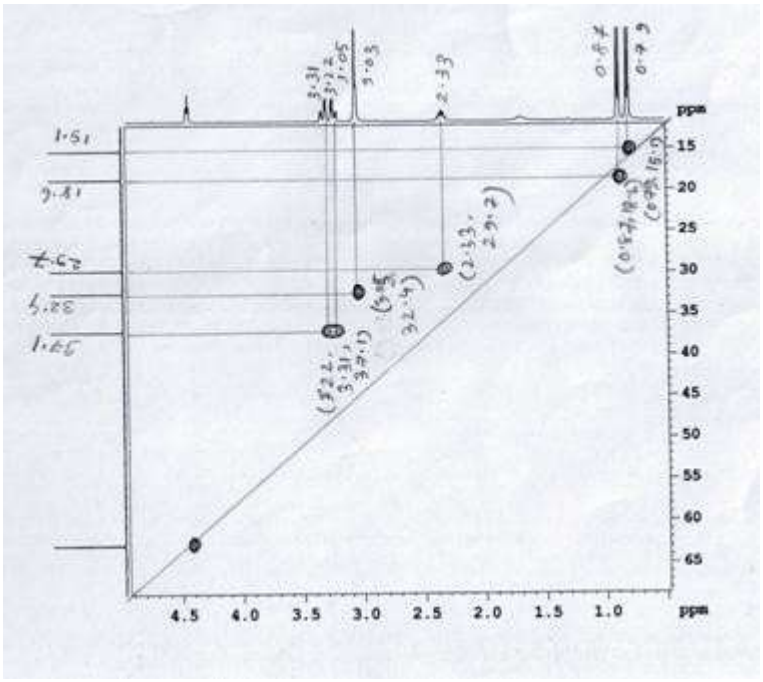

Figure 3.51: HSQC spectrum of CLE-7

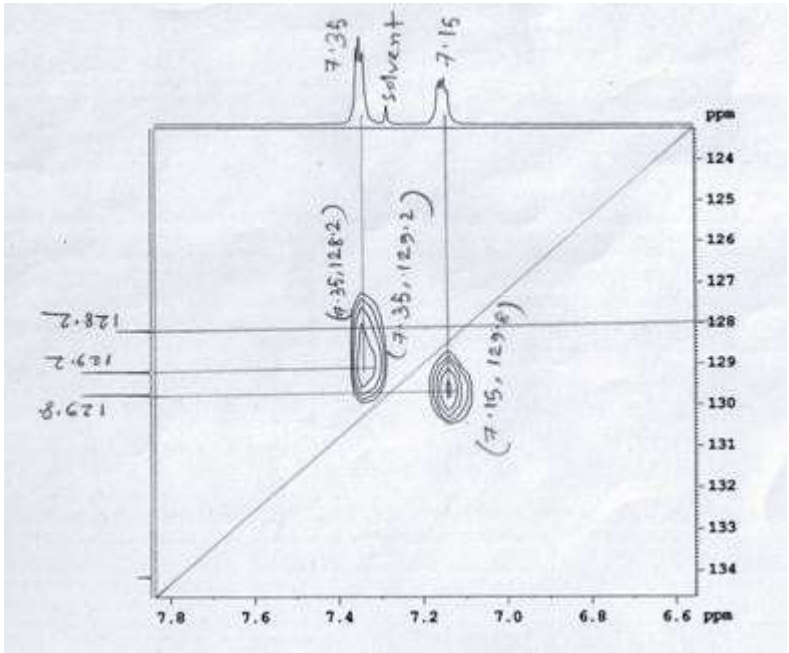

Figure 3.52: HSQC spectrum of CLE-7

2. Characterization of compound CLE-14 as Nectriafurone

CLE-14 was obtained as a yellow-brown crystal (10 mg) (R_f = 0.42, toluene/20% ethyl acetate). A dark quenching spot was seen on the TLC plate under UV light at 254 nm and a bright yellow spot was seen under UV light at 365 nm. In the ^{1}H NMR spectrum, the resonance of two 1H singlets at δ 13.44 and δ 13.12 ppm could be attributed to phenolic hydroxyl groups attached to C-5 and C-8 positions chelated with carbonyl groups. The ^{1}H NMR also showed the presence of singlets at δ 4.03 and δ 1.67 for methoxy and methyl groups in the molecule. But a unique system emerged at δ 1.67 (d, 3H) and 5.22 (q, 1H) specified a Me-CH-OH substitution, this being further maintained on the acetate of the structure. The singlet observed at δ 8.11 (1H) for the acetate, was typical of the isofuranic proton at C-3 as already ascertained for a similar benzoquinone isofuran [Cragg et. al., 1975]. The ^{1}H singlet in the aromatic region at δ 6.73 ppm is integrated for the proton attached to C-6 position.

In the ^{13}C NMR spectrum, carbonyl carbons may be responsible for the resonance at δ 182.2 and δ 186.1 ppm. Three aromatic carbon signals δ 157.5, δ 161.0 and δ 150.6 ppm are attached to the oxygen atom. The signals at δ 56.7 and δ 21.1 ppm indicated the methoxy and methyl carbons present in the molecule.

The 2D NMR spectra analysis including COSY and HMBC led to the assignment of the structure ‘a’ as shown in Figure 3.53. In this structure, the (C10-C11) was assigned by tracing of cross peaks in the COSY spectrum. The ring moiety of the structure was also disclosed by HMBC correlation of (11-CH_3/C-1), (6-H/C-7), (12-CH_3/C-7) and (3-H/C-9a).

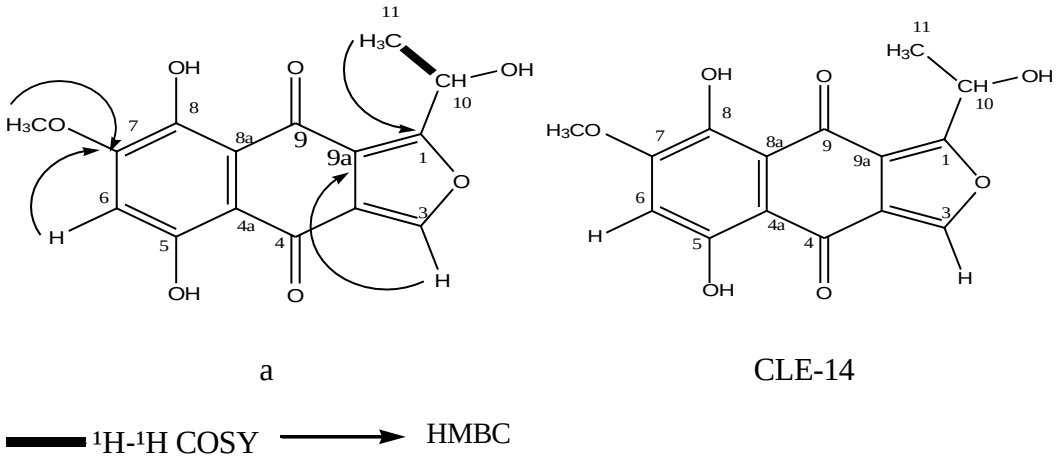

Figure 3.53: Connectivities of CLE-14 (a) and structure of CLE-14

On the basis of this spectral evidence (^{1}H, ^{13}C-NMR, DEPT-135 and 2D-NMR) and comparison with literature data, the compound was characterized as Nectriafurone [Kagamizono et. al., 1995; Ola et. al., 2014], which is a quinone type compound. The obtained NMR data are presented in Table 3.18. NMR spectra are presented in Figures 3.54 to 3.61.

Table 3.18: ^{1}H NMR ($CDCl_3$, 400 MHz) and ^{13} C NMR ($CDCl_3$, 100 MHz) NMR and 2D spectrum data for CLE-14

position	δ_H (mult., *J* in Hz)	δ_c	COSY	HMBC
1		166.6		
3	8.11 (1 H, s)	143.1 (CH)		117.1
4		182.2		
4a		114.1		
5	13.44 (1 H, s)	161.0 (C_5-OH)		
6	6.73 (1H, s)	107.2 (CH)		157.5
7		157.5		
8	13.12 (1 H, s)	150.6 (C_8-OH)		
8a		114.2		
9		186.1		
9a		117.1		
10	5.22 (1H, q, J= 13.6; 6.8 Hz)	64.3 (CH)	1.67	
11	1.67 (3H, d, J=6.4 hz)	21.1(CH_3)	5.22	64.3, 166.6
12	4.03 (3H, s)	56.7 (CH_3)		157.5

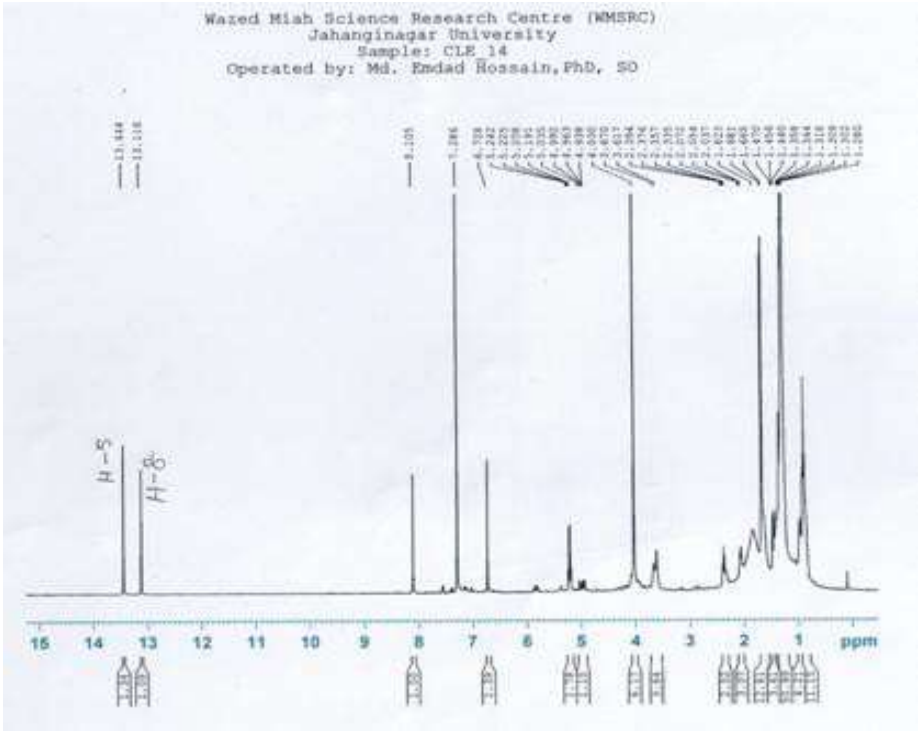

Figure 3.54: ^{1}H NMR spectrum of CLE-14 (Full)

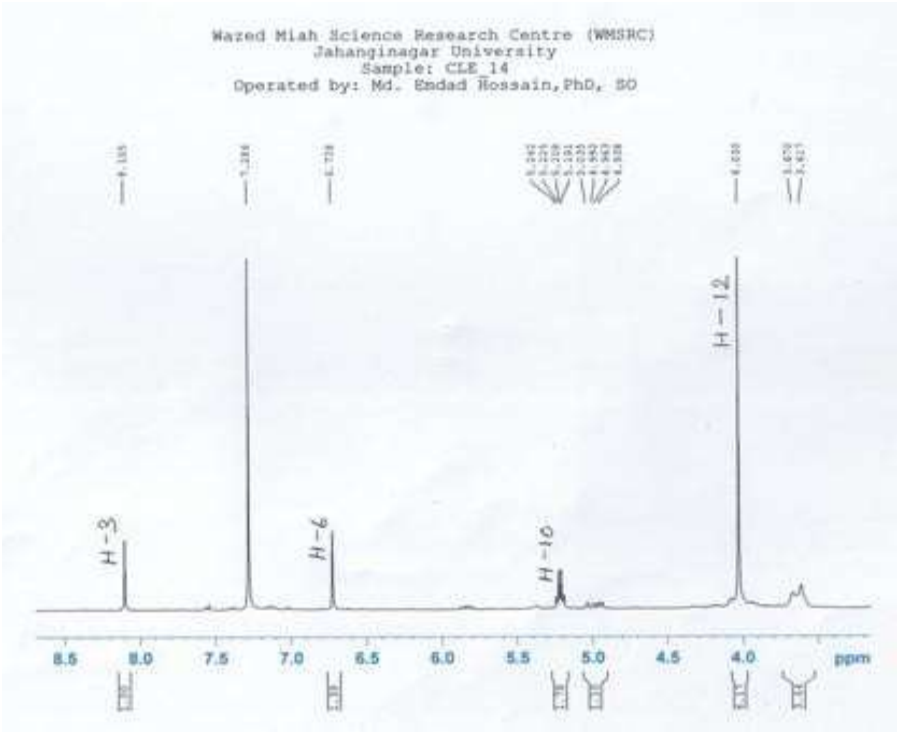

Figure 3.55: ^{1}H NMR spectrum of CLE-14 (Expanded)

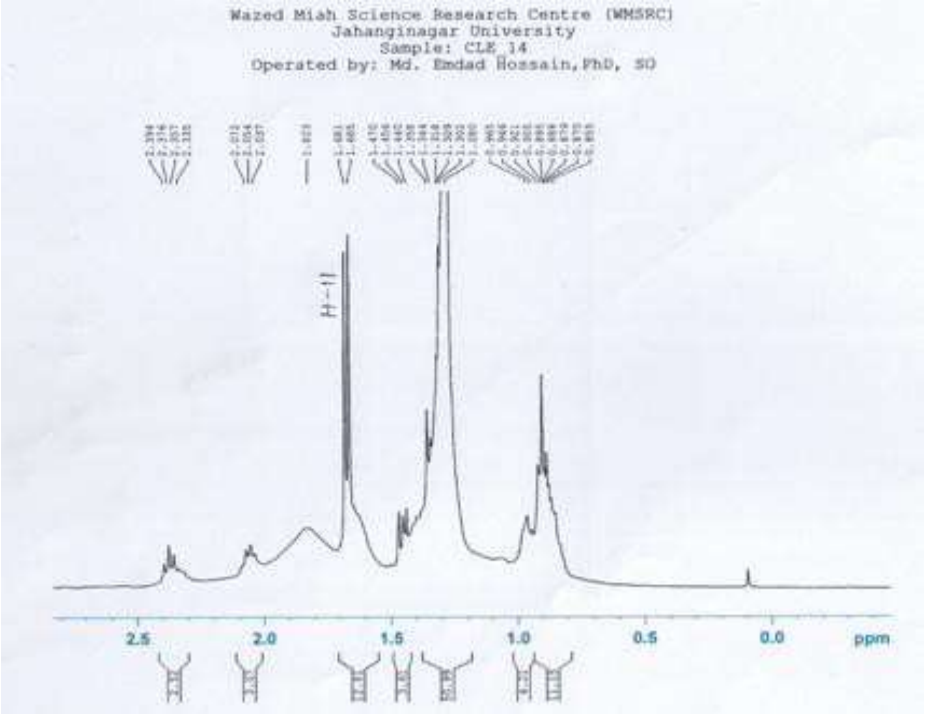

Figure 3.56: ^{1}H NMR spectrum of CLE-14 (Expanded)

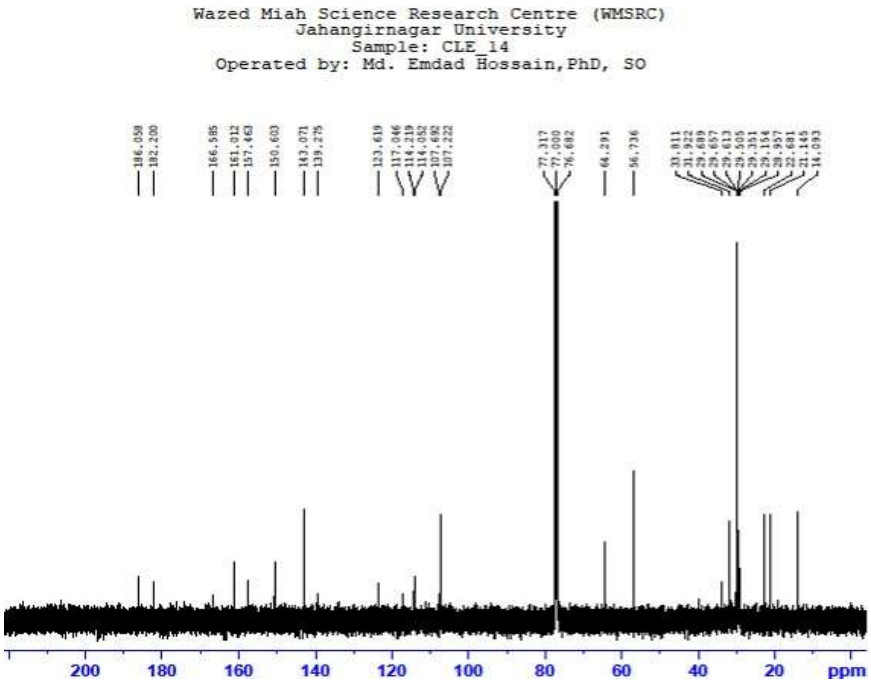

Figure 3.57: ^{13}C NMR spectrum of CLE-14 (Full)

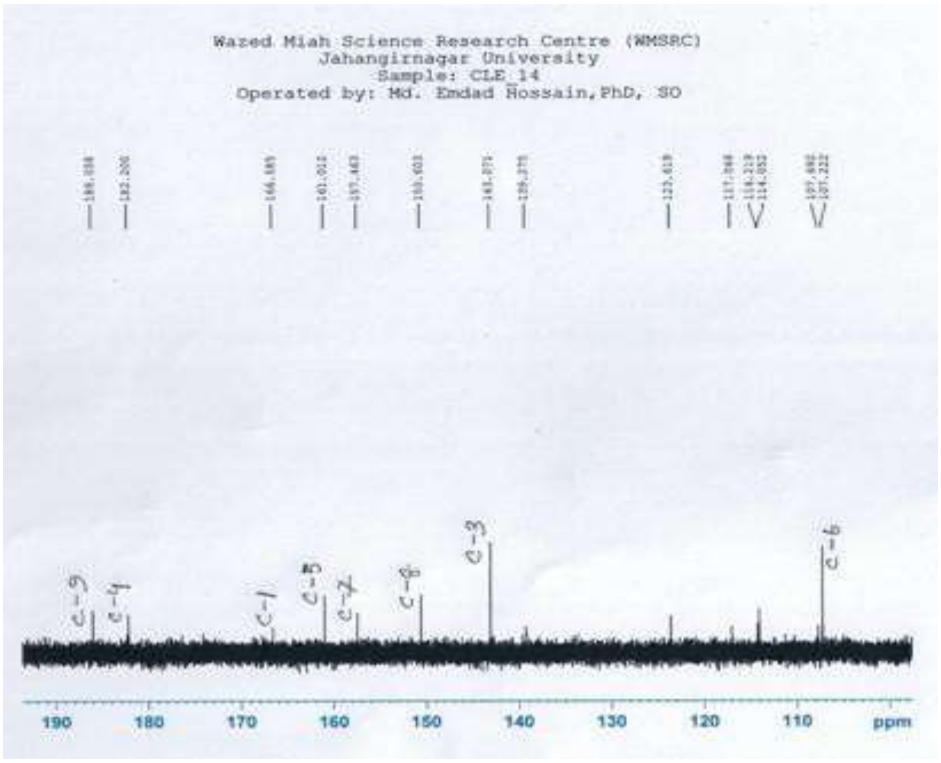

Figure 3.58: ^{13}C NMR spectrum of CLE-14 (Expanded)

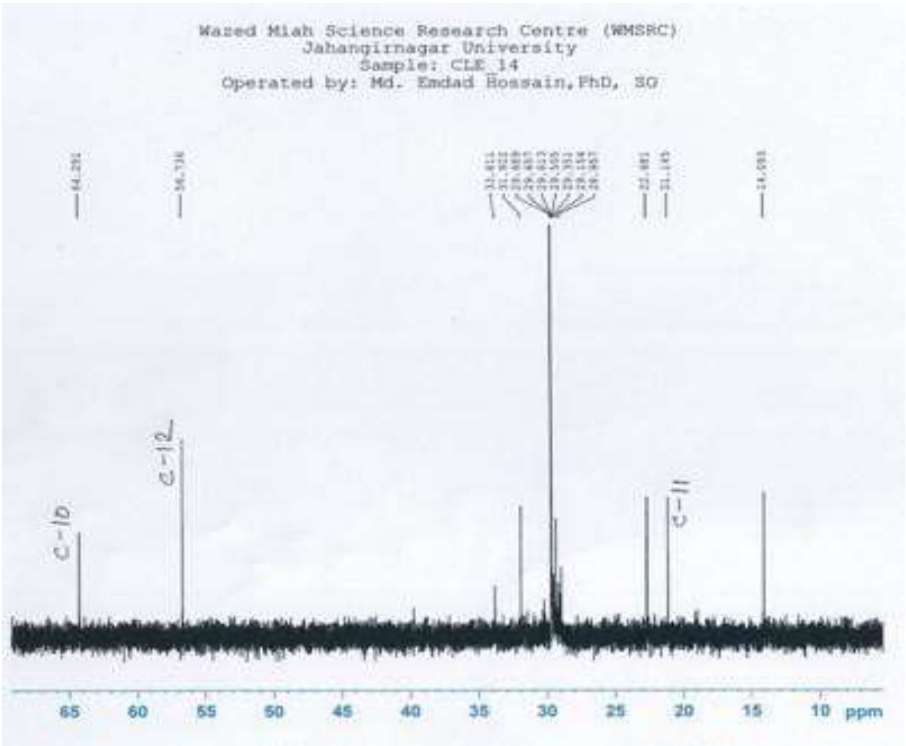

Figure 3.59: ^{13}C NMR spectrum of CLE-14 (Expanded)

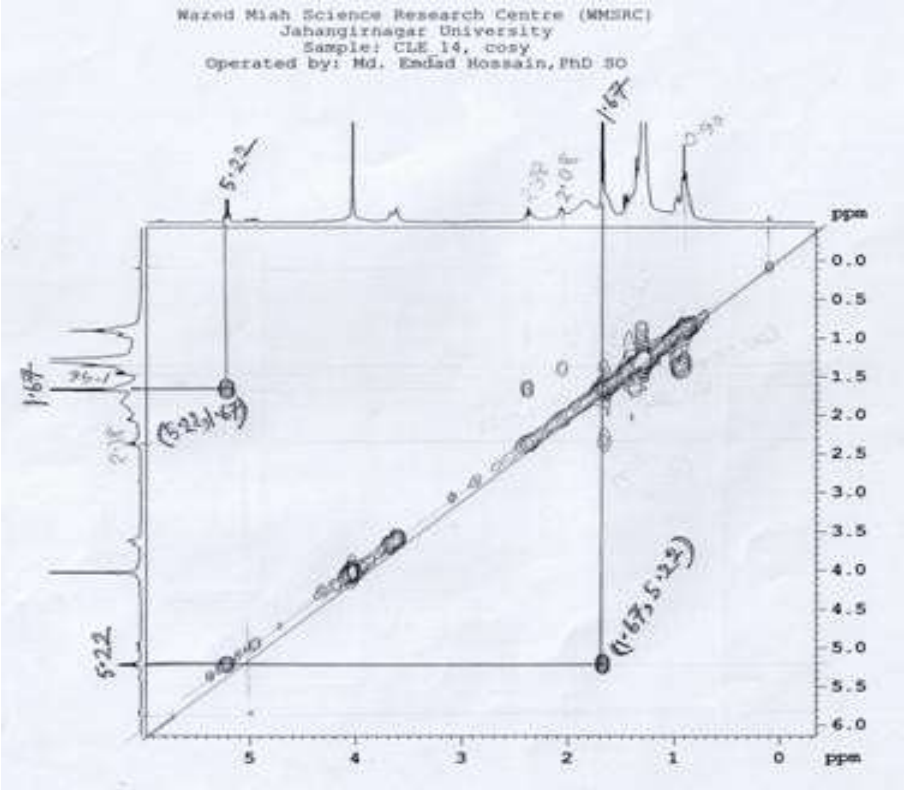

Figure 3.60: ^{1}H-^{1}H COSY spectrum of CLE-14

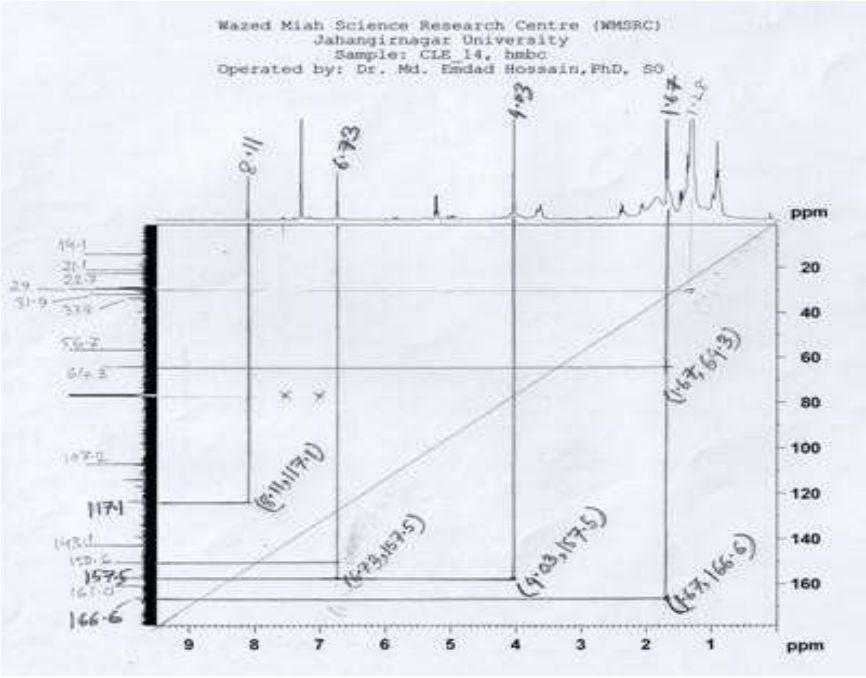

Figure 3.61: HMBC spectrum of CLE-14

3. Characterization of compound CLE-11 as 8-O-methyl Nectriafurone

Compound was also obtained as yellow-brown crystals (3 mg) (R_f = 0.45, chloroform/0.05% methanol). In the ^{1}H NMR spectrum, the resonance of one 1H singlet at δ 13.03 ppm could be attributed to phenolic hydroxyl groups attached to C-5 position chelated with the carbonyl group. The ^{1}H NMR also showed the presence of singlets at δ 4.01 and 4.03 for two methoxy groups and δ 1.65 for the methyl group in the molecule. A new system here also appeared as in Nectriafurone at δ 1.65 (d, 3H) and 5.17 (m, 1H) indicating a Me-CH-OH substitution, this being further supported on the acetate of the structure. The singlet at δ 8.01 (1H) was also observed for the acetate as in Nectriafurone. The ^{1}H singlet in the aromatic region at δ 6.86 ppm is integrated for the proton attached to the C-7 position.

Based on this spectral evidence and comparison with literature data, the compound was characterized as 8-O-methyl Nectriafurone [Tatum et. al., 1987], which is a derivative of Nectriafurone and quinone-type compound. The obtained NMR data are presented in Table 3.19. The structure of the compound and NMR spectra are presented in Figures 3.62 to 3.66.

Table 3.19: ^{1}H NMR ($CDCl_3$, 400 MHz) spectrum data for CLE-11

Position	**δ_H (mult., *J* in Hz)**
3	8.01(1H, s)
5-OH	13.03 (1 H,s)
6-OMe	4.01(3H,s)
8-OMe	4.03(3H, s)
7	6.86 (1 H,s)
10	5.17 (m, 1H)
11-CH_3	1.65(3H, d, J=6.8 Hz)

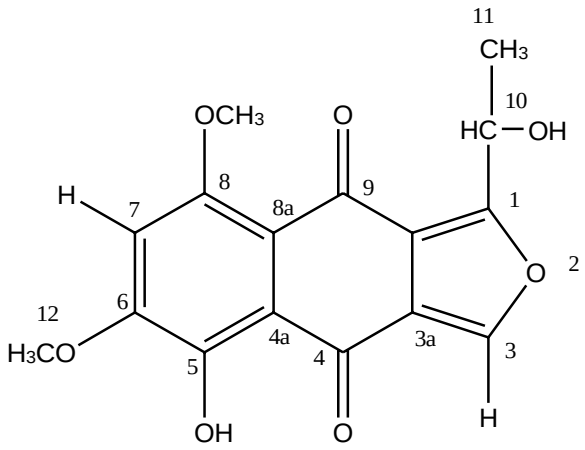

Figure 3.62: Structure of CLE-11

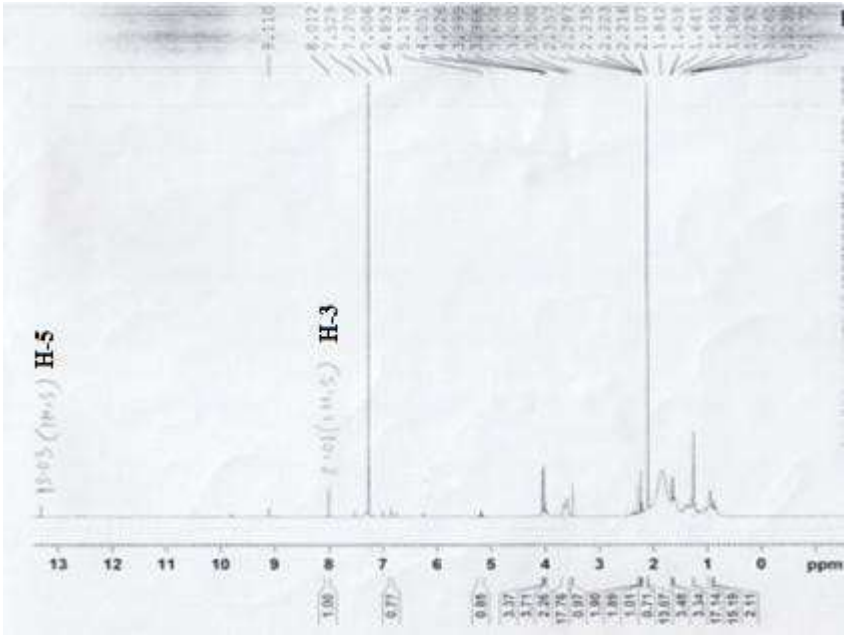

Figure 3.63: ^{1}H NMR spectrum of CLE-11 (Full)

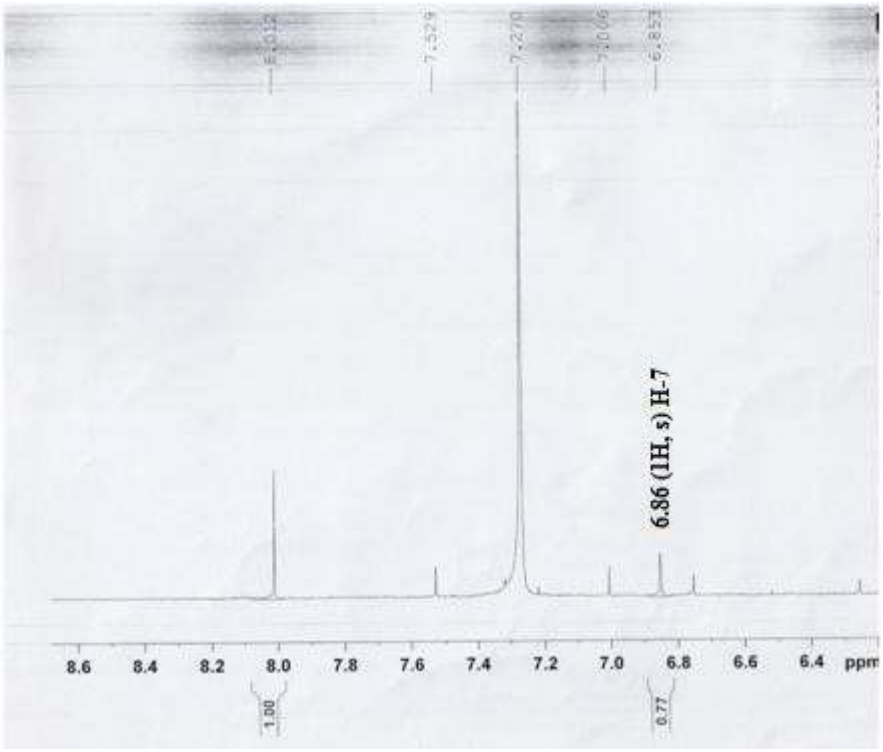

Figure 3.64: ^{1}H NMR spectrum of CLE-11 (Expanded)

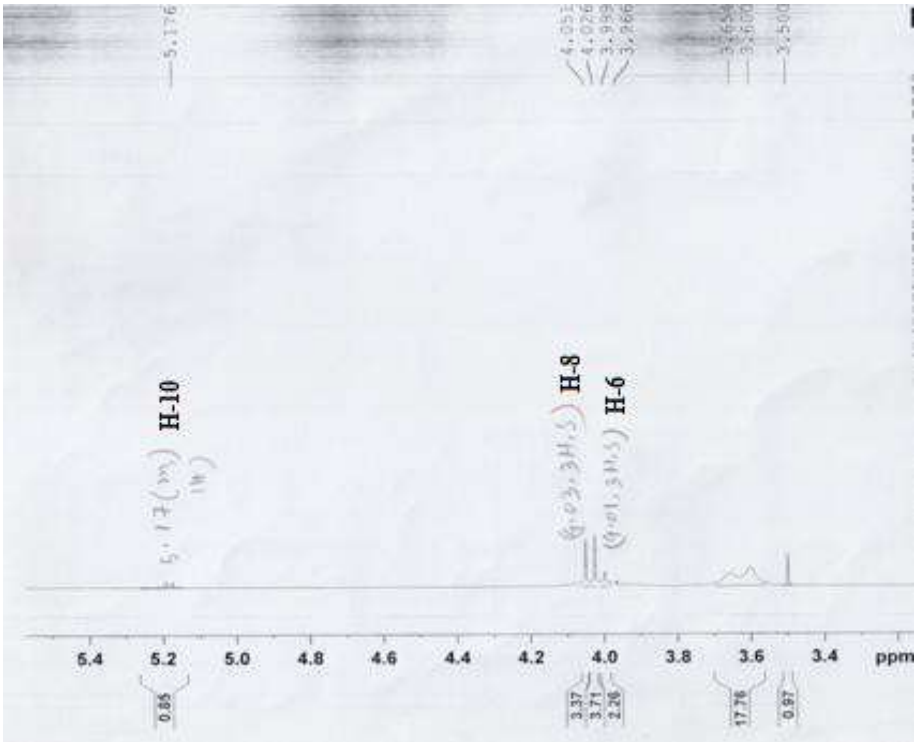

Figure 3.65: ^{1}H NMR spectrum of CLE-11 (Expanded)

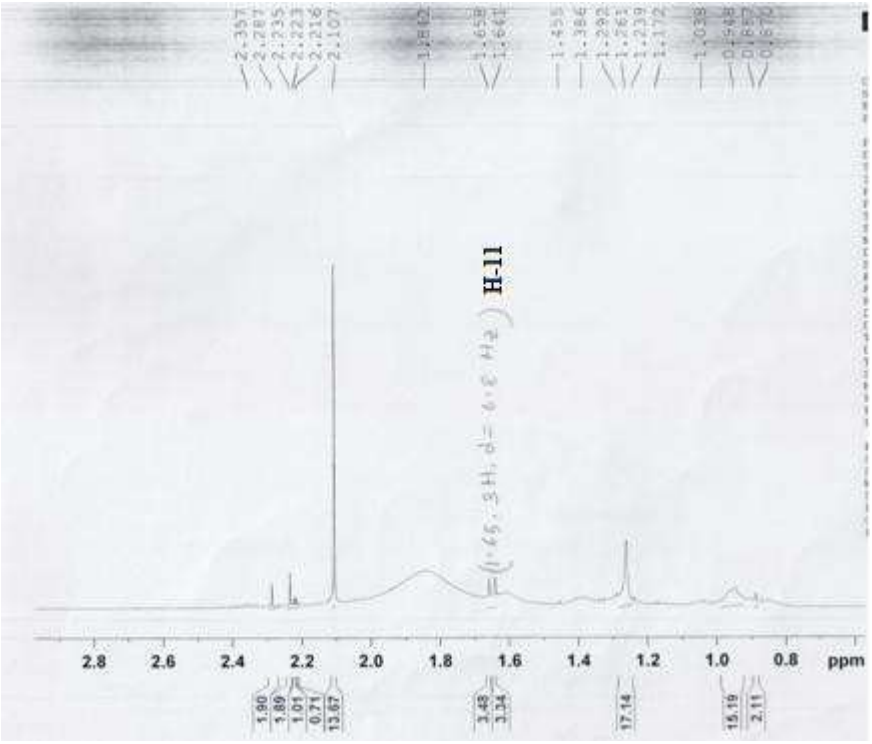

Figure 3.66: ^{1}H NMR spectrum of CLE-11 (Expanded)

4. Characterization of compound CLE-18 (2) as 8-O-methyl Bostrycoidin

Compound CLE-18 (2) was obtained as a red crystal (3 mg) (R_f = 0.55, chloroform/0.05% methanol). A dark quenching spot was seen on the TLC plate under UV light at 254 nm and a dark red spot was seen under UV light at 365 nm.

In the ^{1}H NMR spectrum, the three one-proton singlets at δ 9.46, δ 7.88, δ 6.90 could be attributed to three aromatic protons at C-1, C-4 and C-7, respectively. The singlet δ 9.46 is connected to the C-1, which is immediately linked to the nitrogen atom. The ^{1}H NMR also showed the presence of singlets at δ 4.06 and 4.06 for two methoxy groups and δ 2.77 for the methyl group in the molecule. The resonance of one 1 proton singlet δ13.28 suggested the presence of one phenolic hydroxyl group that was chelated.

On the basis of this spectral evidence and comparison with literature data, the compound was characterized as 8-O-methyl Bostrycoidin [Steyn et. al., 1979] which is an aza-anthraquinone type of compound. The obtained NMR data are presented in Table 3.20. The structure of the compound and NMR spectra are presented in Figures 3.67 to3.70.

Table 3.20: ^{1}H NMR ($CDCl_3$, 600 MHz) spectrum data for CLE-18(2)

Position	δ_H (mult., *J* in Hz)
1	9.46, s
4	7.88, 1 H, s
5	13.28, 1 H, s
7	6.90, 1 H, s
15	2.77, 1 H, s
6-OCH_3	4.06
7-OCH_3	4.06

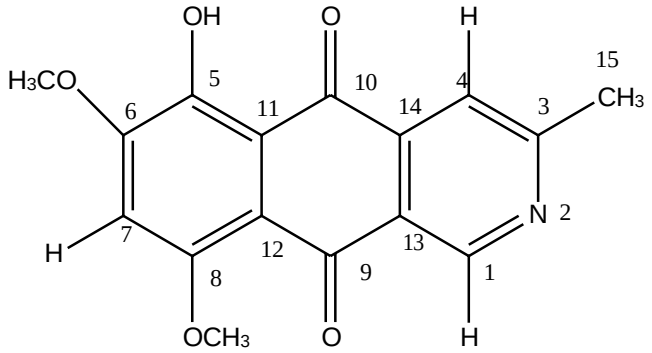

Figure 3.67: Structure of CLE-18(2)

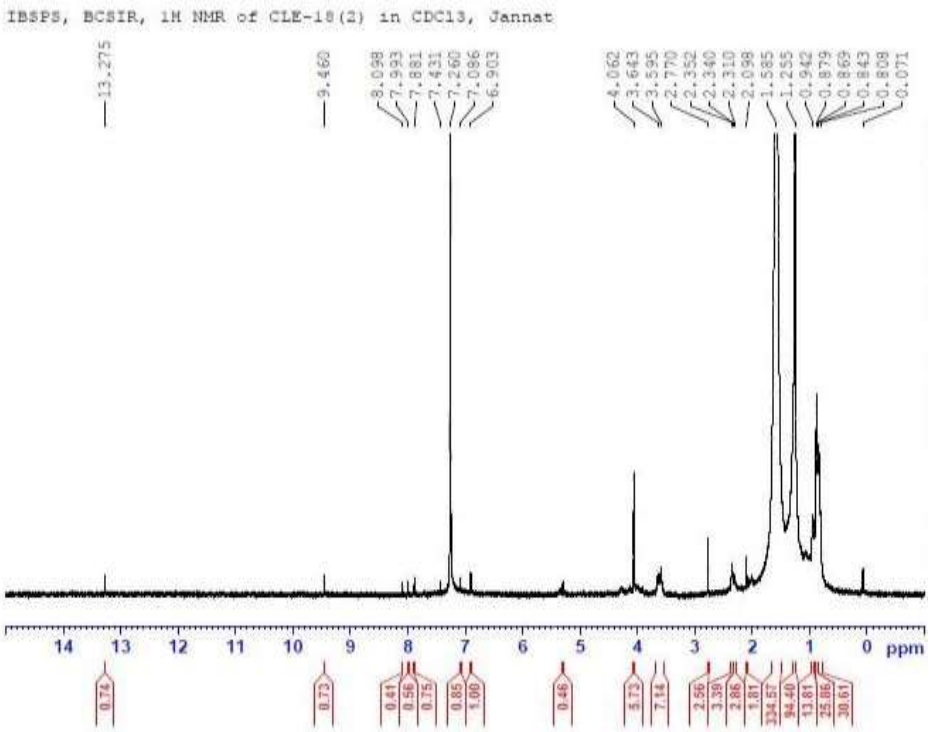

Figure 3.68: ^{1}H NMR spectrum of CLE-18(2) (Full)

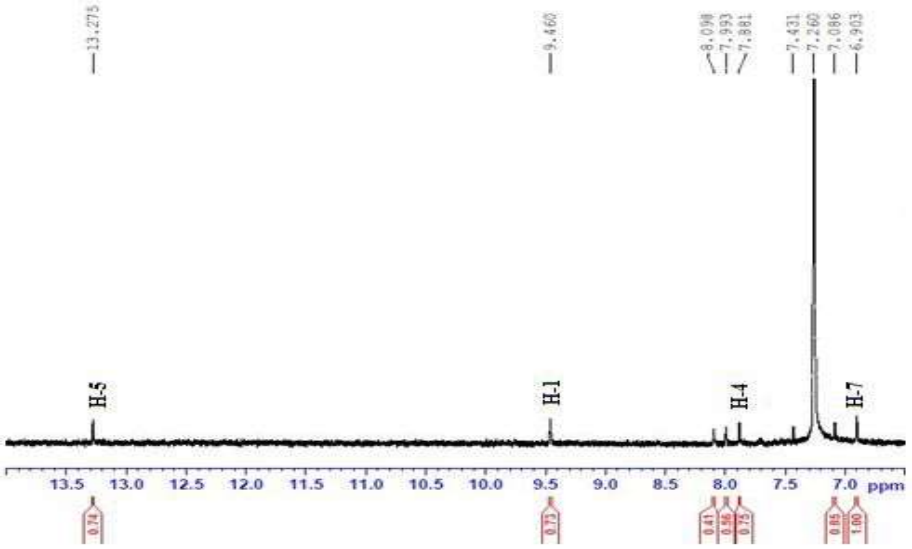

Figure 3.69: ^{1}H NMR spectrum of CLE-18(2) (Expanded)

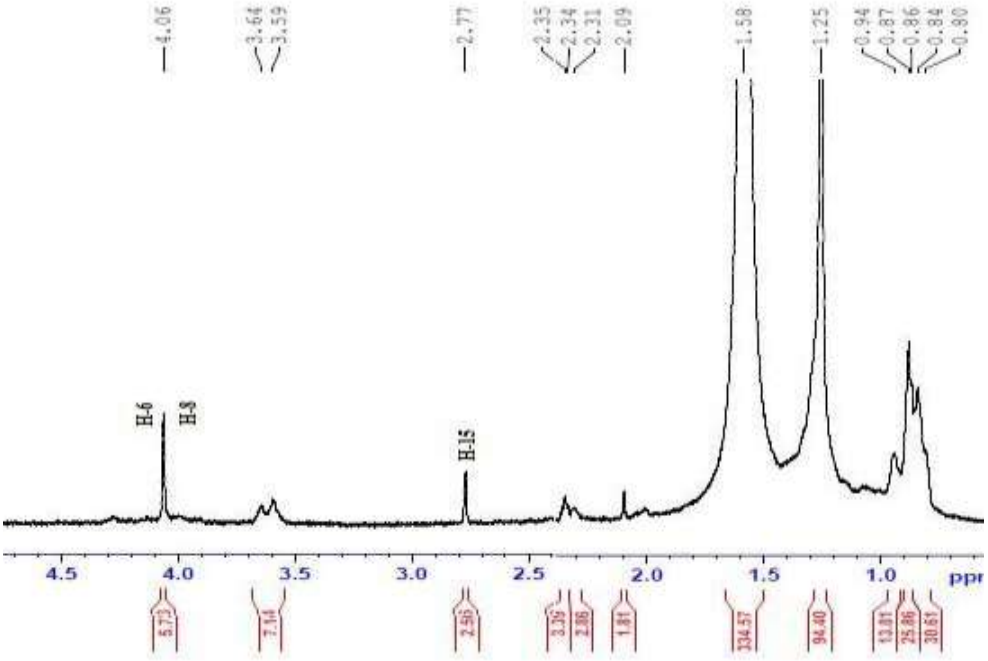

Figure 3.70: ^{1}H NMR spectrum of CLE-18(2) (Expanded)

3.5.2. Structure elucidation of compound isolated from endophytic fungus *Cladosporium cladosporoides* (ZOLE-2) from plant *Z. officinale*

Cladosporium cladosporioides is the pathogen of many different host plants. Bioactive secondary metabolites that have been obtained from *C. cladosporioides* include cladosporin, isocladosporin, cladospolides A and B, cladosporol and the calphostins [Grove & Pople, 1981; Anke et. al., 1978; Sakagami et. al., 1995; Kobayashi et. al., 1989]. A strain LF70 of *C. cladosporioides* produced Huperzine A (HupA) that was identified through TLC and HPLC with authentic HupA [Zhang et. al., 2011]. Cladosporol was isolated from culture filtrate of *C. cladosporioides* [Sakagami Y, 1995]. Zou et. al., identified three steroids, ergosta-5,7,22-triene-3β-ol, eburicol and β-sitosterol from *C. cladosporioides* [Zou & Dai, 2009]. One steroidal compound, ergosterol peroxide (3β-hydroxy-5,8-epidioxy-ergosta-6,22-diene) was isolated from *C. cladosporioides* JG-12 derived from *Ceriops tagal* [Cui et. al., 2017]. Additionally, two steroids, myristate-4-en-3-one and 3β-hydroxy-5α,8α-peroxidized ergot-6,22-diene were isolated from the endophytic fungi *C. cladosporioides* [Liu & Luo, 2019]. GC-MS analysis of the extract of *C. cladosporioides* isolated from the leaves of endemic plant *Zygophyllum mandavillei* successfully identified six major compounds: Cladosporin, Isocladosporin, 5′-

hydroxyasperentin, Di (2-ethylhexyl) phthalate, 1-acetyl-17-methoxyaspidospermidin-20-ol, and 3-phenylpropionic acid [Yehia et. al., 2020].

In the present study two steroidal compounds have been isolated from *C. cladosporoides* endophytic fungus which was isolated from *Z. officinale*. The obtained NMR data were compared to relevant literature that helped solve the structure of the isolated compound. The compounds are described below.

1. Characterization of compound ZOE-1 as Ergosterol

Compound ZOE-1 was obtained as a colorless needle-like crystal (5 mg). It appeared as a dark quenching spot on the TLC plate (R_f = 0.28, Tolune/10% EtOAc) under UV light at 254 nm and also exhibited blue fluorescence at 365 nm. It is soluble in chloroform.

The ^{1}H NMR (600 MHz, $CDCl_3$) and ^{13}C NMR (100 MHz, $CDCl_3$) data of ZOE-1 displayed 28 carbon signals, including six methyls, seven methylenes, eleven methines and four non-protonated carbons.

In the ^{1}H NMR spectrum, the two one proton multiplets at δ 5.57 and δ 5.38 ppm and one two-proton multiplet at δ 5.28 and δ 5.19 ppm indicated the presence of four olefinic protons at C-6, C-7, C-22 and C-23, respectively. It was strongly supported by the six signals in the region at δ 117.6 to δ 147.6 ppm in the ^{13}C NMR spectrum, which indicated the presence of three double bonds in the molecule. The ^{1}H multiplet at δ 3.63 ppm in the ^{1}H NMR spectrum indicated the methine proton at C-3, which is attached to a hydroxyl group and it was also confirmed by a signal at δ 71.6 ppm in the ^{13}C NMR spectrum. The six methyl groups present in ZOE-1 were confirmed by the four doublets and two singlets in the region at δ 0.81 to δ 1.03 ppm in the ^{1}H NMR spectrum.

The ^{13}C NMR spectrum showed 28 signals for 28 carbons. All the above spectral data suggested that ZOE-1 is a sterol compound which is ergosterol [Goulston & Mercer, 1975]. The obtained NMR data are presented in Table 3.21. The structure of the compound and NMR spectra are presented in Figures 3.71 to 3.80.

Table 3.21: ^{1}H NMR ($CDCl_3$, 400 MHz) and ^{13}C NMR ($CDCl_3$, 100 MHz) NMR spectrum data for ZOE-1

Position	δ_H (mult., *J* in Hz)	δ_c
1		38.1, CH_2
2		31.6, CH_2
3	3.63, m	71.6, CH
4		41.1, CH_2
5		139.7, C
6	5.57, m	117.9, CH
7	5.38, m	117.6, CH
8		147.6, C
9		48.3, CH
10		37.3, C
11		21.3, CH_2
12		39.1, CH_2
13		43.0, C
14		55.3, CH
15		21.7, CH_2
16		29.6, CH_2
17		56.1, CH
18	0.63, s	12.2, CH_3
19	0.95, s	19.6, CH_3
20		40.4, CH
21	1.03, d (8.0)	20.1, CH_3
22	5.28, m	132.0, CH
23	5.19, m	135.6, CH
24		42.9, CH
25		33.2, CH
26	0.81, d (8.0)	21.1, CH_3
27	0.84, d (6.0)	19.8, CH_3
28	0.91, d (4.4)	17.8, CH_3

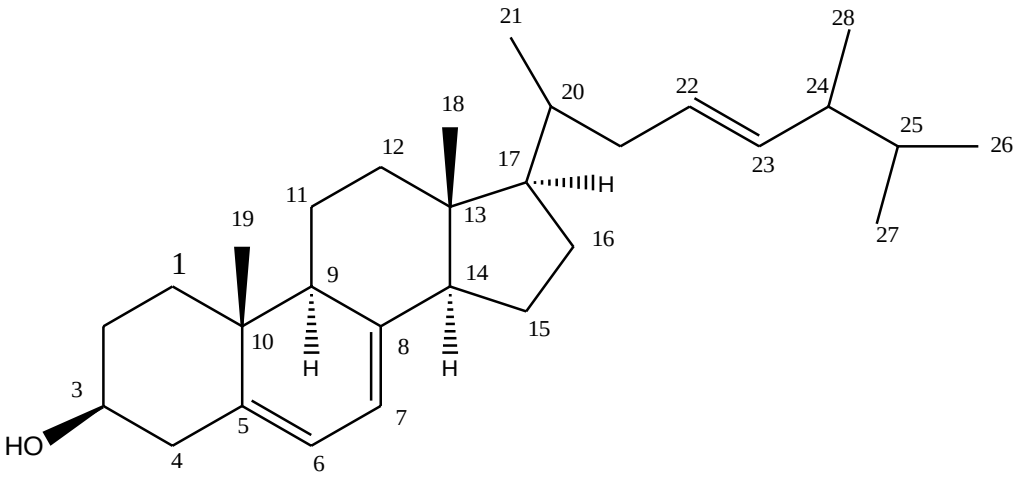

Figure 3.71: Structure of ZOE-1

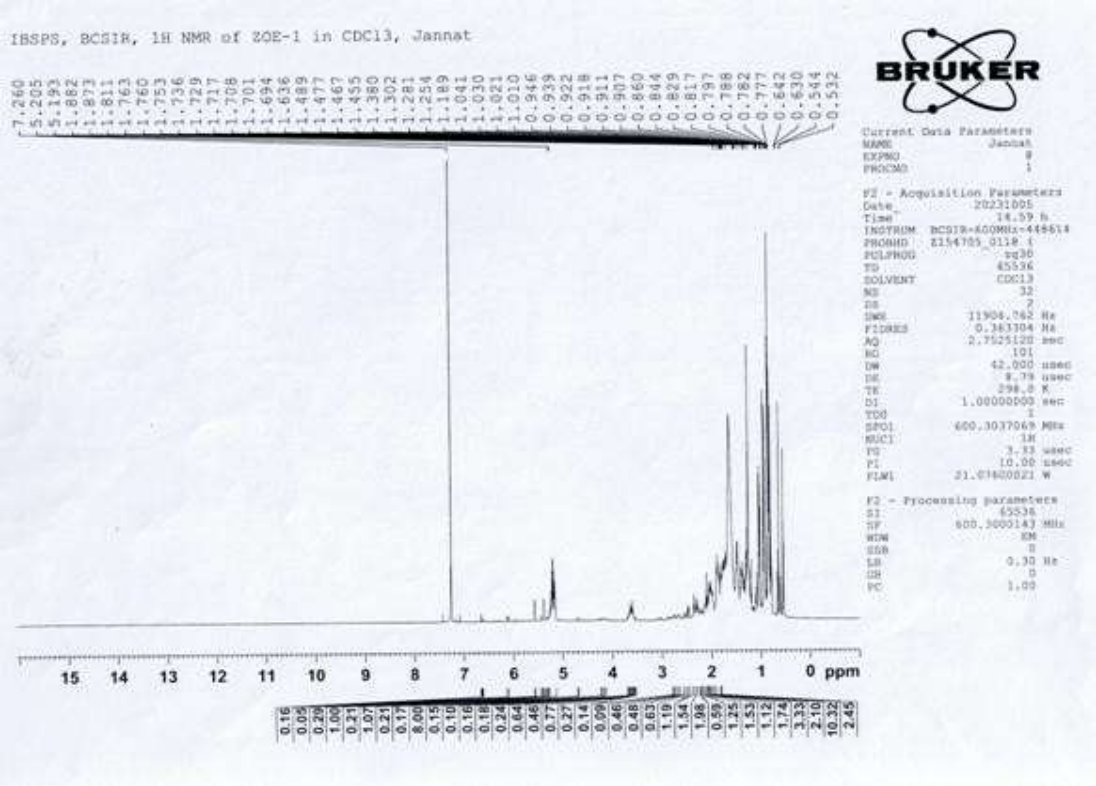

Figure 3.72: ^{1}H NMR spectrum of ZOE-1 (Full)

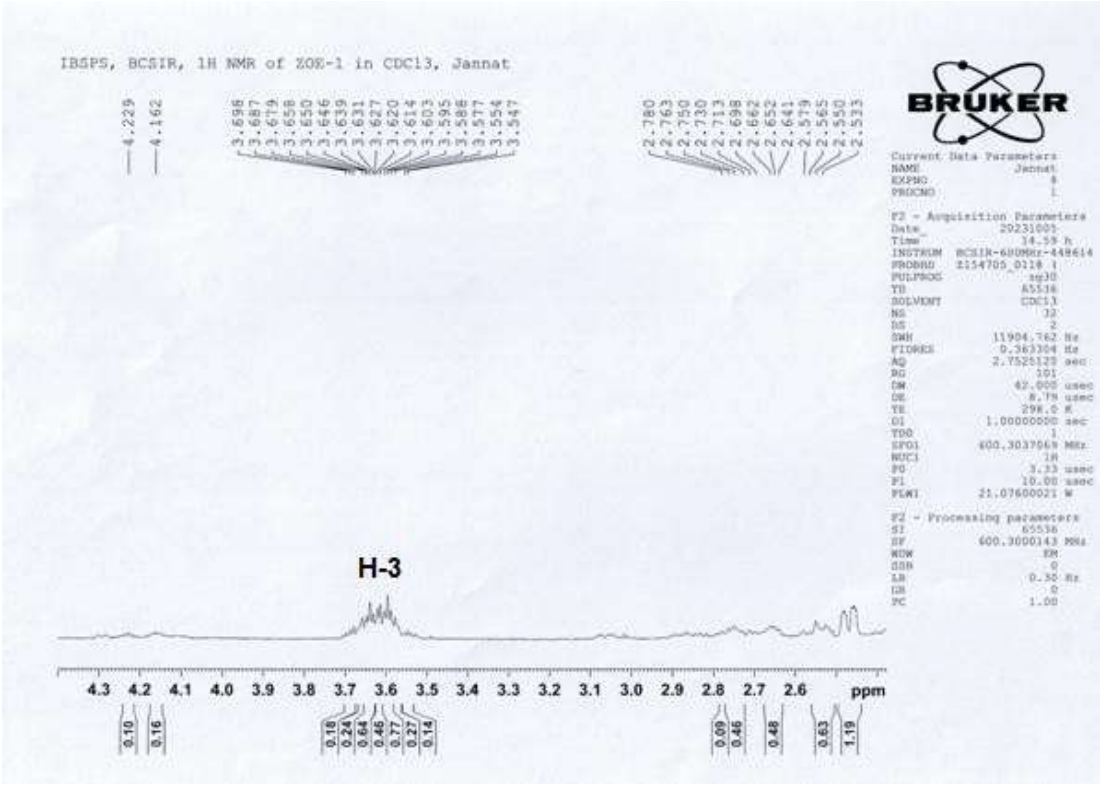

Figure 3.73: ^{1}H NMR spectrum of ZOE-1 (Expanded)

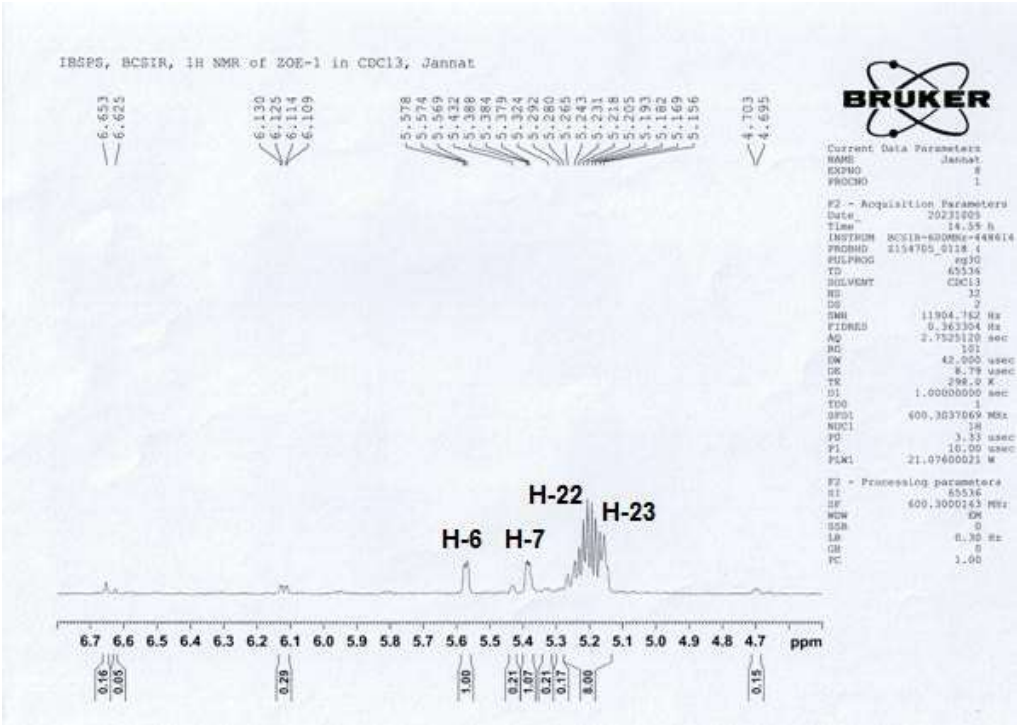

Figure 3.74: ^{1}H NMR spectrum of ZOE-1 (Expanded)

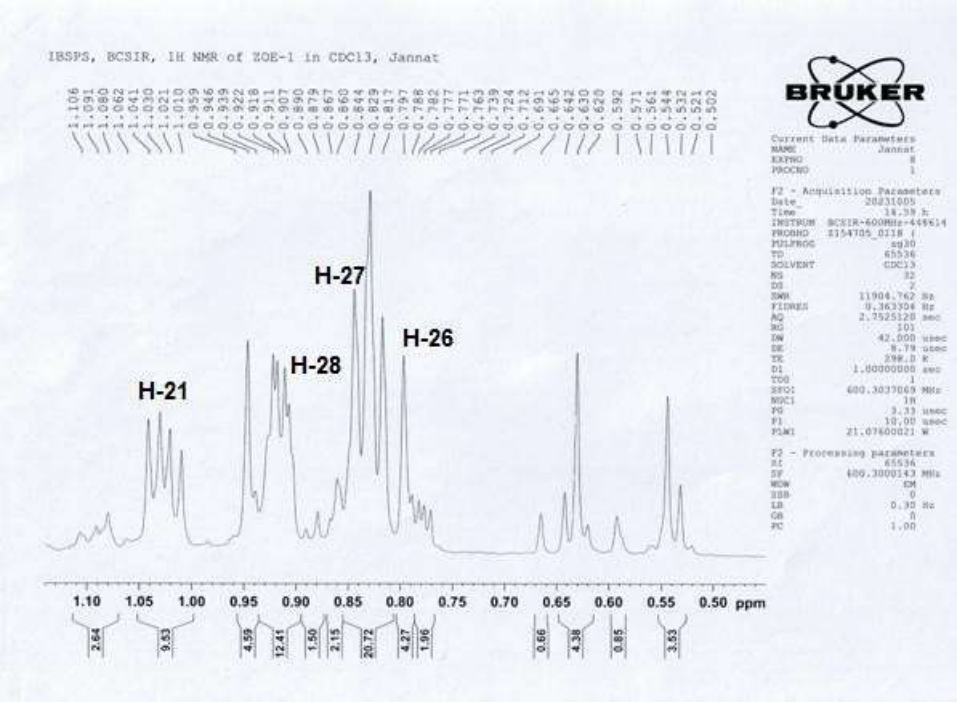

Figure 3.75: ^{1}H NMR spectrum of ZOE-1 (Expanded)

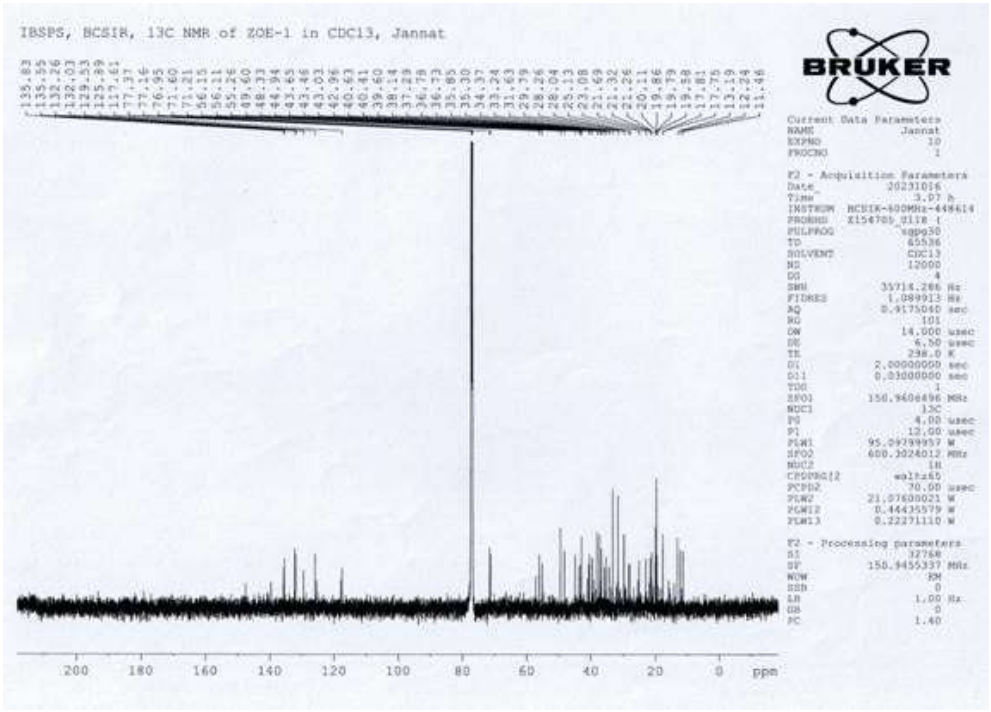

Figure 3.76: ^{13}C NMR spectrum of ZOE-1 (Full)

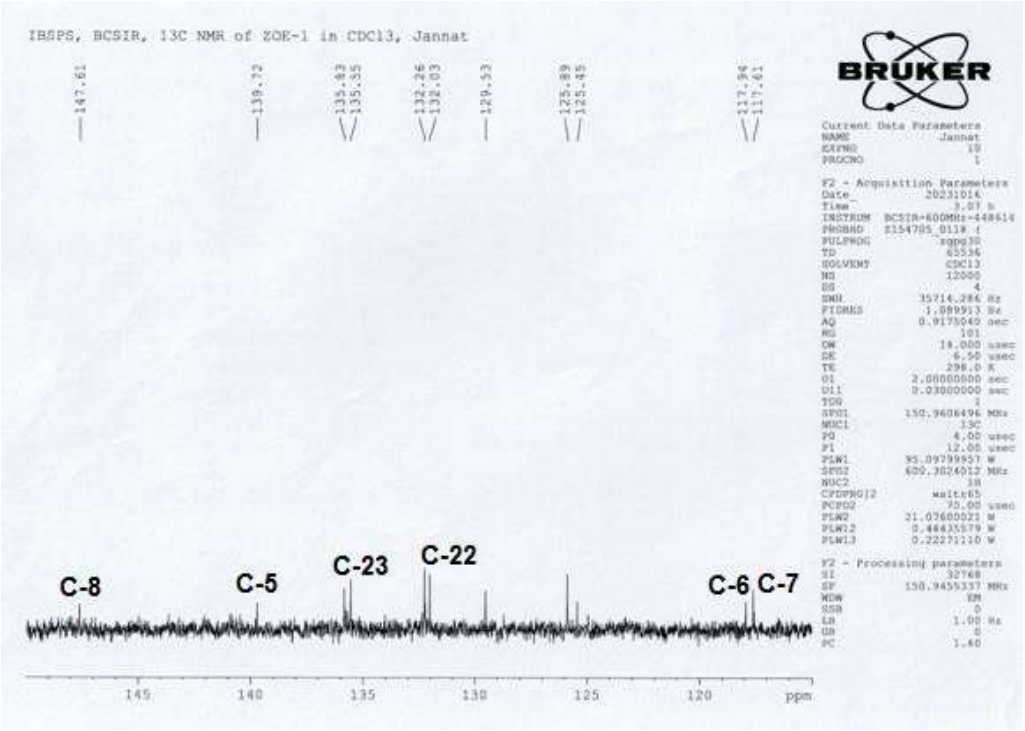

Figure 3.77: ^{13}C NMR spectrum of ZOE-1 (Expanded)

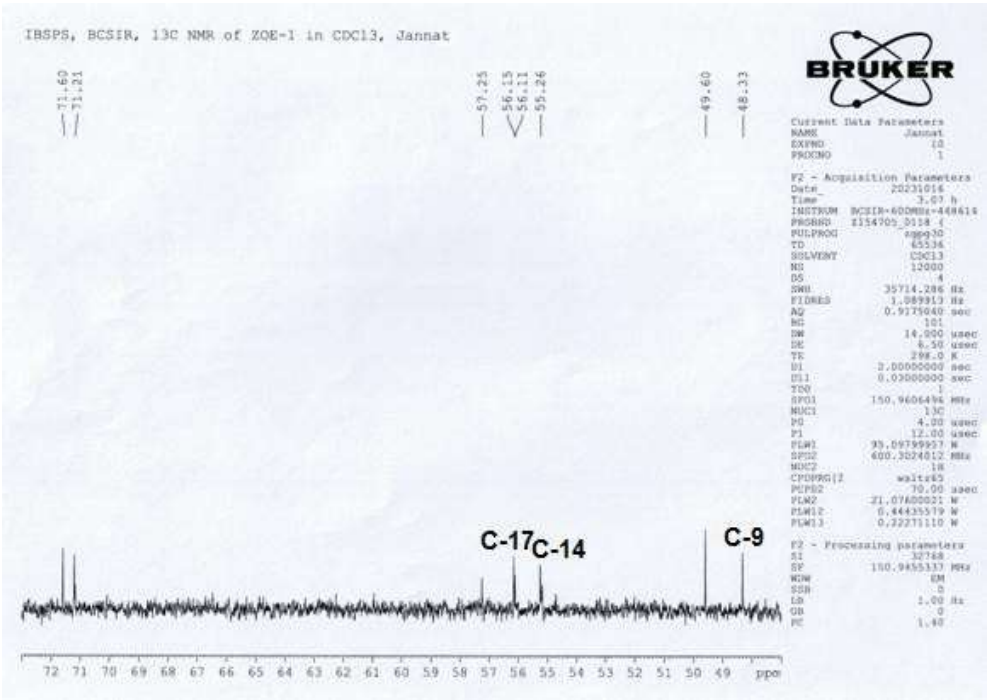

Figure 3.78: ^{13}C NMR spectrum of ZOE-1 (Expanded)

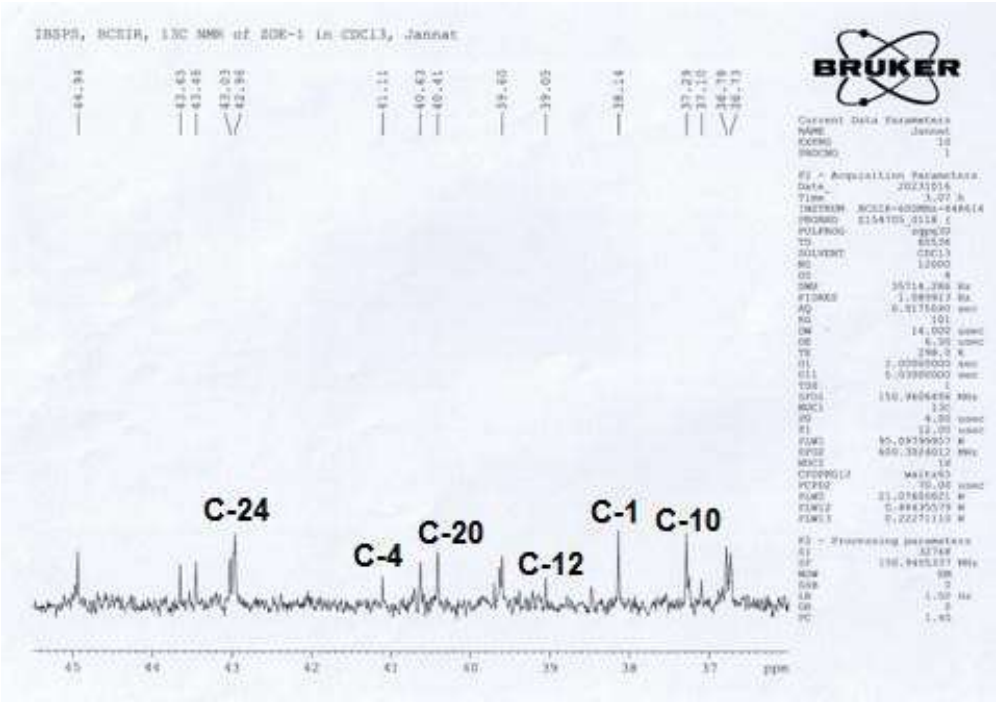

Figure 3.79: ^{13}C NMR spectrum of ZOE-1 (Expanded)

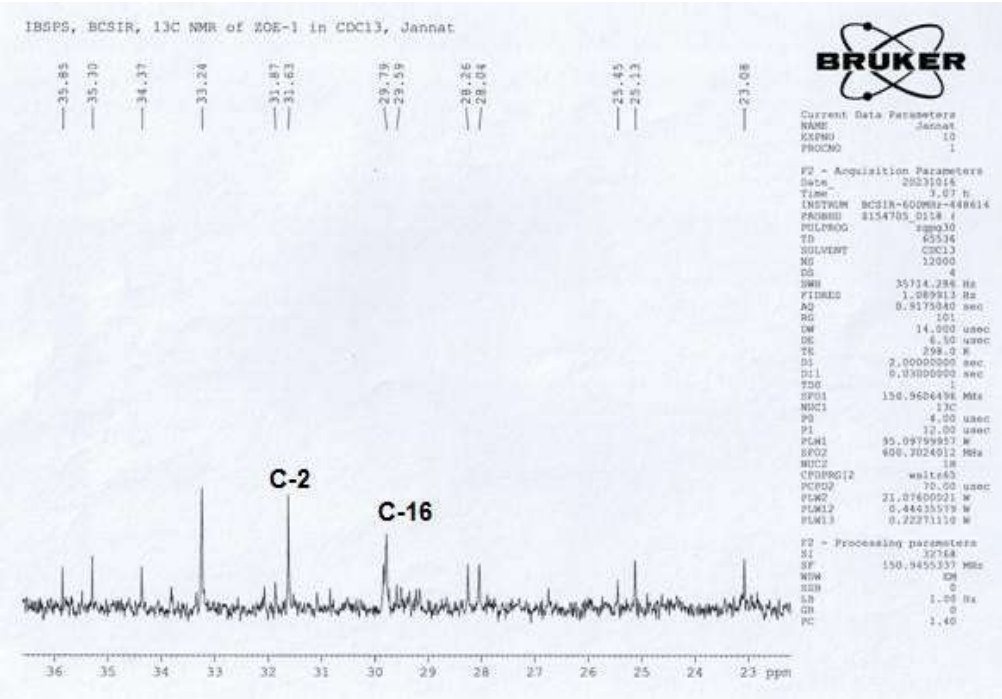

Figure 3.80: ^{13}C NMR spectrum of ZOE-1 (Expanded)

2. Characterization of compound ZOE-6 as 3, 5, dihydroxy-ergosta-7, 22-diene-6-one

Compound ZOE-6 was obtained as a brown oil (3 mg). It appeared as a dark quenching spot on TLC plate (R_f = 0.45, Chloroform/0.2% Methanol) under UV light at 254 nm and also exhibited yellow fluorescence at 365 nm. It is soluble in chloroform.

^{1}H NMR (600 MHz, $CDCl_3$) and ^{13}C NMR (100 MHz, $CDCl_3$) data of ZOE-6 in conjunction with DEPT 135 spectrum showed characteristic signals for sterols with 28 carbon signals including six methyls, seven methylenes, ten methines and five non-protonated carbons.

The ^{1}H NMR spectrum of ZOE-6, the 1H singlet in the olefinic region at δ 5.67 clearly indicated the presence of a proton attached to C-7. The two double-doublets at δ 5.18 ppm (*J* = 5.2 Hz and *J* = 18.4 Hz) and δ 5.22 ppm (*J* = 5.2 Hz and *J* = 18.4 Hz) could be attributed to two olefinic protons located at the side chain (C-22 & C-23), as would be expected for steroidal compounds. This was strongly supported by the four signals at δ 132.5, 135.0, 128.4 and 129.2 in the ^{13}C NMR spectrum which confirmed the presence of two double bonds in the molecule. The 1^H multiplet at δ 4.06 in the ^{1}H NMR spectrum showed the presence of a methane proton at C-3, which is directly attached to a hydroxyl group. The ^{1}H NMR spectral data also suggested that ZOE-6 was a sterol with six methyl signals at δ 0.92 (3H, d, *J* = 4.8 Hz), δ 1.03 (3H, s), δ 0.88 (3H, d, *J* = 4.4 Hz), δ 0.84 (3H, d, *J* = 4.4 Hz), δ 0.82 (3H, d, *J* = 4.4 Hz) and δ 0.62 (3H, s) ppm.

The ^{13}C NMR spectrum showed 28 signals for 28 carbons. The spectrum also showed other comparatively smaller signals due to the presence of some impurities within the compound. The two signals at δ 79.9 and 67.2 clearly indicated the presence of two carbons C-3 and C-5 that are directly attached to the hydroxyl group. The carbonyl carbon (C-6) was indicated by the signal at δ 171.3.

All the above spectral data suggested that ZOE-6 is a sterol compound, an ergosterol derivative named as 3, 5, dihydroxy-ergosta-7, 22-diene-6-one [Yoshihi et. al., 1991; Hirokazu et. al., 1988; Kametani et. al., 1987]. This is the first report of this compound isolated from the endophytic fungus *Cladosporium cladosporoides*. The obtained NMR data are presented in Table 3.22. The structure of the compound and NMR spectra are presented in Figures 3.81 to 3.90.

Table 3.22: ^{1}H NMR ($CDCl_3$, 400 MHz) and ^{13}C NMR ($CDCl_3$, 100 MHz) NMR spectrum data for ZOE-6

Position	δ_H (mult., *J* in Hz)	δ_c
1		34.9, CH_2
2		31.6, CH_2
3	4.06, m	79.9, CH-OH
4		37.2, CH_2
5		67.2, C-OH
6		171.3, C
7	5.67, br, s	128.4, CH
8		129.2, C
9		43.0, CH
10		33.1, C
11		22.4, CH_2
12		22.7, CH_2
13		40.3, C
14		51.9, CH
15		28.9, CH_2
16		29.7, CH_2
17		37.4, CH
18	0.62, s	12.3, CH_3
19	1.03, s	17.6, CH_3
20		33.2, CH
21	0.92, d (4.8)	19.6, CH_3
22	5.18, dd (18.4 & 5.2)	132.5, CH
23	5.22, dd (18.4 & 5.2)	135.0, CH
24		31.7, CH
25		29.9, CH
26	0.82, d (4.4)	19.9, CH_3
27	0.84, d (4.4)	21.1, CH_3
28	0.88, d (4.4)	18.4, CH_3

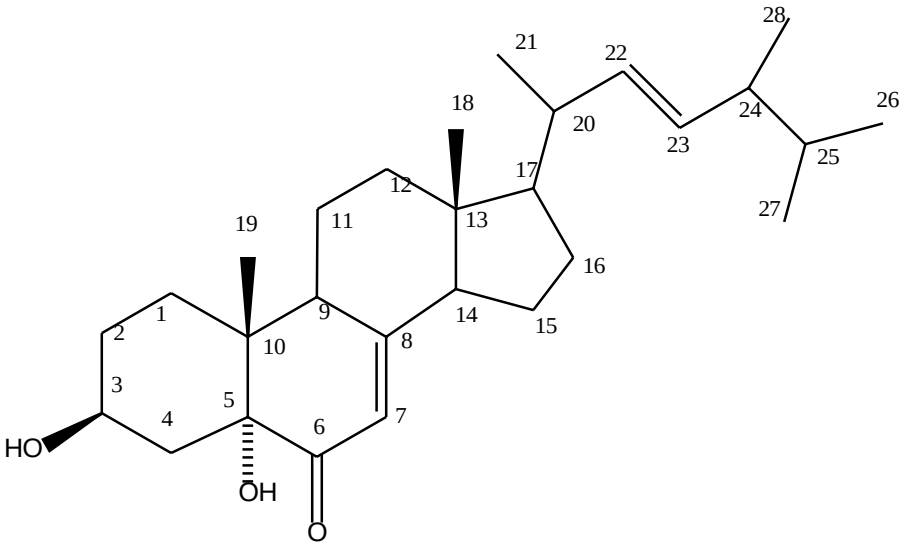

Figure 3.81: Structure of ZOE-6

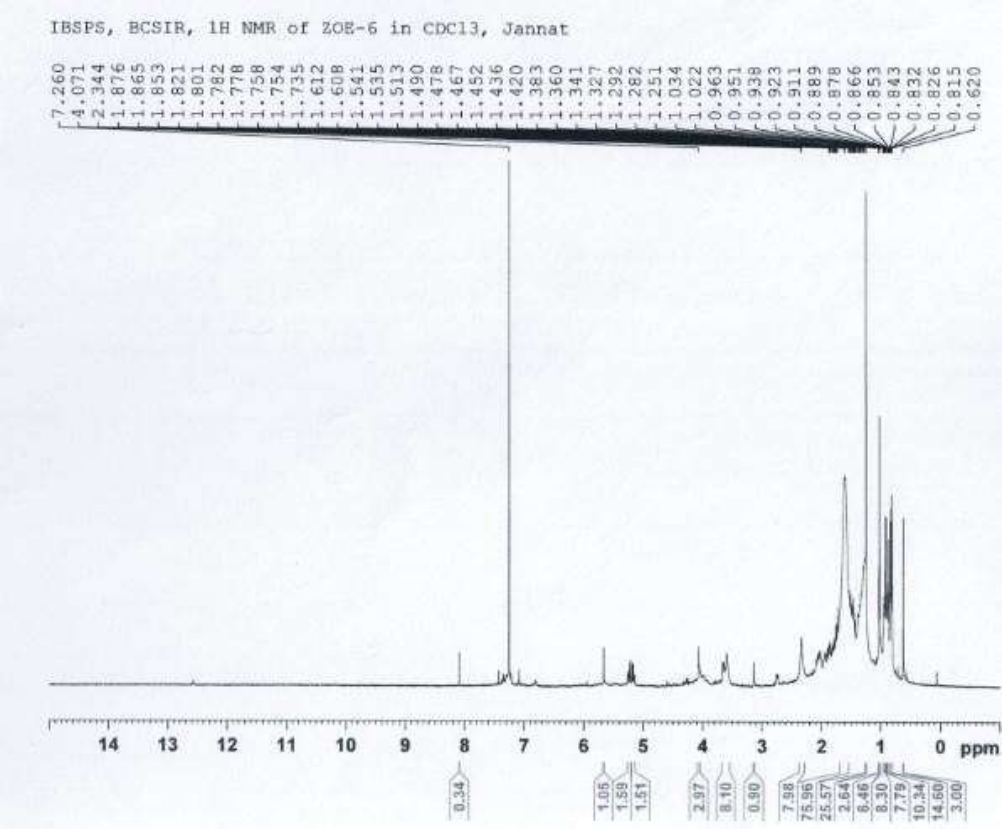

Figure 3.82: ^{1}H NMR spectrum of ZOE-6 (Full)

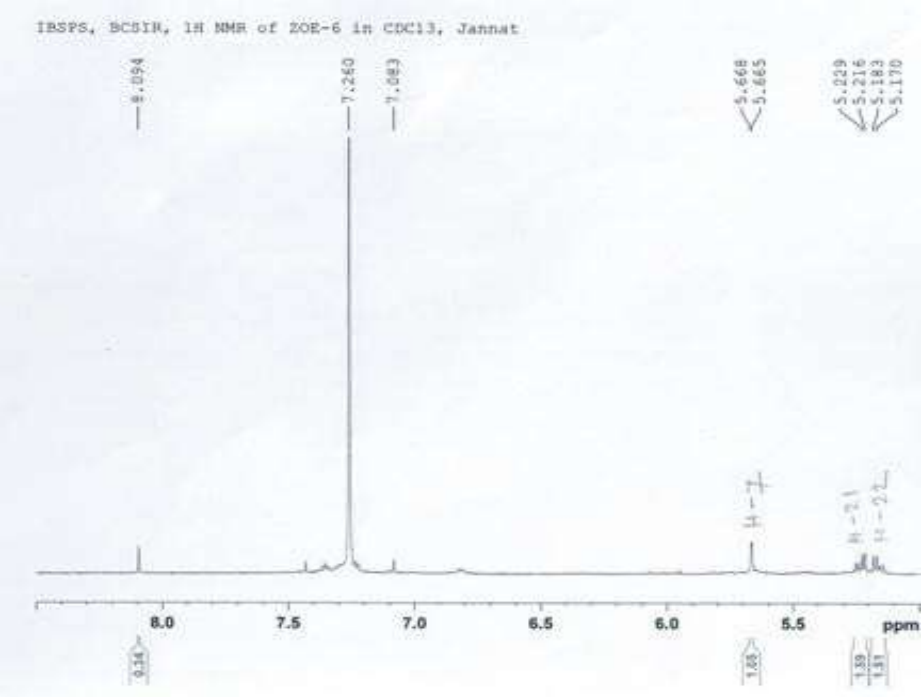

Figure 3.83: ^{1}H NMR spectrum of ZOE-6 (Expanded)

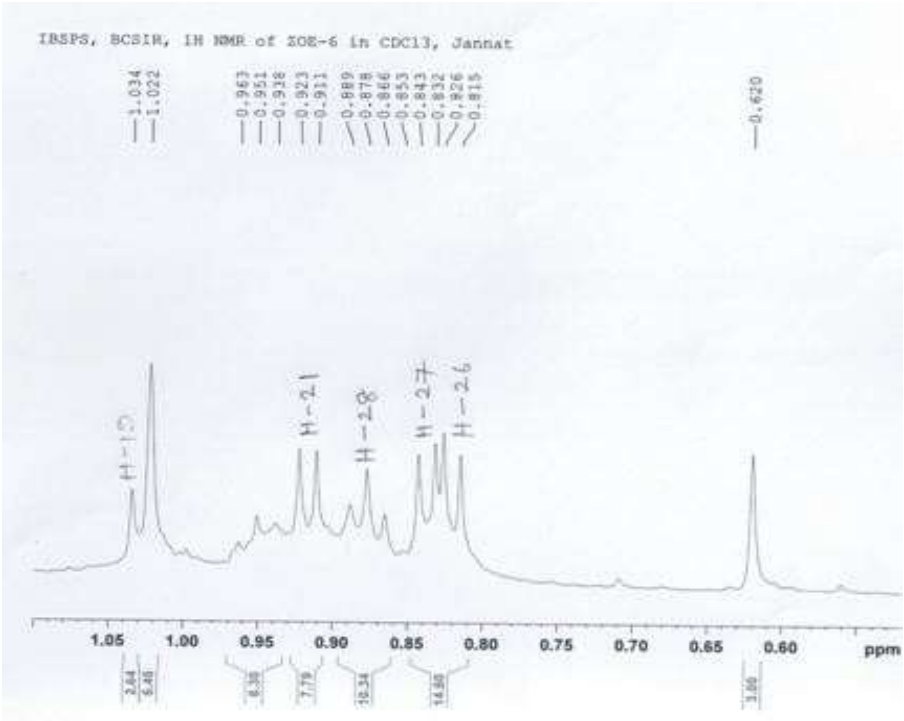

Figure 3.84: ^{1}H NMR spectrum of ZOE-6 (Expanded)

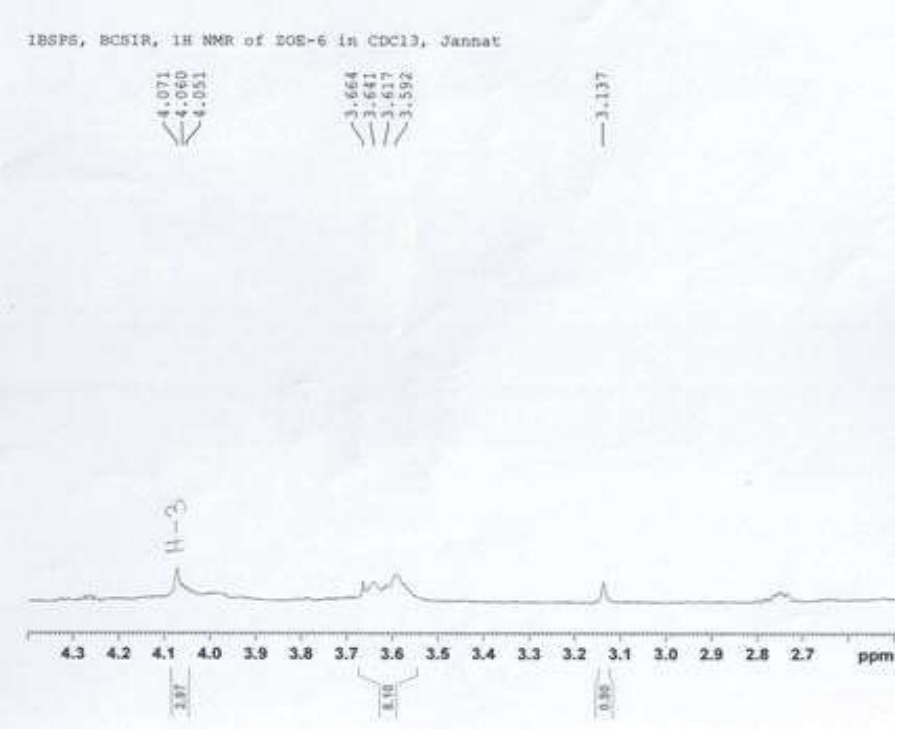

Figure 3.85: ^{1}H NMR spectrum of ZOE-6 (Expanded)

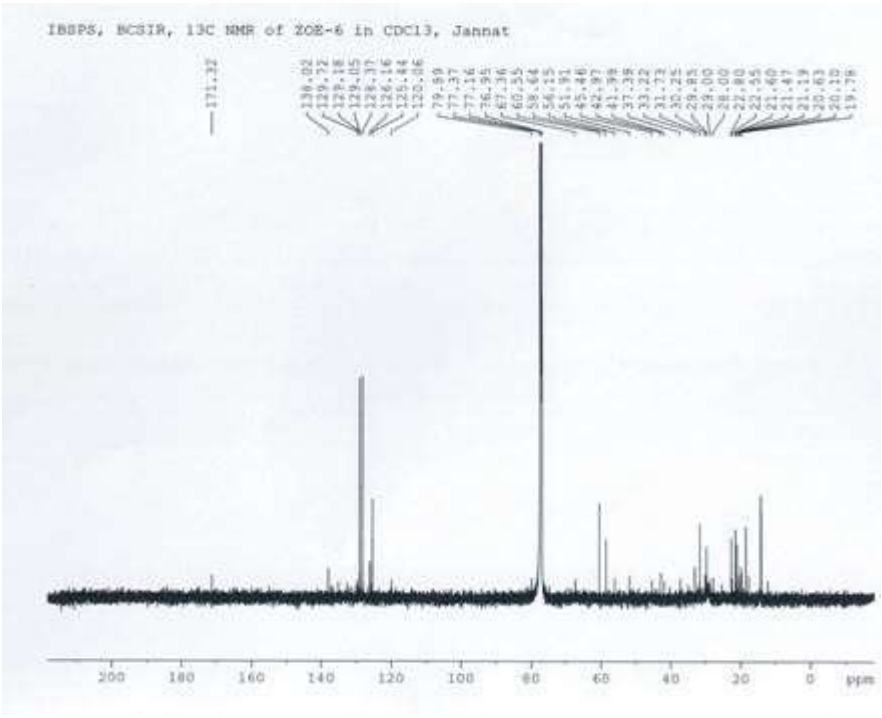

Figure 3.86: ^{13}C NMR spectrum of ZOE-6 (Full)

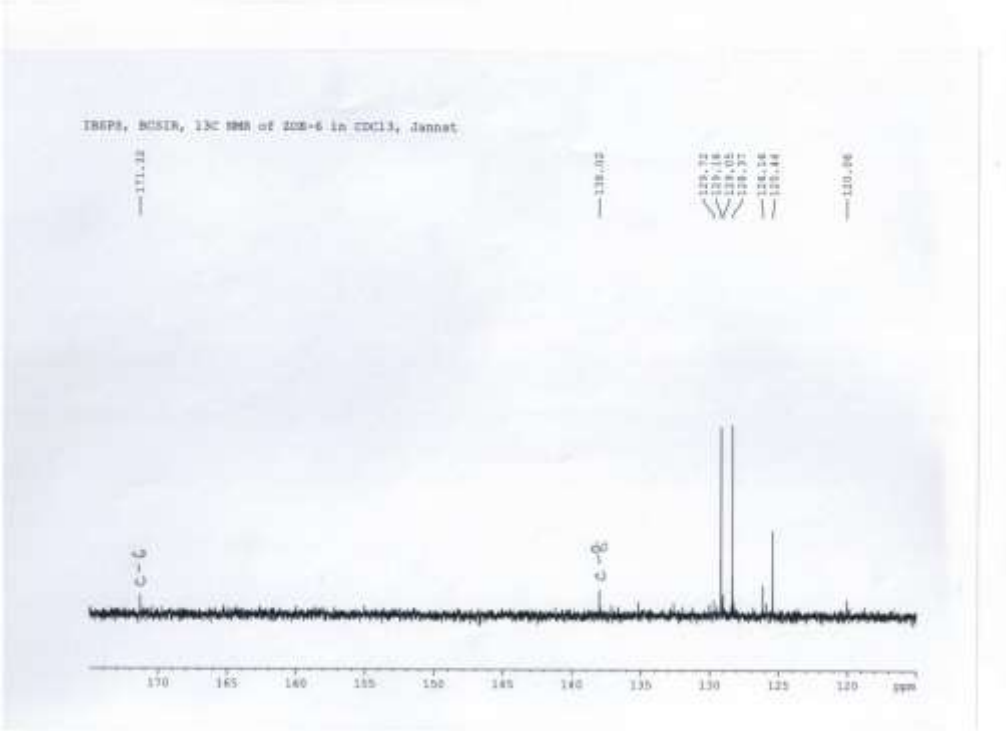

Figure 3.87: ^{13}C NMR spectrum of ZOE-6 (Expanded)

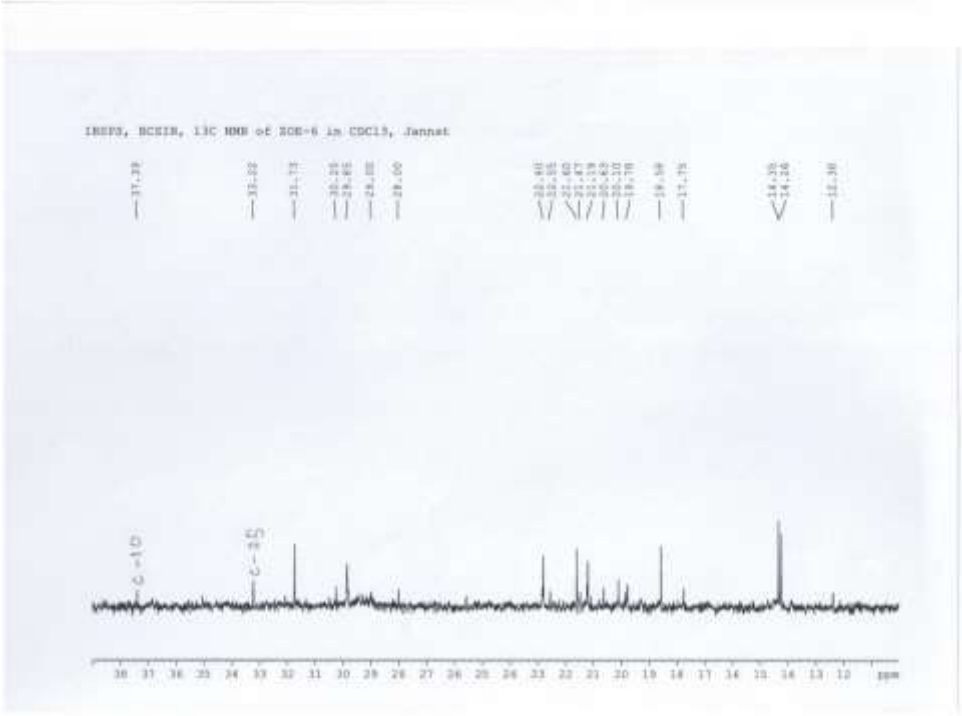

Figure 3.88: ^{13}C NMR spectrum of ZOE-6 (Expanded)

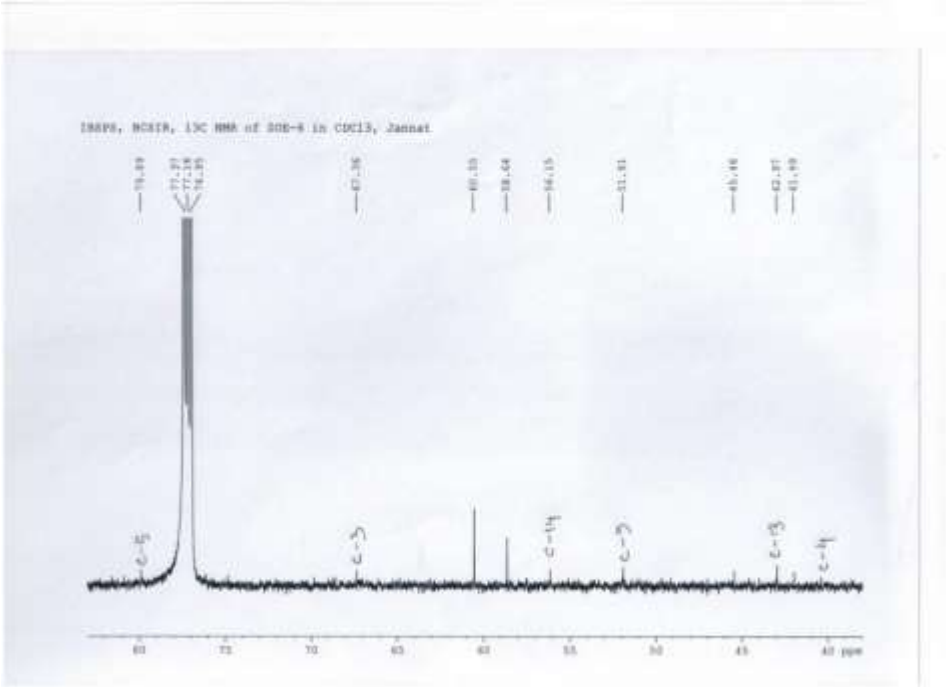

Figure 3.89: ^{13}C NMR spectrum of ZOE-6 (Expanded)

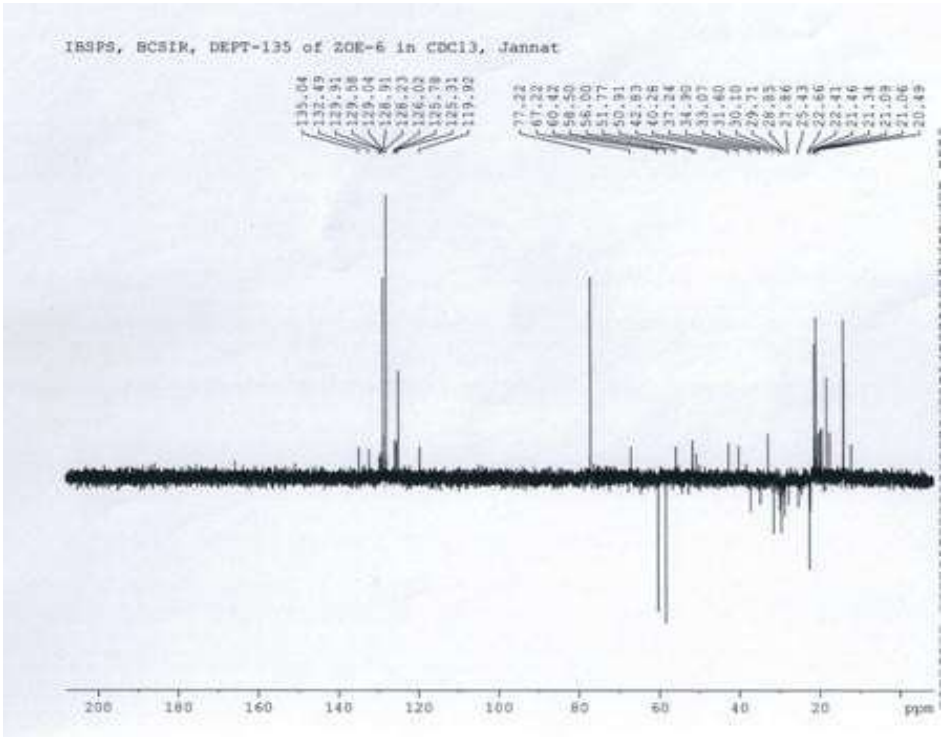

Figure 3.90: DEPT-135 spectrum of ZOE-6 (Expanded)

3.6. Bioassay of the isolated pure compounds

3.6.1. Antimicrobial activity of the isolated compounds

Antimicrobial activities of the isolated compounds were subjected to screening against some pathogenic bacteria and fungi. The results are shown in Table 3.23.

Table 3.23: Antibacterial screening of isolated pure compounds

Name of the organism	**Zone of inhibition (mm)**							**Standard**
	Sample (100 µg/disc)							
Bacteria	**CL-1**	**CL-4**	**CLE-7**	**CLE-11**	**CLE-14**	**CLE-18(2)**	**ZOE-6**	**Kanamycin (30 µg/disc)**
Escherichia coli (gram –ve)	------	10	10	-------	-----	14	10	24
Salmonella typhi (gram –ve)	------		7	-------	10	------	------	25
Pseudomonas aeruginosa (gram –ve)	-----		-------	-------	------	14	10	25
Staphylococcus aureus (gram +ve)	------		-------	--------	-----	16	10	24
Bacillus megaterium (gram +ve)	------		-------	------	-----	------	------	22
Fungi								**Ketoconazole (30 µg/disc)**
Aspergillus niger	-----	-------	------	nd	------	nd	nd	38.5
Aspergillus flavus	-----	-------	------	nd	------	nd	nd	35

CL-1: 4-hydroxy 3-methoxy cinnamic acid; CL-4: Methyl ferulate; CLE-7: Bassiatin; CLE-11: 8-O-methyl nectriafurone; CLE-14: Nectriafurone; CLE-18 (2): 8-O-methyl bostrycoidin; ZOE-6: 3, 5, dihydroxy-ergosta-7, 22-diene-6-one

"------'' indicates no sensitivity; "nd" indicates not done

The zones of inhibition produced by CLE-18(2) and (ZOE-6) were found to be 10 to16 nm which indicates mild to moderate antibacterial sensitivity against *E. coli*, *P. aeruginosa* and *S. aureus* bacteria. CL-4 and CLE-7 showed moderate antibacterial action against *E. coli* bacteria with a zone of inhibition of 10 mm. CLE-7 also showed mild antibacterial activity against *S. typhi*. The antifungal activity was not done with the compounds CLE-11, CLE-18 (2) and ZOE-6 because of their low amount. Other compounds did not show any antifungal activity against the tested fungi.

Narasimhan and co-workers have reported some cinnamic acid derivatives antibacterial activity against *E. coli and S. aureus, Bacillus subtilis* and antifungal activity against *C. albicans* and *A. niger* [Narasimhan et. al., 2004]. Again another report showed that a cinnamic acid derivative 4-hydroxy-3-methoxy benzoic acid from *Gomphrena celosioides* exhibited prominent antibacterial activity against *S. aureus* and *S. typhi* [Xavier et. al., 2004]. 3,4- dihydroxy cinnamic acid methyl ester from *Dendranthema zawadskii* var. *latilobum* also displayed antimicrobial potential [Rahman & Moon, 2007]. The results from the present study showed that 4-hydroxy-3 methoxy cinnamic acid showed did not show any antibacterial and antifungal activity against tested microorganisms. The compound methyl ferulate, similar to ferulic acid did not show any activity because of its small side chain [Borges et. al., 2013]. In this experiment methyl ferulate showed moderate activity against *E. coli*. There is no previous experimental evidence on antimicrobial activity of compounds CLE-7, CLE-14, CLE-18(2) and ZOE-6. Here these compounds showed moderate antibacterial activity against some pathogenic bacteria. Some plate pictures from the experiment are given in Figure 3.91.

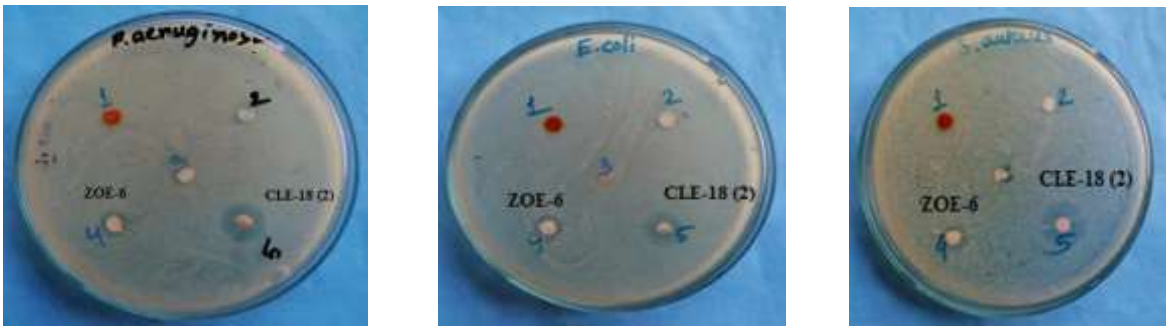

ZOE-6 and CLE-18 (2) against *P.aeruginosa*, *E. coli* and *S. aureus*

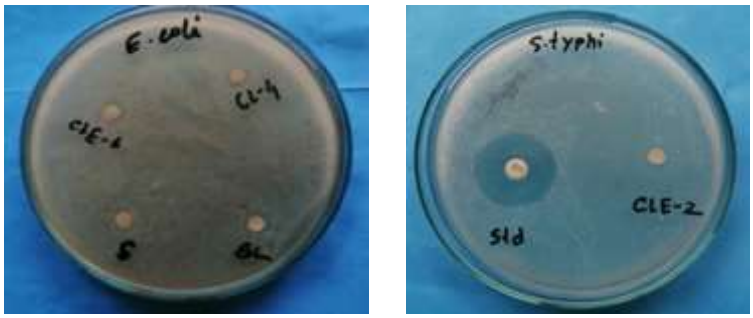

CLE-6/7 and CL-4 against *E. coli* and CLE-2/14 against *S. typhi*

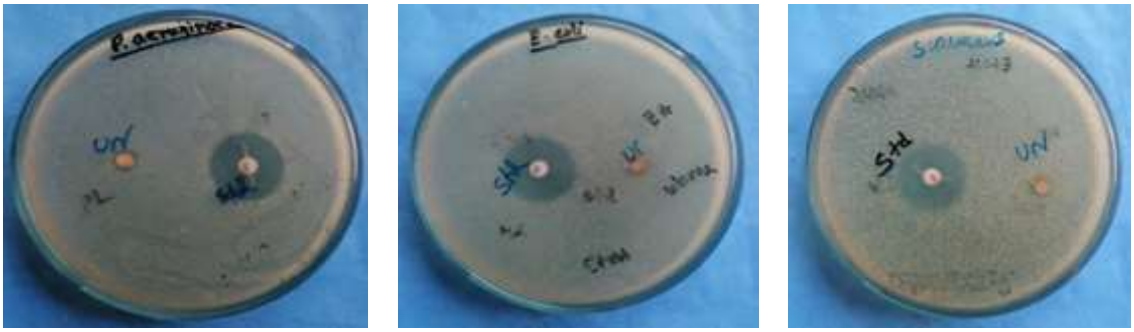

Standards (*P. aeruginosa*, *E. coli* and *S. aureus*)

Figure 3.91: Plate pictures of antibacterial activity of pure compounds. Here, ZOE-6: 3, 5, dihydroxy-ergosta-7, 22-diene-6-one; CLE-18 (2): 8-O-methyl bostrycoidin; CLE-6/7: Bassiatin; CL-4: Methyl ferulate and CLE-2/14: Nectriafurone

3.6.2 Compound CL-1 (4-hydroxy-3-methoxy cinnamic acid) showed antioxidant and cytotoxic activity

Compound CL-1 showed significant antioxidant activity with an IC_{50} value of 4.77 compared to standard ASA (IC_{50} value 9.01) and BHA (IC_{50} value 11.42). The results are shown in Figure 3.92.

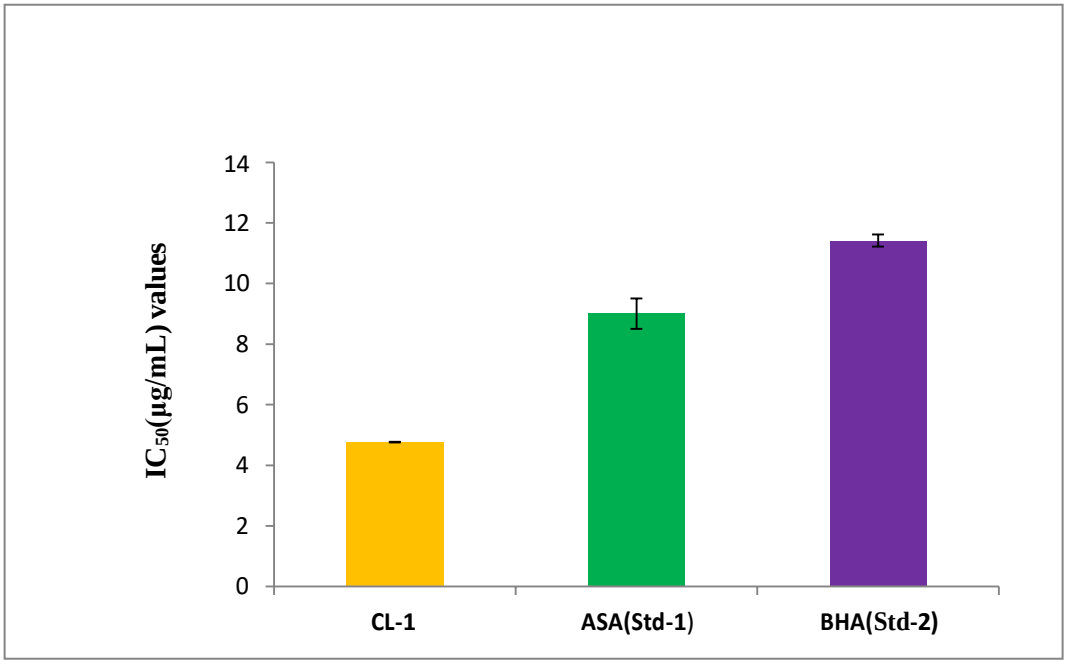

Figure 3.92: Antioxidant activity of compound CL-1. Values are expressed as mean±SD; n=3.

Like several other phenols CL-1 also exhibits antioxidant activity. Other researchers also showed antioxidant activity of cinnamic acid [Chen & Ho, 1997; Itagaki et. al., 2009].

CL-1 also showed cytotoxic activity against the Human lung cancer cell line (A-549) after 24 h of exposure. Toxicity measurement of the compound was achieved by measuring the decrease in cell viability in a dose-dependent manner. It was found that, with increasing concentration, cell viability was reduced for CL-1 (Figure 3.93).

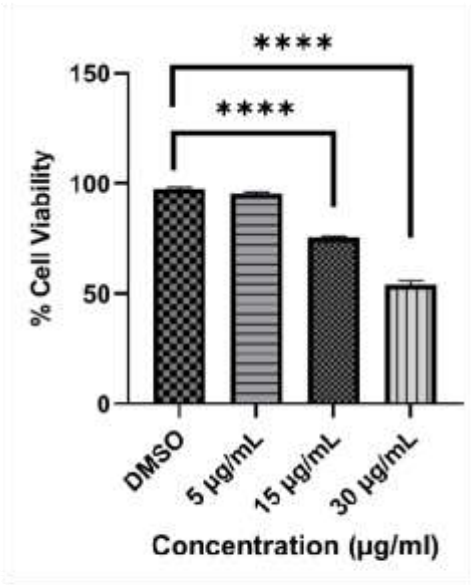

a

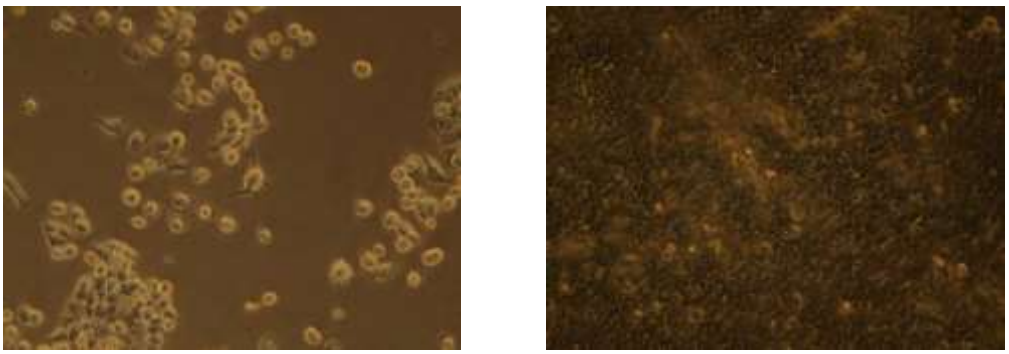

CL-1 b Control

Figure 3.93: Effect of the CL-1 on lung cancer cell line compared to the control (DMSO). a) The compound reduced the cell viability at a concentration of 30.0 µg/ml. The results are expressed as the mean ± SEM. The degree of significance calculated by employing one-way ANOVA was $p<0.0001$. b) Morphological changes observed in Lung cancer cell lines.

In many tumor cell lines such as human osteosarcoma, human glioblastoma (U87MG) and prostate cancer Ferulic acid (FA) can induce cytotoxicity [Zhang et. al., 2017; Markiewicz-Żukowska et. al., 2013]. Besides, studies also found that FA inhibits the cell activities and enhances oxidative DNA damage in HeLa and ME-180 human cervical cancer cells [Karthikeyan et. al., 2011]. In the current study, CL-1 compound showed very significant anti-proliferative activity in Lung cancer cell line which can be correlated with previous data. The compound may inhibit cell proliferation activity or activate apoptosis or necrosis in transformed lung cancer cells.

3.6.3. Compound CLE-14 (Nectriafurone) showed cytotoxic activity

Compound CLE-14 showed cytotoxic activity against a baby hamster kidney fibroblast cell line (BHK-21) with IC_{50} value 663.4 µg/ml compared to standard doxorubicin (IC_{50} value 327.1 µg/ml). It was found that with increasing concentration mortality increases. The results are shown in Figure 3.94. From literature review it is shown that Nectriafurone (specifically, nectriafurone-8-methyl ether and 5-O-methylnectriafurone) and its related compounds have demonstrated cytotoxic activity in various biological assays, primarily against cancer cell lines and parasites (Han et. al., 2020).

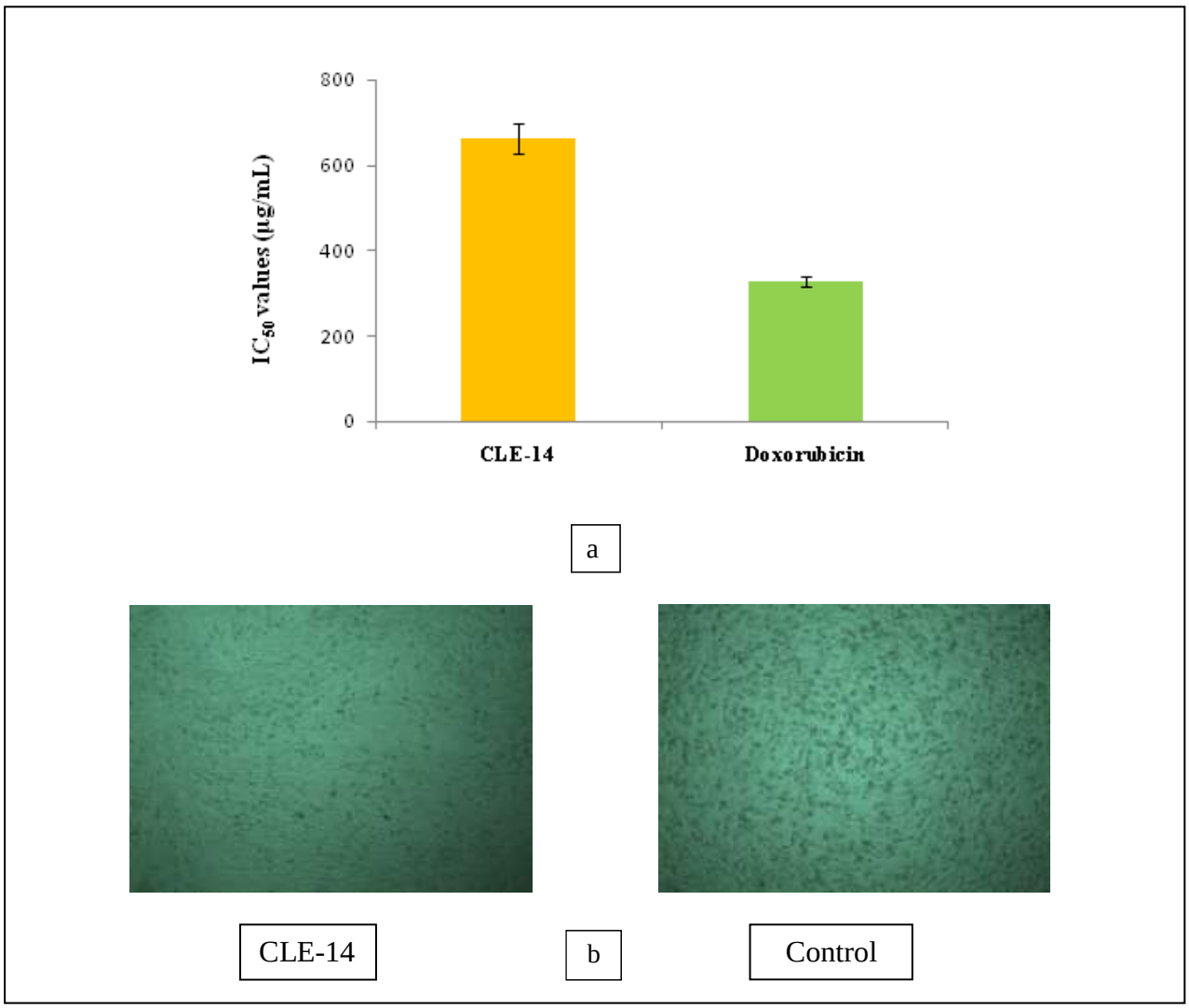

Figure 3.94: Effect of the CLE-14 on kidney fibroblast cell line compared to the control (Doxorubicin). a) IC_{50} values were calculated for the compound and the standard. Values are expressed as ± SD (n=3). b) Morphological changes observed in a fibroblast cell line.

3.6.4. Compound CLE-7 (Bassiatin) showed cytotoxic activity

The cytotoxic effectiveness of CLE-7 was evaluated against A-549 after 24 h of exposure. The toxicity measurement of the compound was achieved by measuring the decrease in cell viability. It was found that, with increasing concentration cell viability was reduced for CLE-7 (Figure 3.95).

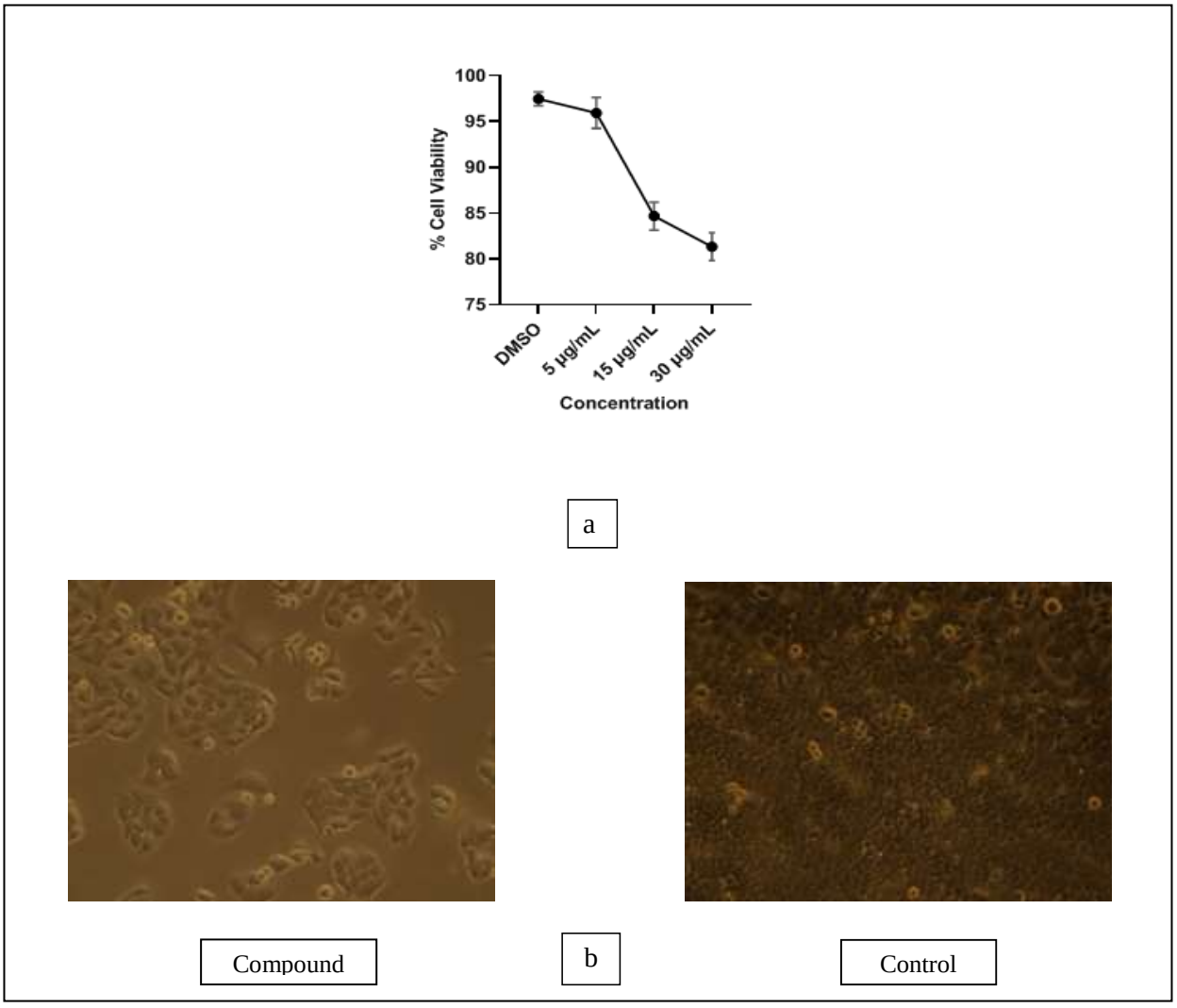

Figure 3.95: Effect of the bassiatin on lung cancer cell line compared to the control (DMSO). a) The compound reduced the cell viability at a concentration of 30.0 µg/ml. Values are expressed as Mean ± SD (n=3). b) Morphological changes observed in Lung cancer cell lines.

3.6.4.1. Computational study of Compound CLE-7 (Bassiatin) based on cytotoxicity

In vitro cytotoxicity assay revealed that Bassiatin shows encouraging results in the cytotoxicity analysis against lung cancer. The substance has the potential to suppress the growth of transformed lung cancer cells by restraining cell proliferation or stirring up apoptosis or necrosis. Thus, it was subjected to network pharmacology-based analysis to develop an understanding of its underlying mechanism which may have influenced its activity against the lung cancer cell line.

When applied to bassiatin and lung cancer, the network pharmacological approach unveiled MMP9, PTGS2 and ERBB2 as the top three common targets between the diseases and compound. When molecular docking was performed against these three targets, the binding affinity of Bassiatin was compared to that of the respective standards. Binding affinities of Bassiatin and respective standards against MMP9 (PDB Id: 4XCT), PTGS2 (PDB Id: 5IKT) and ERBB2 (PDB Id: 3PP0) is shown in Table 3.24 and Figures 3.96a, 3.96b. Against all three proteins, bassiatin has exerted good binding affinity. For, MMP9 and PTGS2, bassiatin showed -7.5 kcal/mol binding score in both cases, which was almost equal to the binding affinity of standard 14R (-7.6 kcal/mol) and aceclofenac (-7.8 kcal/mol), respectively. For, ERBB2 the binding affinity of Bassiatin was -7.9 kcal/mol, whereas standard tucatinib had the affinity of -10 kcal/mol.

Table 3.24: Binding affinity and binding interaction of Bassiatin and standards against MMP9, PTGS2 and ERBB2

Ligand	Binding affinity (kCal/mol)	H-bond	Hydrophobic interaction
MMP9(PDB Id: 4XCT)			
14R (Standard)	-7.6	LEU A:188, ALA A:189, HIS A:226	PRO A:246, HIS A:226, TYR A:248, LEU A:187VAL A:223
Bassiatin	-7.5	-	LEU A:187, LEU A: 188, VAL A:223, HIS A:226, TYR A:248
PTGS2 (PDB Id: 5IKT)			
Aceclofenac (standard)	-7.8	ASN A:375, VAL A:228, ASN A: 537. VAL A:538	GLY A:225, HIS A:226, PHE B:142
Bassiatin	-7.5	ARG A:376	VAL A:538, ASN A: 375, PHE B: 142
ERBB2 (PDB Id: 3PP0)			
Tucatinib (standard)	-10	THR A:862	LYS A:753, LEU A:852, ALA A:751, VAL A:734, CYS A:805, LEU A:796, ARG A:849, ASP A:808
Bassiatin	-7.9	-	ASAP A:863, LEU A:852, VAL A: 734, ALA: 751, LEU A:796, LYS A: 753, THR A:798. LEU A:785

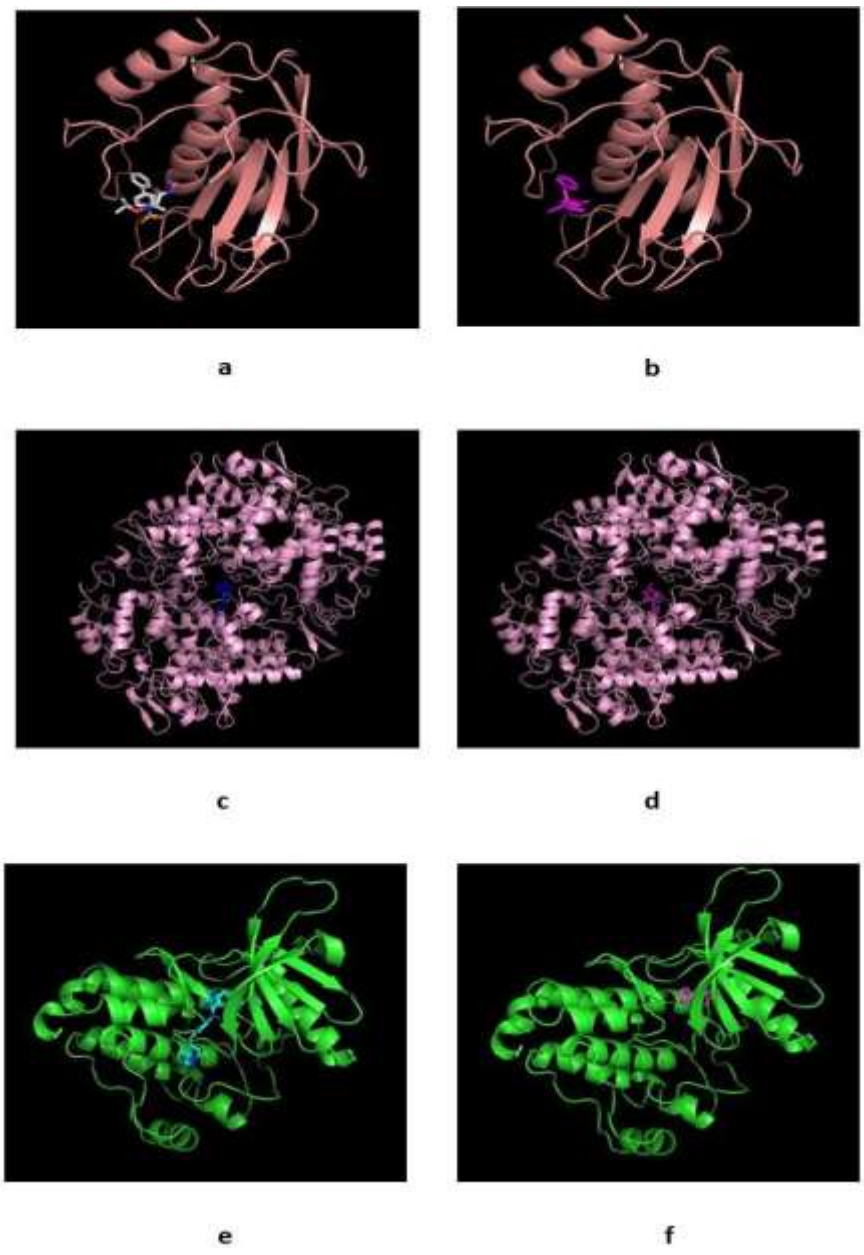

Figure 3.96a: 3D interaction of MMP9 with a) 14 R, b) Bassiatin, PTGS2 with c) aceclofenac and d) Bassiatin, ERBB2 with a) tucatinib and f) Bassiatin

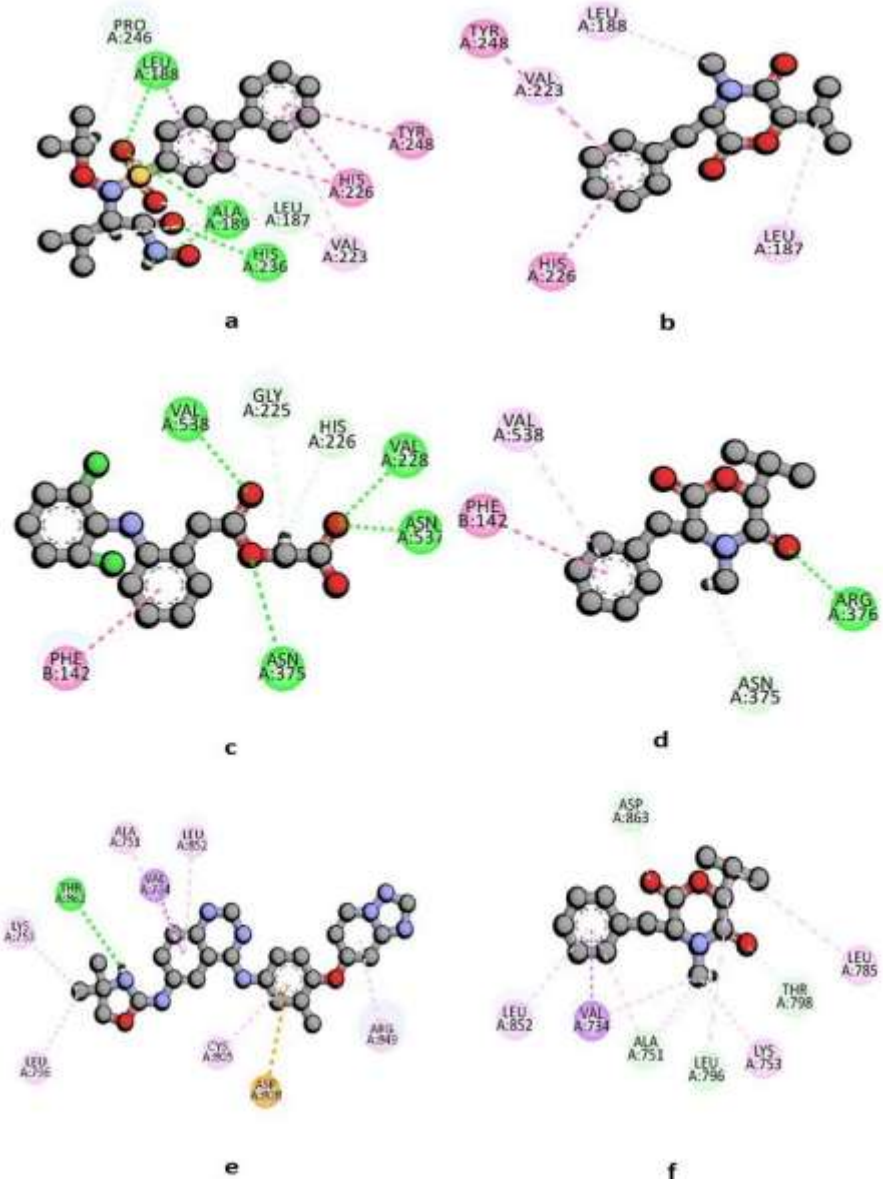

Figure 3.96b: 2D interaction of MMP9 with a) 14 R, b) Bassiatin, PTGS2 with c) aceclofenac and d) Bassiatin, ERBB2 with a) tucatnib and f) Bassiatin. Green: conventional hydrogen bond, pink-violet: hydrophobic, orange: pi-cation/pi-anion/pi-sulfur, cyan: carbon-hydrogen bond

Non-small cell lung carcinoma (NSCLC) has previously been associated with an upregulation of MMP9 [El-Badrawy et. al., 2014]. Moreover, MMP9 has been found to impact the survival rate of patients [Zhang et. al., 2021]. Similarly, cyclooxygenase2 (COX-2) which is encoded by PTGS2 has been shown to be overexpressed in lung cancer patients even their involvement in the development of invasive and metastatic type lung cancer has also been suggested [Takahashi et. al., 2002]. Application of COX-2 inhibitors along with other approaches is under consideration for the healing of lung cancer [Han et. al., 2017]. On the contrary, ERBB2 mutation has been reported in 1% to 4% cases of lung adenocarcinoma [Stephens et. al., 2004]. Thus, targeting MMP9, PTGS2 and ERBB2 positive outcomes in the treatment of lung carcinoma can be expected. As bassiatin targets these proteins with a fairly good binding score based on molecular docking analysis, thus it can be considered as a potential candidate for lung cancer treatment. The compound did not show activity against non-tumor cell line (BHK-21), which determines its selectivity and explores its potential as anticancer compound.

Chapter 4
CONCLUSION

CONCLUSION

A total of twelve endophytic fungi were isolated from *C. longa* and *Z. officinale*. The fungi were identified through morphological and molecular analysis. Two endophytic fungi *Clonostachys rosea* (CLRE-3) and *Cladosporium cladosporoides* (ZOLE-2) were selected for isolation of secondary metabolites through chemical screening and biological investigation. Preliminary chemical screening of all extracts exposes the presence of alkaloids, flavonoids, carotenoids, coumarins, anthrocyanins, isocoumarins or their derivatives, types of compounds. A total of eight (8) compounds were isolated from these plants and their endophytic fungi. The compounds were characterized using spectroscopic data. The biological activities of the isolated compounds were investigated. 8-O-methyl bostrycoidin (CLE-18(2)) and 3, 5, dihydroxy-ergosta-7, 22-diene-6-one (ZOE-6), Methyl ferulate (CL-4) and Bassiatin (CLE-7) showed mild to moderate antibacterial activity against tested pathogenic bacteria. 4-hydroxy-3-methoxy cinnamic acid (CL-1) showed antioxidant activity and cytotoxic activity in the lung cancer cell line (A-549). Nectriafurone (CLE-14) showed cytotoxic activity in the kidney fibroblast cell line (BHK-21). CLE-7 also exhibited cytotoxic activity on lung cancer cell line. Based on encouraging result of cytotoxic activity of CLE-7 on lung cancer cell line a computation study was approached where some common targets (MMP9, PTGS2 and ERBB2) were identified between the compound and the disease through network pharmacological investigation. By molecular docking analysis it was shown that CLE-7 targets these three proteins with a fairly good binding score compared to standards. The compound did not show activity against non tumor cell line (BHK-21) which determines its selectivity. Thus CLE-7 can be considered as a prospective candidate for lung cancer treatment.

In brief, it can be said that these ethnophamacologically important plants and their endophytic fungi are potent source of bioactive compounds like phenolic, quinones, aza-anthraquinones, sterols etc. which can be considered as lead compound for antibiotic, antiproliferative or anticancer agent by further investigation in large scale for including these compounds to drug development process.

REFERENCES

REFERENCES

Adwan, G.M., Abu-Shanab, B.A., & Adwan, K.M. (2008). *In vitro* activity of certain drugs in Combination with plant extracts against Staphylococcus aureus infections. *Pak J Med Sci*., 24(4), 541-4.

Aissaoui, N., Mahjoubi, M., Nas, F., mghirbi, O., Arab, M., Souissi, Y., Hoceini, A., Masmoudi, A.S., Mosbah, A., Cherif, A. & Klouche-Khelil, N. (2019). Antibacterial potential of 2, 4-di-tert-butylphenol and calixarene-based prodrugs from thermophilic *Bacillus licheniformis* isolated in Algerian hot spring. *Geomicrobiology*, 36, 53–62.

Alzoreky, N.S., & Nakahara, K. (2003). Antibacterial activity of extracts from some edible plants commonly consumed in Asia. *Int. J. Food Microbiol*. 80, 223-230.

Ammon, H.P., & Wahl, M.A. (1991). Pharmacology of *Curcuma longa*. *Planta Med*, 57, 1-7.

Anjusha, S., & Gangaprasad, A. (2014). Phytochemical and Antibacterial Analysis of Two Important Curcuma Species, *Curcuma aromatic* Salisb. And *Curcuma Xanthorrhiza* Roxb. (Zingiberaceae). *Journal of Pharmacognosy and Phytochemistry*, 3(3), 50-53.

Anke, H., Zaehner, H., & Koenig, W. (1978). Metabolic products of microorganisms 170: On the antibiotic activity of cladosporin. *Archives of Microbiology*, 116, 253-257.

Asif, M. (2016). Mini review on important biological properties of benzofuran derivatives. *Journal of Analytical & Pharmaceutical Research*., 3(2). DOI: 10.15406/japlr.2016.03.00050

Barnett, H.L., & Hunter B.B. (1998). *Illustrated genera of imperfect fungi*. 4th ed. APS Press, St Paul.

Baum, L., & Ng, A. (2004). Curcumin interaction with copper and iron suggests one possible mechanism of action in Alzheimer's disease animal models. *Journal of Alzheimer's Disease*, 6, 367-377.

Bernard, M.M., McConnery, J.R., & Hoskin, D.W. (2017). [10]-Gingerol, a major phenolic constituent of ginger root, induces cell cycle arrest and apoptosis in triple-negative breast cancer cells. *Exp. Mol. Pathol*., 102, 370–376.

Biologydictionary.net Editors. "Endophytic Fungi." *Biology Dictionary*, Biologydictionary.net, 24 Jan. 2018. https://biologydictionary.net/endophytic-fungi/

Bolsinger, C., & Jaramillo, A.E. (1990). Taxus brevifolia Nutt. Pacific Yew,. In: Burns R.M., Honkala B.H. Silvics of forest trees of North America. (rev ed). Portland, OR: Pacific Northwest Research Station, USDA Forest Service; 17.

Borges, A., Ferreira, C., Saavedra, M.J., & Simões, M. (2013). Antibacterial activity and mode of action of ferulic and gallic acids against pathogenic bacteria. Microb Drug Resist., 19(4): 256-265.

Brown, A.C., Shah, C., Liu, J., Pham, J.T., Zhang, J.G., & Jadus, M.R. (2009). Ginger's (Zingiber officinale Roscoe) inhibition of rat colonic adenocarcinoma cells proliferation and angiogenesis *in vitro*. *Phytotherapy Research*, 23(5), 640-5.

Bustanussalam, R.F., Septiana, E., Lekatompessy, S.J., Widowati, T., Sukiman, H.I., & Simanjuntak, P. (2015). Screening for endophytic fungi from turmeric plant (*Curcuma longa* L.) of Sukabumi and Cibinong with potency as antioxidant compounds producer. *Pak. J. of Biol.Sci*., 18:42-45.

Chakraborty, B., Nath, A., Saikia, H., & Sengupta, M. (2014). Bactericidal activity of selected medicinal plants against multidrug resistant bacterial strains from clinical isolates. *Asian Pac J Trop Med*., 7, 435-441.

Chandra, D., & Gupta, S.S. (1972). Antiinflammatory and antiarthritic activity of volatile oil of *Curcuma longa* (Haldi). *Indian J. Med. Res*., 60, 138-142.

Chandran, U., Mehendale, N., Patil, S., Chaguturu, R., & Patwardhan, B. (2017). Network Pharmacology. *Innov. Approaches Drug Discov.*, 127.

Chatterjee, A., & Pakrashi, S.C. (2001). The Treatise on Indian Medicinal Plants. *NISCAIR, CSIR*, New Delhi, 6, 155-156.

Chen, J.H., & Ho, C.T. (1997). Antioxidant Activities of Caffeic Acid and Its Related Hydroxycinnamic Acid Compounds. *J. Agric. Food Chem.*, 45, 7, 2374-2378.

Chen, Y. & Dai, G. (2015). Acaricidal, repellent, and oviposition-deterrent activities of 2,4-

ditert-butylphenol and ethyl oleate against the carmine spider mite *Tetranychus cinnabarinus*. *J. Pest. Sci*., 88, 645–655.

Choudhary, N., & Sekhon, B.S. (2012). Potential therapeutic effect of curcumin - an update. *Journal of Pharmceutical Education and Research*, 3(2), 218-222.

Chowdhury, N.S., Sohrab, M.H., Rony, S.R., Sharmin, S., Begum, M.N., Rana, M.S., & Choudhury, M.H. (2016). Identification and bioactive potential of endophytic fungi from *Monochoriahastata* (L.) *Solms. J. Bot.*, 45(1), 187-193.

Christenhusz, M.J.M., & Byng, J.W. (2016). The number of known plants species in the world and its annual increase. *Phytotaxa*., 261 (3), 201–217. http://dx.doi.org/10.11646/phytotaxa.261.3.1

Chuang, S.E., Chen, A.L., Lin, J.K. & Kuo, M.L. (2000). Inhibition by curcumin of diethyl nitrosa-mine-induced hepatic hyperplasia, inflammation, cellular gene products and cell-cycle-related proteins in rats. *Food Chem. Toxicol*., 38, 991-995.

Cordell, G.A., Quinn-Beattie, M.L., & Farnsworth, N.R. (2001). The potential of alkaloids in drug discovery. *Phytother. Res*., 15, 183-205.

Cragg, G.M.L., Giles, R.G.F. & Roos, G.H.P. (1975). Syntheses of isobenzofuran-4, 7-quinone and isoindole-4,7-quinone. *J Chem Sot Perkm Trans*. 1, 1339. DOI: 10.1039/P19750001339

Cui, Y., Wang, P., Kong, F., Mei, W., Guo, Z., Chen, H., & Dai, H. (2017). Secondary metabolites from the endophytic fungus *Cladosporium cladosporioides* JG-12 of Ceriops tagal and their biological activity. *J. Trop. Ecol*., 8, 29–36.

Devi, N.N., & Prabakaran, J.J. (2014). Bioactive Metabolites from an Endophytic Fungus *Penicillium* sp. Isolated from *Centella asiatica*. *Current Research in Environmental & Applied Mycology*, 4, 34-43. https://doi.org/10.5943/cream/4/1/3

El-Badrawy, M.K., Yousef, A.M., Shaalan, D., & Elsamanoudy, A.Z. (2014). Matrix metalloproteinase-9 expression in lung cancer patients and its relation to serum mmp-9 activity, pathologic type, and prognosis. *J BronchologyIntervPulmonol*., 21, 327–34.

Emon, N.U., Alam, S., Rudra, S., Chowdhury, S., Rajbangshi, J.C. & Ganguly, A. (2020). Evaluation of pharmacological potentials of the aerial part of Achyranthes aspera L.: in vivo, in vitro and in silico approaches. *Adv. Tradit. Med.*, 1-14.

Faeth, S.H., & Fagan, W.F. (2002). Fungal endophytes: common host plant symbionts but uncommon mutualists. *Integr. Comp. Biol.*, 42, 360–368. doi: 10.1093/icb/42.2.360

Firáková, S., Šturdíková, M., & Múčková, M. (2007). Bioactive secondary metabolites produced by microorganisms associated with plants. *Biologia.*, 62, 251–257. doi: 10.2478/s11756-007-0044-1

Gomes, Dde. C., Alegrio, L.V., de Lima, M.E., Leon, L.L., & Araujo, C.A. (2002). Synthetic derivatives of curcumin and their activity against *Leishmania amazonensis*. *Arzneimittelforschung*., 52, 120-124.

Goulston, G., & Mercer, E.I. THE IDENTIFICATION OF 24-METHYLENE-24.25-DIHYDROLANOSTEROL AND OTHER POSSIBLE ERGOSTEROL PRECURSORS IN *PHYCOMYCES BLAKESLEEANUS* AND *AG'ARICUS CAMPESTRIS. Phpocheminrv.*, 1975, 14, 457-462.

Grove, J.F., & Pople, M. (1981). The insecticidal activity of some fungal dihydroisocoumarines. *Mycopathologia*, 76, 65-67.

Gujral, M.L., Chowdhury, N.K., & Saxena, P.N. (1953). The effect of certain indigenous remedies on the healing of wounds and ulcers. *J Indian State Med. Assoc*., 22, 273-276.

Hadi, M.Y., Mohammed, G.J. & Hameed, I.H. (2016). Analysis of bioactive chemical compounds of Nigella sativa using gas chromatography-mass spectrometry. *Journal of Pharmacognosy and Phytotherapy*., 8(2), 8-24.

Gupta, A., Meshram ,V., Gupta, M., Goyal, S., Qureshi, K.A., Jaremko, M., & Shukla, K.K. (2023). Fungal Endophytes: Microfactories of Novel Bioactive Compounds with Therapeutic Interventions; A Comprehensive Review on the Biotechnological Developments in the Field of Fungal Endophytic Biology over the Last Decade. Biomolecules, 13, 1038. https://doi.org/10.3390/biom13071038

Han, P., Zhang, X., Xu, D., Zhang, B., Lai, D., & Zhou, L. (2020). Metabolites from *Clonostachys* Fungi and Their Biological Activities. *J. Fungi*, 6, 229. doi: 10.3390/jof6040229

Han, T., Li, H., Zhang, Q., Zheng, H., & Qin, L. (2006). New thiazinediones and other components from *Xanthium strumarium*. Chem Nat Compd., 42, 567–570. https://doi.org/10.1007/s10600-006-0215-2

Han, Z.Q., Liao, H., Shi, F., Chen, X.P., Hu, H.C., Tian, M.Q., Wang, L.H., & Ying, S. (2017). Inhibition of cyclooxygenase-2 sensitizes lung cancer cells to radiation-induced apoptosis. *Oncology Letters*, 14(5), 5959–65.

Hanks, G.R. (1996). Control of *Fusarium oxysporum* f. sp. narcissi, the cause of narcissus basal rot, with thiabendazole and other fungicides. *Crop Prot*., 15,549–558.

Harborne, A.J. (1998). Phytochemical methods: a guide to modern techniques of plant analysis. (21–72). London: Chapman and Hall Ltd.

Hasan, A.E.Z., Artika, I.M., Kuswandi, and Tukan, G.D. (2014). Analysis of Active Components of *Trigona spp* Propolis from Pandeglang Indonesia. *Global Journal of Biology, Agriculture & Health Sciences*, 3(1), 215-219.

Hirokazu, K., Ryosuke, K., Toshimi, S., Takashi, M., Toshihiko, H., & Takuji, N. (1988). Cytotoxic steroids from the mushroom *Agaricus* blazei. *Phytochemistry*, 27, 2777-2779.

Hooker, J.D. (1990). Flora of British India. Connaught palace. Dehradun., 4, 214.

Hsiang, C., Lo, H., Huang, H., Li, C., Wu, S., & Ho, T. (2013). Ginger extract and zingerone ameliorated trinitrobenzene sulphonic acid-induced colitis in mice via modulation of nuclear factor-kappa B activity and interleukin-1 beta signalling pathway. *Food Chem*., 136, 170–177.

Ignjatov, M., Vlajić, S., Milošević, D., Nikolic, Z., Tamindzic G. & Gvozdanović-Varga, J (2019). Identification and phylogenetic analysis of *Fusarium proliferatum* isolated from elephant garlic *Allium ampeloprasum* L. *Zbornik Matice srpske za prirodne nauke.,* 137, 49-55. https://doi.org/10.2298/ZMSPN1937049I

Ilmiawati, A., Anggraini, D., Syahbirin, G., Rahayu, D.U.C. & Sugita, P. (2020). Methyl

Ferulate from Methanol Extract of Indonesian Sausage Fruit (*Kigelia africana*). *AIP Conference Proceedings*, 2243, 030009. https://doi.org/10.1063/5.0001095

Issuriya, A., Kumarnsit, E., Wattanapiromsakul, C., & Vongvatcharanon, U. (2014). Histological studies of neuroprotective effects of *Curcuma longa* Linn. on neuronal loss induced by dexamethasone treatment in the rat hippocampus. *Acta Histochem.*, 8(116), 1443-1453.

Itagaki, S., Kurokawa, T., Nakata, C., Saito, Y., Oikawa, S., Kobayashi, M., Hirano, T., & Iseki, K. (2009). In vitro and in vivo antioxidant properties of ferulic acid: A comparative study with other natural oxidation inhibitors. *Food Chemistry*, 114, 466–471.

Jeffrey, A.D., Kyeonghee, M.L., Roger, A.R., Rodney, A.M., Alfred, F.F., Kathy, M.G., Po, C.C., Leo T.B., & Joseph H.R. (2003). 2u-Globulin Nephropathy and Carcinogenicity following Exposure to Decalin (Decahydronaphthalene) in F344/N Rats. *TOXICOLOGICAL SCIENCES*, 72, 223–234.

Ji, K., Fang, L., Zhao, H., Li, Q., Shi, Y., Xu, C., Wang, Y., Du, L., Wang, J., & Liu, Q. (2017). Ginger oleoresin alleviated gamma-ray irradiation-induced reactive oxygen species via the Nrf2 protective response in human mesenchymal stem cells. *Oxid. Med. Cell. Longev.*, (1), 1-12. https://doi.org/10.1155/2017/1480294

Jitoe, A., Masuda, T., Tengah, I.G.P., Suprapta, D.N., Gara, I.W., & Nakatani, N. (1992). Antioxidant activity of tropical ginger extracts and analysis of the contained curcuminoids. *J Agric Food Chem*, 40(8), 1337-40.

Kagamizono, T., Nishino, E., Matsumoto, K., Kawashima, A., Kishimoto, M., Sakai N., He, B-M., Chen, Z-X., Adachi, T., Morimoto, S., & Hanada, K. (1995). Bassiatin, a new platelet aggregation inhibitor produced by *Beauveria bassiana* K-717. *J Antibiot (Tokyo)*, 48(12), 1407–12.

Kametani, T., & Furayam, H. Synthesis of vitamin *Dj* and related compounds. (1987). *Med. Res. Rev.*, 7, 147-171.

Karthikeyan, S., Kanimozhi, G., Prasad, N.R., & Mahalakshmi, R. (2011). Radiosensitizing

effect of ferulic acid on human cervical carcinoma cells in vitro. Toxicol In Vitro, 25(7), 1366–75.

Keskın, D., Ceyhan, N., Uğur, A., & Durgan, D.A. (2012). Antimicrobial activity and chemical constitutions of West Anatolian olive. *Journal of Food, Agriculture& Environment*, 10(2), 99-102.

Khan, M.G.U., Nahar, K., Rahman, M.S., Hasan, C.M., & Rashid, M.A. (2008). Phytochemical and Biological Investigations of *Curcuma longa*. *Dhaka Univ. J. Pharm. Sci*., 8(1), 39-45.

Khattak, S., Rehman, S., Ullah, S.H., Ahmad, W. & Ahmad, M. (2005). Biological effects ofindigenous medicinal plants *Curcuma longa* and *Alpinia galangal*. *Fitoterapia*, 76, 254-257.

Kirtikar, K.R., & Basu, B.D. (1993). *Indian Medicinal Plants.* 2nd Ed, I Vol, (2435-2438). International Book Distributors, Dehradun, India.

Kobayashi, E., Ando, K., Nakano, H., Iida, T., Ohno, H., Morimoto, M., & Tamaoki, T. (1989). Calphostins (UCN-1028), novel and specific inhibitors of protein kinase C. I. Fermentation, isolation, physico-chemical properties and biological activities. *The Journal of Antibiotics*, 42, 1470-1474.

Kumar, A.P., Garcia, G.E., Ghosh, R., Rajendran, V., Rajnarayanan, Y., Alworthy, W.L., & Slaga, T.J. (2003). 4-Hydroxy-3-Methoxybenzoic Acid Methyl Ester: A Curcumin Derivative Targets Akt/NFKB Cell Survival Signaling Pathway: Potential for Prostate Cancer Management. *Neoplasia*, 5(3), 255 – 266.

Kupchan, S. M., & Tsou, G. (1973). *J. Org. Chem.*, 38, 178. https://doi.org/10.1021/jo00941a049

Kuroda, M., Mimaki, Y., Nishiyama, T., Mae, T., Kishida, H., Tsukagawa, M., Takahashi, K., Kawada, T., Nakagawa, K. & Kitahara, M. (2005). Hypoglycemic Effects of Turmeric (*Curcuma longa* L. Rhizomes) on Genetically Diabetic KK-Ay Mice. *M Bio. Pharm. Bull*., 28, 937-939.

Lee, H.S. (2006). Antiplatelet property of *Curcuma longa* L. rhizome-derived ar-turmerone. *Biores. Tech*., 97, 1372-1376.

Lee, O.H., & Lee, B.Y. (2010). Antioxidant and antimicrobial activities of individual and combined phenolics in *Olea europaea* leaf extract. *Bioresource Technology*, 101, 3751–3754.

Liu, C., Kao, C., Tseng, Y., Lo, Y., & Chen, C. (2017). Ginger phytochemicals inhibit cell growth and modulate drug resistance factors in docetaxel resistant prostate cancer cell. Molecules, 22, 1477.

Liu, H., & Luo, D. Study on secondary metabolites of Cladosporium. (2019). *Chem. Eng. Commun*., 45, 2.

Luettig, J., Rosenthal, R., Lee, I.M., Krug, S.M., & Schulzke, J.D. (2016). The ginger component 6-shogaol prevents TNF-alpha-induced barrier loss via inhibition of PI3K/Akt and NF-kappa B signaling. *Mol. Nutr. Food Res*., 60, 2576–2586.

Lutomski, J., Kedzia, B., & Debska, W. (1974). Effect of an alcohol extract and of active ingredients from *Curcuma longa* on bacteria and fungi. *Planta Med*., 26, 9-19.

Mahmud, S.M.N., Sohrab, M.H., Begum, M.N., Rony, S.R., Sharmin, S., Moni, F., Akhter, S., Mohiuddin, A.K.M., & Afroz, F. (2020). Cytotoxicity, antioxidant, antimicrobial studies and phytochemical screening of endophytic fungi isolated from *Justicia gendarussa*. *Ann Agri Sci*., 65(2), 225–32.

Mao, Q-Q., Xu, X-Y., Cao, S-Y., Gan, R-Y., Corke, H., Beta, T., & Li, H-B. (2019). Bioactive Compounds and Bioactivities of Ginger (*Zingiber Officinale* Roscoe). *Foods*, 8, 185. doi: 10.3390/foods8060185

Marasini, B.P., Baral, P., Aryal, P., Ghimire, K.R.S., Neupane, S., Dahal, N., Singh, A., Ghimire, L., & Shrestha, K. (2015). Evaluation of Antibacterial Activity of Some Traditionally Used Medicinal Plants against Human Pathogenic Bacteria. *BioMed Research International*.

Markiewicz-Żukowska, R., Naliwajko, S,K., Bartosiuk, E., Moskwa, J., Isidorov, V., Soroczyńska, J., Borawska, M.H. (2013). Chemical composition and antioxidant activity of beebread, and its influence on the glioblastoma cell line (U87MG). *J Apic Sci*., 57(2), 147–57.

Masuda, Y., Kikuzaki, H., Hisamoto, M., & Nakatani, N. (2004). Antioxidant properties of gingerol related compounds from ginger. *Biofactors*, 21(1-4), 293-6.

Narasimhan, B., Belsare, D., Pharande, D., Mourya, V., & Dhake, A. (2004). *European Journal of Medicinal Chemistry*, 39, 827–834.

Nasri, H., Sahinfard, N., Rafieian, M., Rafieian, S., Shirzad, M., & Rafieian-kopaei, M. (2014). Turmeric: A spice with multifunctional medicinal properties. *J Herb Med Pharmacol.*, 3(1), 5-8.

Nasrin, M., Afroz, F., Sharmin, S., Rana, M.S., & Sohrab, M.H., (2019). Cytotoxic, antimicrobial and antioxidant properties of *Commelina diffusa* Burm. f. *Pharmacol. Pharm.*, 10, 82–93.

Ohta, T. (1993). Modification of genotoxicity by naturally occurring flavorings and their derivatives. *Crit Rev Toxicol*., 23, 127–146.

Ola, A.R.B., Aly, A.H., Lin, W., Wray, V., & Debbab, A. (2014). Structural revision and absolute configuration of lateritin. *Tetrahedron Letters*, 55, 6184–7.

Pari, L., & Murugan, P. (2004). Protective role of tetrahydrocurcumin against erythromyvin estolate-induced hepatotoxicity. *Pharmacological Research*, 49, 481-486.

Park, G.H., Park, J.H., Song, H.M., Eo, H.J, Kim, M.K., & Lee, J.W., Lee, M.H., Cho, K-H., Lee, J.R., Cho, H.J., & Jeong, J.B. (2014). Anti-cancer activity of Ginger (*Zingiber officinale*) leaf through the expression of activating transcription factor 3 in human colorectal cancer cells. BMC complementary and alternative medicine, 14(1), 408.

Rahman, M.A.A., & Moon, S. (2007). Antimicrobial phenolic derivatives from Dendranthema zawadskii var. latilobum Kitamura (Asteraceae). *Archives of Pharmacal Research*, 30, 1374-1379.

Rahman, M.S., Hossain, R., Saikot, F.K., Rahman, S.M., Saha, S.K., Hong, J. & Kim, K. (2017). Insights into the *in vitro* germicidal activities of *Acalypha indica*. *Anal. Sci. Techno*., 30, 26-31.

Rampogu, S., Baek, A., Gajula, R.G., Zeb, A., Bavi, R.S., Kumar, R., Kim, Y., Kwon, Y.J., &

Lee, K.W. (2018). Ginger (Zingiber o_cinale) phytochemicals-gingerenone-A and shogaol inhibit SaHPPK: molecular docking, molecular dynamics simulations and in vitro approaches. *Ann. Clin. Microb. Anti*., 17, 16.

Rios, J.L., Recio, M.C., & Villar, A. (1988). Screening methods for natural products with antimicrobial activity: A review of the literature. *J.Ethnopharmacol.*, 23,127-149.

Ross, I.A. (2001). Medicinal Plants of the World. Humana Press, New Jersey, 1, 139-143.

Rudra, S., Sawon, M.S.U., Emon, N.U., Alam, S., Tareq, S.M., Islam, M.N., & Shakil, M. (2020). Biological investigations of the methanol extract of Tetrastigma leucostaphylum (Dennst.) Alston ex Mabb. (Vitaceae): In vivo and in vitro approach. *J. Adv. Biotechnol. Exp. Ther*., 3, 216-224.

Sadananda, T.S., Govindappa, M., Ramachandra, Y.L. (2014). *In Vitro* Antioxidant Activity of Lectin from Different Endophytic Fungi of *Viscum album* L. British Journal of Pharmaceutical Research, 4(5), 626-643.

Sakagami, Y., Sano, A., Hara, O., Mikawa, T., & Marumo, S. (1995). Cladosporol, β-1,3-glucan biosynthesis inhibitor isolated from fungus, *Cladosporium cladosporioides*. *Tetrahedron Letters*, 36, 1469-1472.

Sarangthem, K., & Haokip, M.J., (2010). Bioactive component in *Curcuma caesia* Roxb. Grown in Manipur. *The Bioscan*., 5, 113-115.

Schadich, E., Hlavac, J., Volna, T., Varanasi, L., Hajduch, M., & Dzubak, P. (2016). Effects of ginger phenylpropanoids and quercetin on Nrf2-ARE pathway in human BJ fibroblasts and HaCaT keratinocytes. *Biomed Res.Int*., 2173275. http://dx.doi.org/10.1155/2016/2173275

Schroers, H.J. (2001). A Monograph of Bionectria (Ascomycota, Hypocreales, Bionectriaceae) and its clonostachys anamorphs. (46). *Studies in mycology*. Centraalbureau voor Schimmel cultures. ISSN 0166-0616.

Schroers, H.J., Samuels, G.J., Seifert, K.A., & Gams, W. (1999). Classification of the mycoparasite Gliocladium roseum in *Clonostachys* as *C. rosea*, its relationship to *Bionectria ochroleuca*, and notes on other Gliocladium-like fungi. *Mycologia*, 91, 365–385.

Sekiwa, Y., Kuboto, K., & Kobayashi, A. (2000). Isolation of novel glucosides related to gingerdiol from ginger and their antioxidant activities. *J Agric Food Chem*, 48(2), 373-7.

Shahidi, F., Janitha, P.K., & Wanasundara, P.D. (1992). Phenolic antioxidants. *Crit. Rev. Food Sci. Nutr.*, 32, 67-103.

Shan, B., Cai, Y.Z., Sun, M., & Corke, H. (2005). Antioxidant capacity of 26 spice extracts and characterization of their phenolic constituents. *J. Agric. Food Chem*., 53, 7749–7759.

Shareef, H.K., Muhammed, H.J., Hussein, H.M. & Hameed, I.H. (2016). Antibacterial Effect of Ginger (*Zingiber officinale*) Roscoe and Bioactive Chemical Analysis using Gas Chromatography Mass Spectrum. *ORIENTAL JOURNAL OF CHEMISTRY.*, 32(2), 817-837.

Shi, Y., Ji, M., Dong, J., Shi, D., Wang, Y., Liu, L., Feng S., & Liu L. (2024). New bioactive secondary metabolites from fungi: 2023. *Mycology*, 15(3), 283-321, DOI: 10.1080/21501203.2024.2354302.

Shukla, Y., & Singh, M. (2007). Cancer preventive properties of ginger: A brief review. *Food Chem Toxicol*, 45(5), 683-90.

Shusterman, A.J., McDougal, P.G., & Glasfeld, A. (1997). Dry-Column Flash Chromatography. *J Chem Educ*., **74** (10), 1222. doi:10.1021/ed074p1222.

Stahl, E. (1969). *Thin Layer Chromatography, A Laboratory Hand Book*. 2nd ed., Springer, Verlag, New York.

Stephens, P., Hunter, C., Bignell, G., Edkins, S., Davies, H., Teague, J., et al. (2004). Lung cancer: intragenic ERBB2 kinase mutations in tumours. *Nature*, 431(7008), 525–6.

Steyn, P.S., Wessels, P.L., Marasas, W.F.O. (1979). Pigments from *Fusarium moniliforme* Sheldon. *Tetrahedron*, 35, 1551-1555.

Strober, W. (2015). Trypan Blue Exclusion Test of Cell Viability. Current Protocols in Immunology, 111(1). https://doi.org/10.1002/0471142735.ima03bs111

Supratman, U. (2010). Elusidasi Struktur Senyawa Organik. *Widya Padjajaran, Bandung*, 94-

102.

Sutarno, H., Hadad, E.A., & Brink, M. (1999). "Zingiber officinale Roscoe". In De Guzman CC, Siemonsma JS (eds.), *Plant resources of South-East Asia: no.13: Spices* (pp. 238–244). Leiden (Netherlands), Backhuys Publishers.

Sutton, J.C., Li, D.W., Peng, G., Yu, H. & Zhang, P.G. (1997) Gliocladium roseum: a versatile adversary of Botrytis cinerea in crops. *Plant Dis*., 81, 316–328.

Takahashi, T., Kozaki, K. I., Yatabe, Y., Achiwa, H., & Hida, T. (2002). Increased expression of COX-2 in the development of human lung cancers. *J Environ PatholToxicol Oncol*., 21(2), 177–81.

TATUM, J.H., BAKER R.A., & BERRY, R.E. (1987). NAPHTHOFURANS PRODUCED BY FUSARIUM OXYSPORUM ISOLATED FROM CITRUS. *Phytochemistry*, 26(9), 2499-2500.

Taylor, A., Armitage, D.A., Handy, C., Jackson, C.A., Hulin, T.M., Harrison, J.R., & Clarkson, P.J. (2019). Basal rot of narcissus: Understanding pathogenicity in *Fusarium oxysporum* f. sp. narcissi. *Front Microbiol*., 10,1–17.

Thomas, F. (2000). PDR of Herbal Medicine. *Medical Economics Company*, Montvale, New Jersey, 775-776.

Touchstone, J. C., & Dobbins, F. M. (1978). *Practice of Thin Layer Chromatography.* (170-199). John Wiley and Sons Ltd.

Tsuda, H., Uehara, N., Iwahori, Y., Asamoto, M., Iigo, M., Nagao, M., Matsumoto, K., Ito, M. & Hirono, I. (1994). Chemopreventive effects of beta-carotene, alpha-tocopherol and five naturally occurring antioxidants on initiation of hepatocarcinogenesis by 2-amino-3-methylimidazo sbd (4,5-f)-quinoline in the rat. *Jpn J Cancer Res*., 85, 1214–1219.

Van-Wagenen, B. C., Larsen, R., Cardellina II, J. H., Randazzo, D., Lidert, Z. C., & Swithenbank, C. (1993). *J. Org. Chem.*, 58, 335. https://doi.org/10.1021/jo00054a013

Varsha, K.K., Devendra, L., Shilpa, G., Priya, S., Pandey, A. and Nampoothiri, K.M. (2015). 2,4-Di-tert-butyl phenol as the antifungal, antioxidant bioactive purified from a newly isolated *Lactococcus sp*. *Int. J. Food Microbiol*., 211, 44–50.

Wainwright, M. (1993). The Mystery of the Plate: Fleming's Discovery and Contribution to the Early Development of Penicillin. *Journal of Medical Biography*, 1(1). https://doi.org/10.1177/096777209300100113

White, T.J., Bruns, T.D., Lee, S.B. & Taylor, J.W. (1990). Amplification and Direct Sequencing of Fungal Ribosomal RNA Genes for Phylogenetics. In: Innis, M.A., Gelfand, D.H., Sninsky, J.J. & White, T.J., Eds., (315-322). *PCR Protocols: A Guide to Methods and Applications*, Academic Press, New York. http://dx.doi.org/10.1016/B978-0-12-372180-8.50042-1

Williams, W.B., Cuvelier, M.E., & Berset, C. (1995). Use of a free radical method to evaluate antioxidant activity. *LWT- Food Sc. Technol*., 28(1), 25–30.

Wong, C., Li, H., Cheng, K., & Chen, F. 2006. A systematic survey of antioxidant activity of 30 Chinese medicinal plants using the ferric reducing antioxidant power assay. *Food Chem*., 97, 705-711.

Wu, C.Q., Chen, F., Wang, X., Kim, H.J., He, G.Q., Haley- Zitlin, V., & Huang, G. (2006). Antioxidant constituents in feverfew (*Tanacetum parthenium*) extract and their chromatographic quantification. *Food Chem*., 96, 220-227.

Xavier, de Moura R.M., Pereira, P.S., Januario, A.H., Franca, S.C., & Dias, D.A. (2004). Antimicrobial screening and quantitative determination of benzoic acid derivative of Gomphrena celosioides by TLC densitometry. *Chemical & Pharmaceutical Bulletin*, 52, 1342-1344.

Xiang, H., Zhang, L., Lu, Xi., Yang, Y., Wang, X., Lei, D., Zheng, Xi., & Liu, X. (2018). Phytochemical profiles and bioactivities of essential oils extracted from seven *Curcuma* herbs. *Industrial crops and products*, 111, 298-305.

Yehia, R.S., Osman, G.H., Assaggaf, H., Salem, R., & Mohamed, M.S.M. (2020). Isolation of potential antimicrobial metabolites from endophytic fungus *Cladosporium cladosporioides* from endemic plant Zygophyllum mandavillei. *South African Journal of Botany*, 134, 296-302.

Yoshihi, A.T., Mn, R.U., Takashi, O., Kimikc, N., Koutarou, M. & Toshiakit, O. (1991). Glycosides of ergosterol derivatives *fromffericum erinaceus. Phytochemistry*, 12, 4117-4120.

Zhang, H., Zhao, B., Zhai, Z.G., Zheng, J.D., Wang, Y.K., & Zhao, Y.Y. (2021). Expression and clinical significance of MMP-9 and P53 in lung cancer. *Eur Rev Med Pharmacol Sci*., 25, 1358–65.

Zhang, X-d., Wu, Q., Yang, S-h. (2017). Ferulic acid promoting apoptosis in human osteosarcoma cell lines. *Pak J Med Sci*., 33(1), 127.

Zhang, Z.B., Zeng, Q.G., Yan, R.M., Wang, Y., Zou, Z.R & Zhu, D. Endophytic fungus *Cladosporium cladosporioides* LF70 from Huperzia serrata produces Huperzine A. (2011). *World J Microbiol Biotechnol*., 27, 479–486. DOI 10.1007/s11274-010-0476-6

Zou, J. & Dai, J. (2009). Study on chemical constituents in marine fungus of *Cladosporium cladosporioides*. *Chin. Pharm. J*., 44, 418–421.